MASTER THESIS

POSSIBILITIES FOR IMPROVING ASSESSMENT TOOLS OF DIKES SAFETY

Author: Q.T. Tran

Enschede, the Netherlands,

Date: 12th August, 2012

Version: final

Examination Committee:

Graduation supervisor	:	Prof. Suzanne Hulscher
UT supervisor	:	Dr. Sam Karim
Deltares supervisor	:	André Van Hoven

University of Twente
Enschede - The Netherlands

Master Thesis

POSSIBILITIES FOR IMPROVING ASSESSMENT TOOLS OF DIKES SAFETY

Author	TRUNG QUOC TRAN
Date	August 12, 2012
Examination Committee:	Prof.dr. S.J.M.H. Hulscher Faculty of Engineering Technology Department of Water Engineering and Management Email: s.j.m.h.hulscher@ctw.utwente.nl
	Dr.ir. U.F.A. Karim University of Twente Faculty of Engineering Technology (Engineering Technology Sciences) Department of Building / Infrastructure Email: U.F.A.Karim@utwente.nl
	Andre Van Hoven Deltares Institute, Delft Department of Dike Safety Email: Andre.vanHoven@deltares.nl

University of Twente
P.O. Box 217
7500 AE Enschede
The Netherlands
Telephone: +31 (0)53-489 9111
Fax: +31 (0)53-489 2000
E-mail: info@utwente.nl
Website: http:/www.utwente.nl

UNIVERSITY OF TWENTE.

Deltares
Enabling Delta Life

Preface

This report is the result of the work that I have followed for last six months in Delft. Regarding to the direction of thesis work, it still took me a lot of time to finish defining the research problem. When I met André in January and discussed a possibility about my graduation topic. I recognized that I would take a big challenge for my final assignment. I am interested in understanding soil mechanics in terms of stability of earth structures. At that time, I also had my own idea about what I would like to work for my thesis. However, being afraid of time limitation and complicated situation, I decided to divert my thesis direction and took an option that André proposed to me.

I started with learning different stability analyses methods, of which some methods that I had not learned before. Fortunately, background of soil mechanics and the preparation about marine dynamics helped me in understanding the procedure and made progress. In addition, some insights from summer internship gave me more confidence to involve in the project.

Looking at the entire progress, I would like to say thank to André first, my daily supervisor in Deltares. Regular meetings with him helped me to clarify difficult problems and keep my work being on time and on track. Secondly, many thanks to the close supervision of Mr. Karim, who encouraged me to gain much progress both professional knowledge and English reporting skills. Also, I would like to show my gratitude towards Mrs. Hulscher who kept looking after my progress and helped my plan to be finished on time. Next, I would like to thank all Vietnamese and Dutch friends in Enschede for the good time we shared altogether. Unforgettable trips, parties, discussions, and encouragements would stay with me wherever I go. Living far from home is very hard at the beginning, but useful experience ensuing from difficulties surrounding. Last but not least, special thanks are dedicated to my family where I receive endless energy to overcome difficulties. Without their support and spiritual advices, I would not have done many things to date.

Even though considerable effort of mine was spent on this document, it is hard to avoid having mistakes or shortcomings occurring here and there. Any contribution is always highly appreciated. Finally, I hope you will enjoy reading this report.

Tran Quoc Trung

Enschede, August 2012

Abstract

Currently, Edelman – Joustra equation is used as an assessment tool for evaluating dike safety in terms of potentially surficial sliding. Application of this statutory is relatively simple, but gives a conservative judgment since it stemmed from one-dimensional analysis. In practice, many dike sections are still safe even though the Edelman – Joustra condition is not satisfied. In those cases, further detailed evaluations are usually required, including groundwater flow and advanced stability analyses. To some extent, such costly and time-consuming tests can be avoided if the accuracy of the current criterion is improved sufficiently. To achieve this, the 1-D method using Edelman – Joustra equation was compared to other detailed analyses, namely Spencer and finite element method (FEM – PLAXIS) through a set of parametric calculations.

The calculations showed that the accuracy of the one-dimensional Edelman – Joustra equation can be improved by including the effect of L/D ratio. In this ratio, L is the slope length and D is the thickness of the cover layer. With a formulae determining the influence of L/D ratio on sliding mechanism, the accuracy can be improved up to 15% for ratios smaller than 25. This result holds for most conventional dikes. In order to show and determine practical usefulness of the improved function, verification and validation steps have been executed, together with a case study – Afsluitdijk. As part of this case study, the influence of wave overtopping on downstream slopes stability was simulated, of which infiltration process demonstrates a simple method connecting hydraulic loadings and soil mechanics.

In conclusion, an improved safety assessment method was developed, which is useful in instances. Consequently, the improved method has been included in an integrated proposal to improve the current assessment guidelines so that the costly and time-consuming evaluations can be avoided as much as possible in the future.

Contents

Chapter 1. Introduction

This chapter is dedicated to give an overview of the origin of the current thesis. An understanding of the root of the project will provide a fundamental background of the scope of study. The problem statement is defined and solutions need to be found out. Therefore, a set of research questions emerges, followed by the research approach and the thesis boundaries, which in turn steer the thesis activities.

1.1. A need for understanding of failure mechanisms subject to wave overtopping history

In The Netherlands, much attention has been paid to water defenses (as many years ago). Nowadays, dikes and other water defences are generally divided into 53 dike rings with different standard levels of safety. Changes in these standard levels of safety can be dated from 1953. Before 1953, a dike was designed based on as standard in relation with crest height of dike. In this standard, the crest height should be determined so that it has 0.5 m above the highest food level with a certain amount of surcharge. With a designed return period of 300 years, a large number of sea dikes collapsed during the storm surge disaster of 1953. 1836 people were killed and approximately 14% Dutch GNP was lost after the complete region was flooded with water. This standard was re-investigated and new guidelines were made to protect the country from such kind of flooding disasters in the future. According to investigations of these situations, overtopping waves were attributed to the failure of a number of sea dikes. Large volumes of water passed the crest of the dikes and damaged the inner slope of the dikes. A dike failed when the inner slope slides and exposes the core to further erosion leading to a dike breach. As a result, the standard stated that water defences should be designed to withstand a hydraulic loading level, water level and wave conditions, which has a probability of exceedance of 1/10000 or 1/4000 a year, according to the economical value of the protected area. The number of overtopping waves that is allowed to exceed a dike crest level is limited to the value of 2% of the incoming waves. This made the crest height much higher than the storm surge level (about 3 to 5 meters). In the late twentieth century, the average overtopping discharge was introduced as an extra guideline for dike design.

Due to changes in the design guidelines and the climate conditions, increasing dike heights is a conventional approach in design procedure. Typically, dikes consist of a mild outer slope (1:4) and a steeper downstream slope where in between a crest is built with a certain width. A berm is usually constructed at mean sea level. The outer slopes are, in most cases, covered with a place block revetment, rock or asphalt up to or just above the design level, while the rest of the outer slope, crest and landward slopes are covered with grass.

In the future, more and more heavier storms are expected due to climate change. The dikes may not be high enough any more to meet the strict 0.1 or 1.0 l/s per m overtopping discharge guideline, when the sea level rises and more waves attack the structures. Wave overtopping can lead erosion and/or to sliding due to erosion or infiltration process (Van Hoven, Hardeman, Van der Meer, and Steendam, 2010). The solutions that was used in the past (raising the height) may not be sufficient and recommendable in the future. Even though they are applicable, the costs are still high. If the dikes remain unchanged in their height, wave overtopping will occur more frequently. This does not really matter if the dike is strong enough to withstand the overtopping water and if there is a good water management system behind the dike. Reinforcing the dikes can be a good solution, rather than raising the dikes in some cases. However, before it is known whether the dikes are strong enough or need reinforcement, an understanding of the strength of inner slopes in case of wave overtopping is essential.

1.2. Problem statement and the need for improvement of assessment tools

As stated in the previous part, evaluating the shear strength of the inner slopes is very important since the increase in hydraulic loadings keeps going on. Currently, the assessment tools for different failure mechanism provided by government are divided into several levels: simple, detailed and advanced. The simple assessment tools can be described as a limitation of the average overtopping discharge of 0.1 l/s per m and/or maximum slope gradient of 1V:4H[1]. According to these simple criteria (Safety assessment primary flood, 2007), only small percentage of sea dikes (approximately 5%) is considered as safe while other dike sections have to be assessed using more complicated methods. However, sophisticated methods mean more variables to be considered and the procedure of assessment is both costly and time-consuming. A possible solution is avoidance of using complicated assessment tools as much as possible by upgrading the simple tool properly. Acknowledging the scenario mentioned above, Deltares institute is being involved in the SBW program (Strength and Loads on Water Defenses) that creates a framework for safety assessment. Part of the program is the project SBW – Wave Overtopping and Strength of Revetments – focusing on reliable assessment without further reinforcement measures. Improvement and optimization are put on the assessment tool for sliding of the inner slope cover layer in case of wave overtopping. This framework is elaborating on the slope stability with different analysis methods, varying from simple to sophisticated ones. Above all, the goal of this project is to enhance the use of simple assessment as much as possible.

The thesis originates from the idea that it is likely that the simple assessment tools can be extended to have a higher discharge limitation or a steeper slope gradient. Therefore, this study aims at comparing different safety calculation methods to improve the simple assessment method by looking at the difference between them.

1.3. Research objectives

The main objective of this research is to propose an improved method for assessing dikes safety in which the stability of inner slopes against superficial sliding is re-evaluated in a new procedure formulated from current simple assessment tools. The secondary objective is to give

[1] 1V:4H: the ratio representing slope angle, V: vertical and H: horizontal

a description and evaluation of the effect of infiltration process due to wave overtopping on the stability of inner slopes in case of Afsluitdijk.

1.4. Research questions

Main research questions:

1. Can the simple assessment tool for sliding of the cover layer due to wave overtopping be extended?
2. What are the effects of the infiltration process, generated from overtopping waves, on the downstream slope stability of Afsluitdijk?

Sub-research questions 1:

1. How is downstream slope stability assessed by using Edelman – Joustra method?

   To enable development of a new assessment method, it should be known how the current assessment tool evaluates the stability of landward slopes. Having such knowledge, one can determine to which extent the current method is simple and over conservative.

2. What are the properties of complex assessment methods, namely Spencer and FEM, in slope stability?
   Answering this question will help to get an overview about possible difference between the methods, which then pinpoint the significantly additional variables for the new method. As can be seen in Chapter 2, two approaches, namely Spencer method and the finite element method, are presented.
3. What are the limitations of the chosen methods?
   Because these calculation methods consider certain assumptions, which can lower the probability of searching precise solutions, understanding their restrictions will help to choose calculation models to avoid errors as much as possible.
4. What is the pattern of difference between the methods having on stability of downstream slopes?
   The answer to this question shows how the current simple assessment tool can be upgraded.
5. In how far is the improved method effective and efficient?
   Concerning the applicability of the new assessment tool, the validation and verification will be elaborated in Chapter 5.

Sub-research questions 2:

1. What are the properties of wave overtopping?
   Understandings of wave overtopping theory will help to determine how overtopping waves are characterized at upstream slopes and downstream slopes.
2. What are the important properties of the soil being affected through the infiltration process?

In order to get insights onto how the soil strength decreases, some relevant elements have to be investigated, such as permeability and pore water pressure.

3. In what ways does infiltration process simulate different overtopping conditions?
   The purpose is to give a description of how various overtopping discharges are transferred into infiltration rate or infiltration time. Then, we can simulate them using appropriate water boundary condition.
4. Over the infiltration time, what is the relationship between the factor of safety and overtopping discharges in the case study?
   The relationship will give an overview on how much a difference between two overtopping discharges causes a difference in safety factor on a certain inner slope.

1.5. Failure mechanism – Problem description

Given a certain storm condition, overtopping waves will flow over the landward (downstream side) slope, leading to a small amount of water infiltration. The infiltration then increases the pore water pressure in clay-covered slopes. The increase in pore water pressure will decrease the shear strength of the clay cover. If the slope angle is steep or hydraulic loadings are too high, surface layers will start to slide, exposing the dike core to more erosion. In the 1953 storm surge disaster, the far majority of damaged and failed dikes showed this mechanism. It is noted, however, this event does not automatically mean the dike fails if the dike core can withstand the erosive force of the overtopping waves long enough. The infiltration process and the potential slip plane are depicted in

Figure 1.

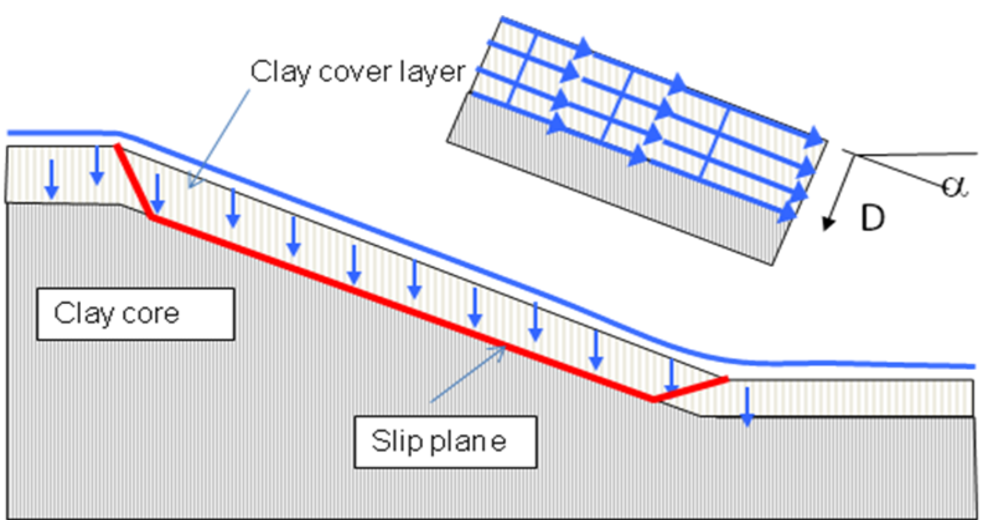

Figure 1. Clay dike cross section

1.6. Thesis Scope

1.6.1. Scope of study

The study is concerned with the technical risk from sliding-potential of the landward slopes of layered dikes subjected to wave overtopping. The dikes can differ in size, construction and materials. The properties of the core and protective cover materials are important elements in the stability of these dikes. The clay material in combination with grass is used as a cover layer on dikes that can have either clay or a sand core. The focus of this study will be on clay dikes with a clay cover layer. The clay cover layer is subjected to different effects than the core layers due to frost, thaw, draught, rain, swelling, shrinking, and infiltration. Moreover, the grass roots on the slope contribute to the so-called soil structure, which makes the clay-covered layer more permeable than the clay core, even though the base material can be the same.

Because of this, the core layer will be different from the cover layer in terms of permeability and shear strength. This research starts with given soil shear strengths parameters, which vary in a range to check the difference between safety factors, calculated from infinite slope analysis (Edelman – Joustra method) and finite analyses. Besides the thickness of the cover layer, the slope length is the main parameter accounting for the difference between infinite and finite analysis. In this study, factors of safety calculated from the Edelman – Joustra method represent infinite slope analysis while factors of safety provided by Spencer's calculation stand for finite slope analysis.

The emphasis is to quantify the effect of the slope length and the thickness of the cover layer on the safety factor. Variations are made regarding to a range of crest height of dikes and the thickness of the cover layer. Table 1 shows which parameters should be changed in calculation models and which should not. The shear strength parameters were kept unchanged so that possible variables affecting research outcomes are minimized. In addition, for a first evaluation, the influence of variation in cohesion and friction angle is significant. It is noted that the sand core covered with clay layer is outside the scope of this study while property of clay in the cover layer is low in cohesion and partially drained, isotropic material.

Table 1. Study variables

Parameter	Vary	Magnitude
The thickness of cover layer	yes	From 0.6 m --> 1.4 m
The Slope angle	yes	From 1V:1.5H ---> 1V:4H
The crest height of dike	yes	From 2.0 ---> 10.0 m
Cohesion	no	4.00 kN/m^2
Friction angle	no	20.0^0

The overtopping wave theory is elaborated up to the degree in which a storm condition is specified by relevant parameters. A typical overtopping condition for the Dutch coast can last for a couple of hours up to 12 hours. In Afsluitdijk case study, the concern is the relationship between the storm conditions and the level of infiltration, which causes the dynamic of pore water pressure in time. Therefore, some hydraulic quantities such as flow velocities and flow depths are beyond the study area. Indeed, even though the magnitude of these parameters are important for evaluating erosion process, they have little influence on the infiltration which is mainly dependent on how long overflow water stays on the slope.

1.6.2. Assumptions

Assumptions are essential to shape the boundary of the study and ensure the occurrence of the failure. In this study, assumptions concern the groundwater conditions. In addition, the effect of ground water flow such as seepage and infiltration are very important for calculating the stability. As depicted in the failure mechanism, due to the large difference in permeability between the clay core and cover layer, only negligible amount of infiltration water pass the interface of the two layers. In addition, many studies and experiment observations (Collins and Znidarcic, 2004) allow researchers to accept the following assumptions:

Superficial sliding occurs in the condition that the infiltration water causes the soil of the cover layer to be saturated and a groundwater flow develops parallel to the slope angle. A critical slip plane then develops parallel to the slope surface.

Infinite slopes are considered as constant slopes of infinite extent. In an infinite slope, the thickness of the cover layer is much smaller than the slope length. On the other hand, finite slopes take into account the effect of the slope length when the ratio of L/D is significant.

Erosion of the inner slope is assumed not to be critical in a wave overtopping event. This assumption holds for slopes covered by a good quality of the grass.

The strength parameters used in this report are considered as design values, and the partial safety coefficients are not taken into account in the scope of this report.

1.7. Research approach

The scope of study and aforementioned assumptions formulate the starting points of the research, it is now essential to describe a linkage between the starting points to the set-up objectives. This will be fulfilled by the research approach. It is clear that the objective of the study aimed at the effect of slope length and cover layer's thickness on the superficial sliding mechanism. Once the effect is quantified, an improved method can be made by upgrading the Edelman – Joustra method with the presence of the slope length parameter. In order to obtain such improved assessment, the approach includes a comparison between Edelman – Joustra and Spencer method under various geometrical situations formulated from the variation of slope length, slope angle, and the thickness of the cover layer. From Figure 2, the approach is depicted, in which the arrow lines shows chronological steps to reach the objectives. The arrow represents the input of those steps. Verification and validation steps are also carried out. Detailed descriptions of Edelman – Joustra, Spencer, and Finite Element Method are discussed in Chapter 2.

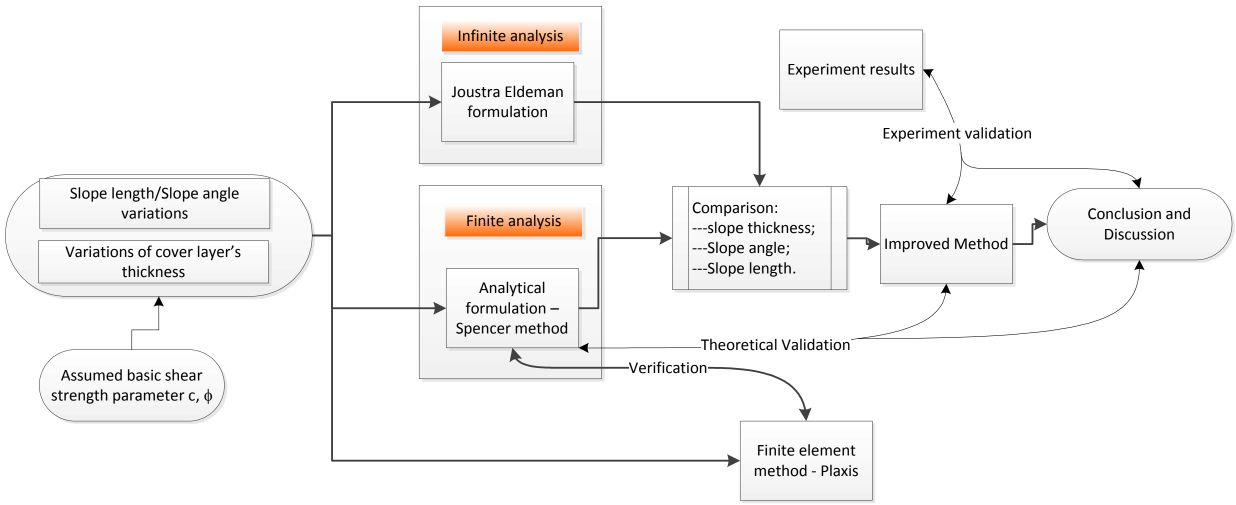

Figure 2. Methodology for determining the effect of slope length

The approach for obtaining the second objective is depicted in the figure below. A simulation model will be built up using data of Afsluitdijk experiment. This model is then forced to undergo five different overtopping discharges so that their influence can be measured in forms of factor of safety. These safety factors will be compared in order that the possibility of extending the limited overtopping discharge of 0.1 l/s per m may emerge.

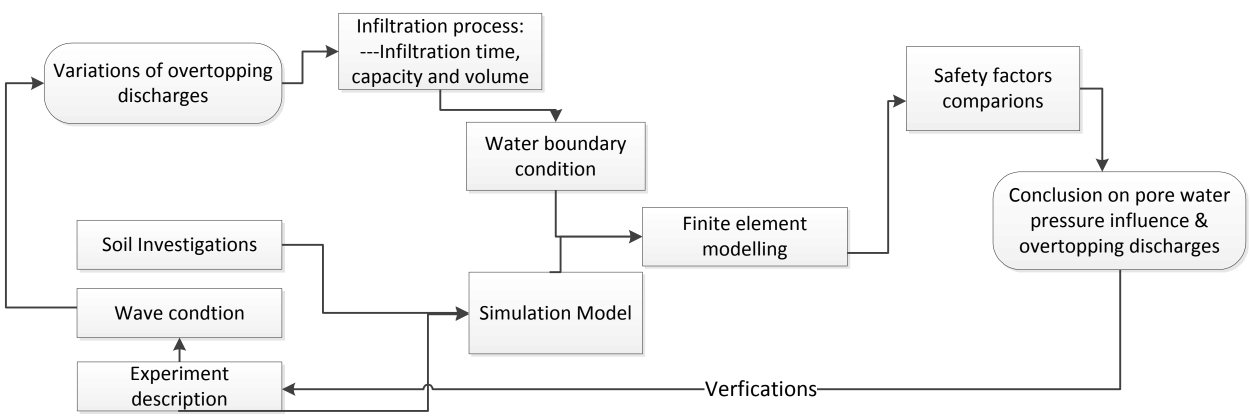

Figure 3. Methodology for determining the influence of overtopping discharges

1.8. Report structure

This document is structured as follows:

Chapter 2: Current Approaches. This chapter elaborates on reflections of three different safety calculation methods including Edelman – Joustra, Spencer, and finite element method (FEM).

Chapter 3: Implementation. Chapter 3 sets up a procedure in which involved steps to achieve the expected outcome are specified in a structured manner. Three safety assessment methods mentioned in Chapter 2 will use the same basic soil parameters to calculate factors of safety. It starts with the general methodology description, followed by the variations of geometry, and ends with calculated results.

Chapter 4: Comparison and Improved Methods. This chapter presents the relationship between the Edelman – Joustra method and Spencer method in terms of the safety factor. This relationship is a function of slope length and the cover layer’s thickness. A new assessment procedure is proposed to improve current assessment guidelines, ensuing on Edelman – Joustra equation.

Chapter 5: Verification and Validation. The first part of this chapter shows evidence to ensure the reliability of safety factor calculated by Spencer method. Secondly, a number of parametric calculations were made to validate the improve function and the accuracy of Spencer method. This is done by comparisons between the improved method, finite element method, and Spencer methods under random situations.

Chapter 6: This chapter attempts to make a description about the relationship between infiltration process with the slope stability, of which infiltration is initiated from overtopping waves. A comparison of simulation result and experiment measurements is also made to give insights on the superficial sliding mechanism.

Chapter 7: Discussion. This chapter brings us the evaluation of the entire thesis work, ranging from the research questions, methodology, and the final findings. Together with the emphasis on the limitations of the research results, the applicability and significance of the proposed improvement are elaborated.

Chapter 8: Conclusions and Recommendations

Chapter 2. Current Approaches

This chapter describes current approaches, which deal with slope stability under different levels of sophistication.

2.1. Edelman – Joustra Method

2.1.1. Theory

Generally, the factor of safety of ordinary methods or analytical methods is stated in the following function:

$$FOS = \frac{\tau_c}{\tau_o} \quad [1]$$

Where:

FOS : factor of safety (-)

τ_c : shear strength at the base of the slice (kN/m^2)

τ_o : mobilized shear stress at the base of the slice (kN/m^2)

In this research, the soil of the cover layer is considered as homogenous, isotropic and highly permeable relative to dike core. As seen in

Figure 4, a developing groundwater flow parallel to the slope is likely to develop when the dike core is much less permeable than the superficial soil layer (Daniel, and Glen, 1993). Because of this, it is assumed that the stability condition mentioned here concerns the ratio of the shear strength and shear stress at the interface between two material layers. In other words, the stability condition for interface behavior is more critical than that just within the layers.

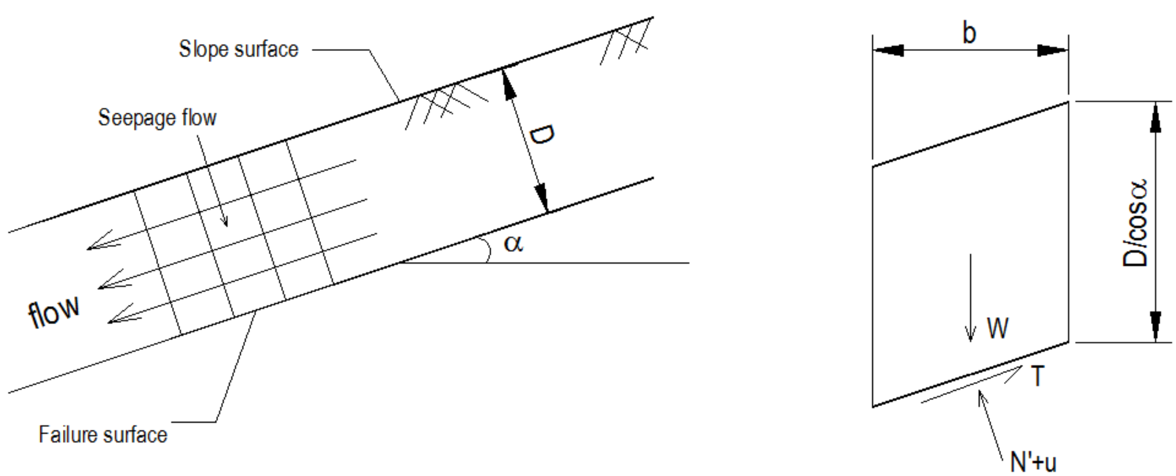

Figure 4. Assumed flow condition

From the observations of damage after the 1953 storm surge disaster, Edelman and Joustra developed a formula for calculating the stability of inner cover layers (TAW, 2001). This formula is based on the equilibrium of the shear strength and shear stress of a soil element when the hypothesis is met. This shear strength is caused by the cohesion c, internal friction angle ϕ', and the effective stress of the soil mass, based on Mohr-Coulomb model and the formulation of the shear strength is as follows (Budhu, 2007):

$$\tau_c = c + \sigma' \tan\phi' \quad [2]$$

$$\sigma' = \sigma - u \quad [3]$$

$$W_2 = \sigma = \gamma_n.D.\cos\alpha \quad [4]$$

Where:

c : effective cohesion (kN/m^2)

ϕ' : effective friction angle (deg)

σ : total stress at the base of slice (kN/m^2)

σ' : effective stress at the base of slice (kN/m^2)

u : pore pressure (kN/m^2)

W_2 : slope-perpendicular force/stress generated by soil weight (kN/m^2)

γ_n : the unit weight of saturated soil (kN/m^3)

α : inclination of slip surface at the middle of the slice (deg)

D : the depth perpendicular distance to the surface of slope from the base of the slice (m)

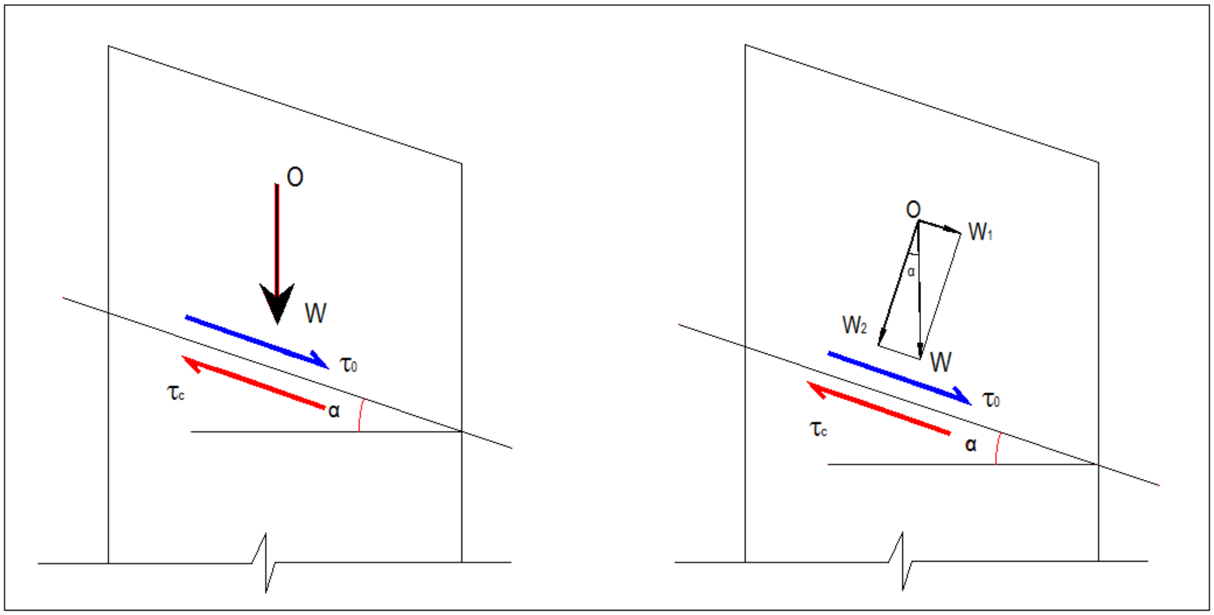

Figure 5. Sliding forces

Figure 5 shows that the stability of the cover layer is no longer ensured or guaranteed once the shear stress, τ_0, which is caused by the forces of soil mass in the direction parallel to the slope to the dike toe, is larger than the shear strength τ_c. The mobilized shear stress is:

$$\tau_o = W_1 = W.\sin\alpha = D.\gamma_n.\sin\alpha \qquad [5]$$

Where:

W : weight of the soil of the slice (kN/m^2)

W_1 : slope-parallel force/stress generated by soil weight (kN/m^2)

Due to:

$u = D.\gamma_w.\cos\alpha$, the shear strength in Equation [1] can be re-written from [2] and [3] as follows:

$$\sigma' = \sigma - u = D.\gamma_n.\cos\alpha - D.\gamma_w.\cos\alpha$$

$$\tau_c = c + \sigma'.\tan\phi' = c + (D.\gamma_n.\cos\alpha - D.\gamma_w.\cos\alpha).\tan\phi' \qquad [6]$$

Substituting [5] and [6] to [1], the safety factor (FOS) is:

$$FOS = \frac{\tau_c}{\tau_o} = \frac{c + \left(D.\gamma_n.\cos\alpha - D.\gamma_w.\cos\alpha\right)\tan\phi'}{D.\gamma_n.\sin\alpha} \qquad [7]$$

Or

$$\tan\phi' \geq \frac{\gamma_n.\sin\alpha + \dfrac{c}{D}}{\gamma_n.\cos\alpha\ -\ \gamma_w.\cos\alpha} \qquad [8]$$

2.1.2. Limitations

According to Edelman – Joustra method, the safety factor tends to decrease with an increasing thickness of the cover layer. However, this is without taking into account the influence of the slope length limitation and the infiltration depth limitation. This method is a part of current statutory assessment tools and may lead to over conservative assessments.

2.1.3. Partial safety factors

The safety factor as stated in previous section should not be confused with partial safety factors. The former factor is the ratio of resisting forces over the driving force, while the latter represents the magnitude of uncertainty quantified for involved design parameters.

For the sake of simplicity and comparability in comparison of different methods, the value of involved parameters in the previous parts is referred to as design values, in which the partial safety factor for each quantity is already taken into account. Although the partial safety factor is not investigated in this report, a short explanation will help the researchers understanding the uncertainty embedded on the used design values, especially cohesion and friction angles.

Due to uncertainties in measuring involved parameters in practice and spatial variability of the parameter, the measured values contain both true (local) values and errors of the measurements. While there is no way to obtain the true soil parameters, covering the spatial variability, the design values are derived from measured values thanks to statistical calculations. The correlation between measured values and design values is then stated in terms of relevant partial safety coefficients to compensate the uncertainties. The following equations express the correlation:

$$\gamma_S = \frac{S^*}{S_k} \qquad [9]$$

$$\gamma_R = \frac{R_k}{R^*} \qquad [10]$$

Where:

S^*, R^* : design value of driving forces, design value of resistance forces

S_k, R_k : mean measured value of driving forces, mean measured value of resistance forces

γ_S, γ_R : partial safety factor of driving forces and resistance forces

The magnitude of partial safety factors is calculated with the aid of probabilistic calculations. The procedure for calculating the partial safety factors involves mean values, a reliability index, and standard deviations (Vrouwenvelder and Siemes, 1987). According to statistic principles, a quantity has a distribution, which explains how the magnitude of such quantity changes depending on the consistency of measurement. This kind of distribution has its mean value and standard deviation. These parameters indicate the level of reliability of the value used in design, and thereby increase the reliability of the calculation. Using these values, many reliability methods aim at obtaining a design value with an acceptable reliability level. For example, the "method of First order second moment" aims at producing a converged reliability index after making sufficient iterations of calculations. Design values produced from such a method then are used to determine partial safety coefficients of different quantities.

From the coastal engineering perspective, the set of partial safety factors ensures that the failure probability for this mechanism is sufficiently low, given a certain hydraulic loading level determined by a statutory return period (for instance 1 every 10.000 years for Zuid Holland). Referring to TAW 2001, there are four factors taken into account. First, a model factor accounts for uncertainties in the calculation mode. For example, when applying Bishop's method, the value of 1.1 is used. Second, damage factor explains the influence of three aspects: the exceeding frequency of design level, the cause of geotechnical instability and the flood defenses around the dike. The spatial safety factors for the internal friction angle and cohesion depend on a few factors which determine the amount of uncertainty around the parameters. For example, when consolidated, undrained triaxial tests are used within a vertical strain range of 2% - 5%, for a clay material, the factors are 1.2 and 1.25, respectively. If the values from the NEN 9997 table 2b are used, the factors are 1.3 and 1.6, respectively.

2.2. Spencer's method

2.2.1. Theory

Like other limit equilibrium methods (LEM), Spencer's method satisfies both force and moment equilibrium. However, the difference is that this method considers both shear and normal forces of the inter-slices (T and E). It assumes a constant inclination of inter-slices forces acting on all inter-slices, which means that the ratio of T over E is presented in a constant angle, θ (Spencer, 1989). The considered forces are sketched in Figure 6 (Krishna, 2006).

Where:

W : the weight of the slice of soil

N' : effective force at the base of the slice

u : pore water pressure

T : shear force at the base of the slice

T_1, T_2 : vertical/shear inter-slice forces

E_1, E_2 : horizontal/normal inter-slice forces.

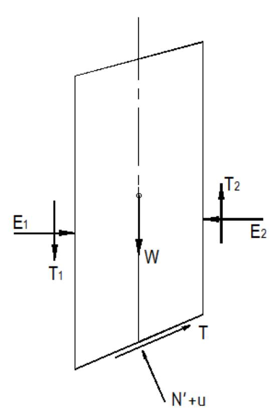

Figure 6. Spencer's considered forces

For each slice, three equations describing the equilibrium conditions of horizontal forces, vertical forces, and moments are derived with the presence of the constant inclination inter-slices forces. From these equations, the FOS is computed for both force and moment equilibriums (Spencer, 1967). The D Geo Stability software computed two factors of safety, one with respect to the moment equilibrium (F_m), the other regarding the horizontal force equilibrium (F_f) under various values of angle θ. The iterative procedure continues until F_m and F_f share more or less the same value. The detailed description of force analysis is presented in Appendix 2.

2.2.2. Limitations

Although Spencer's method satisfies all conditions of equilibrium and gives an accurate result for the factor of safety, it still uses the assumption that soil mass is divided into small vertical slices and the inter-slices forces inclinations are constant. To some extent, this does not give people a feeling of natural failure of the slope.

Another limitation is related to the calculation process. One may realize that Spencer calculation does much iteration to derive an inter-slices side force inclination, which simultaneously satisfies horizontal and vertical force equilibrium and moment equilibrium. This requires convergence of F_m and F_f, which sometimes can be violated in some calculations.

2.3. Finite element method (FEM) – Plaxis

A difficulty with all equilibrium methods is that they are based on the assumption that a failing soil mass are divided into slices. This in turn requires further assumptions related to the side forces directions. The assumption of the side forces direction is one of the main characteristics distinguishing one limit equilibrium method from another. However, this concept of side forces is entirely artificial (Griffiths, and Lane, 1999).

2.3.1. General concept

With the development of computing technology, finite element methods and other numerical approaches have grown rapidly. They help geotechnical engineers in solving a wide range of complex engineering problems such as deformations of complex geometry, bending moments, and so on. This approach decomposes the whole soil mass into finite elements with the help of a generated mesh (Figure 7). This numerical method uses approximations of the connectivity of elements, continuity of displacements, and stresses between elements. In soil stability analysis, this method is useful for calculating the stresses and deformations of a given model with sufficient and complex boundary conditions.

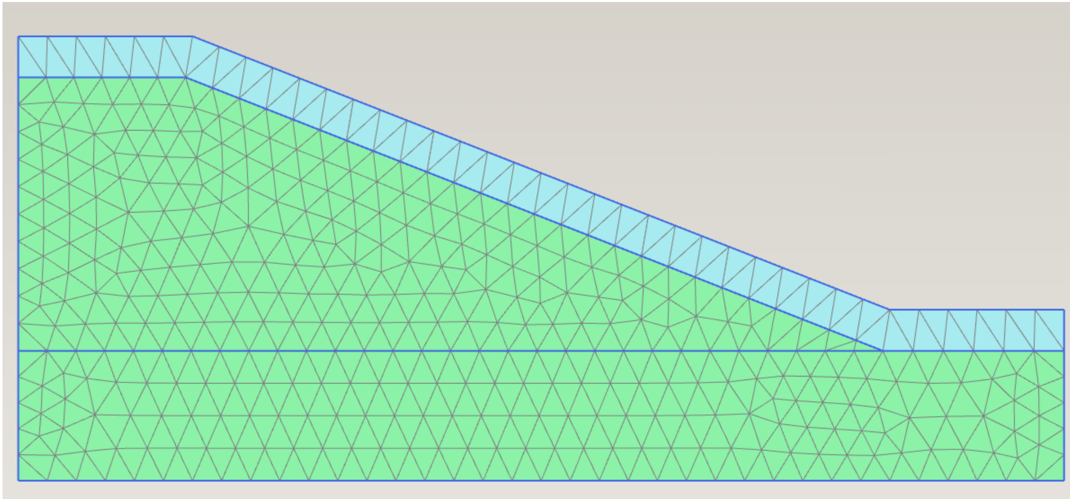

Figure 7. Finite element model.

In this study, Plaxis is used as a tool to execute finite element method, which allows designers to compute the stresses and deformations without assuming a planar failure beforehand. The finite element method finds the instability state by decreasing the strength of relevant parameters. This shear strength reduction technique is elaborated in next paragraphs.

2.3.2. Soil model

In order to make the analytical method and finite element method comparable, choosing an appropriate soil model is essential. In this study, the model of Mohr Coulomb, a linear elastic perfectly plastic model, is chosen. The argumentation for this choice is included in finite element method section of Chapter 3. It would be interesting to find out what kind of soil model is most appropriate to simulate the behavior of clay with soil structure. However, this is outside the scope of this study.

2.3.3. The shear strengths reduction technique

The shear strengths reduction (SSR) technique is commonly used in finite element calculations for stability analyses. The factor of safety calculated from SSR employs the same definition, as it would be in limit-equilibrium methods. The factor of safety is a ratio of 'actual soil shear strength to the minimum shear strength required preventing failure (Cala, Fliksiak, and Tajdus, 2004). In this technique, the material shear strength is reduced progressively until the collapse of the soil body occurs.

Given an initial set of soil strength parameters (c and ϕ') and an initial factor of safety F (usually F=1.0 in the first iteration step), initial shear strength is calculated using the formula:

$$\frac{\tau}{F}=\frac{c}{F}+\frac{\tan\phi'}{F} \quad [11]$$

Then, the equation can be re-written as:

$$\frac{\tau}{F}=c^{*}+\tan\phi^{*} \quad [12]$$

Where:

$$c^{*}=\frac{c}{F} \quad [13]$$

$$\phi^{*}=\arctan\left(\frac{\tan\phi'}{F}\right) \quad [14]$$

These values of c* and ϕ* reduce with an increment of F through many iterations. The process of iterations continue until it reaches a set of values of c* and ϕ*, which are sufficiently small to cause the slope to unstable state. The value of F at this moment is the critical factor of safety, FOS. In order to have a clear procedure, the following paragraphs describe three basic steps for determining the critical factor of safety value.

Step 1: Develop a finite element model of a slope, entering deformation and strength properties. Then, compute the model and monitor the maximum total deformation in the slope.

Step 2: Increase the value of factor F, and recalculate the shear strength parameters, (c* and ϕ*), impute them into the model and re-compute. The maximum total deformation has to be recorded.

Step 3: Repeat step 2, using systematic increments of F, until the slope fails. This indicates that the FEM model does not converge to a solution. The critical value of F just above which failure occurs will be the factor of safety, FOS.

2.3.4. Limitations

Although FEM - Plaxis deals with engineering problems with a higher sophistication, it generally has its own disadvantages. The first drawback concerns the user's experience. Since the method can solve many sophisticated situations, there is a strong temptation to solve problems without doing hard work and understanding the underlying mechanics and physical applications. As a result, inexperienced users can make serious mistakes. Secondly, even though the approach has the advantage of simulating complex restraints successfully, this is still an approximation approach that has inherent errors. These errors include numerical errors, formulation errors, and discretization errors (Brinkgreve, Swolfs, and Engin, 2010). For example, as the accuracy of the solutions is partially the function of mesh resolution, any region of highly concentrated stress, for instances, regions around loading points and supports must be carefully analyzed with the use of a sufficiently refined mesh. Lastly, due to closed-form solutions, using FEM can be time consuming sometimes.

However, the mentioned considerations or limitations do not have considerable influence on our scope of work. Because the geometry profile in this research is not highly sophisticated, the error embedded with the simplicity can be negligible. In addition, the simplicity of investigated slopes decreases the possibility of making serious mistakes. Moreover, since the FEM is based on constitutive law (stress-strain relationship), the critical slip plane has been considered as the most critical one in comparison with other limit equilibrium methods (Krishna, 2006).

Chapter 3. Implementation

For decades, much attraction has been paid to the establishment of knowledge on the hydraulics of wave overtopping of dikes, levees, and embankments (Steendam, Van der Meer, Hardeman, and Van Hoven, 2010). In the current guidelines for safety assessments of dikes, the crest height may be of significant influence on the superficial stability of the downstream slope. However, the effect of crest height on the stability of cover layers has not received much investigation. This chapter aims to identify the quantitative pattern showing the effect of slope length and thickness of the cover layer on the superficial stability by applying three discussed methods.

3.1. Basic Profile

The figure below sketches out the geometrical feature of the inner slopes, with typical parameters: the width of dike crest (i.e. 5m); the thickness of the cover layer (D); the slope length (L); the slope angle (α); the slope height (H); and the width of the dike toe (i.e. 5m).

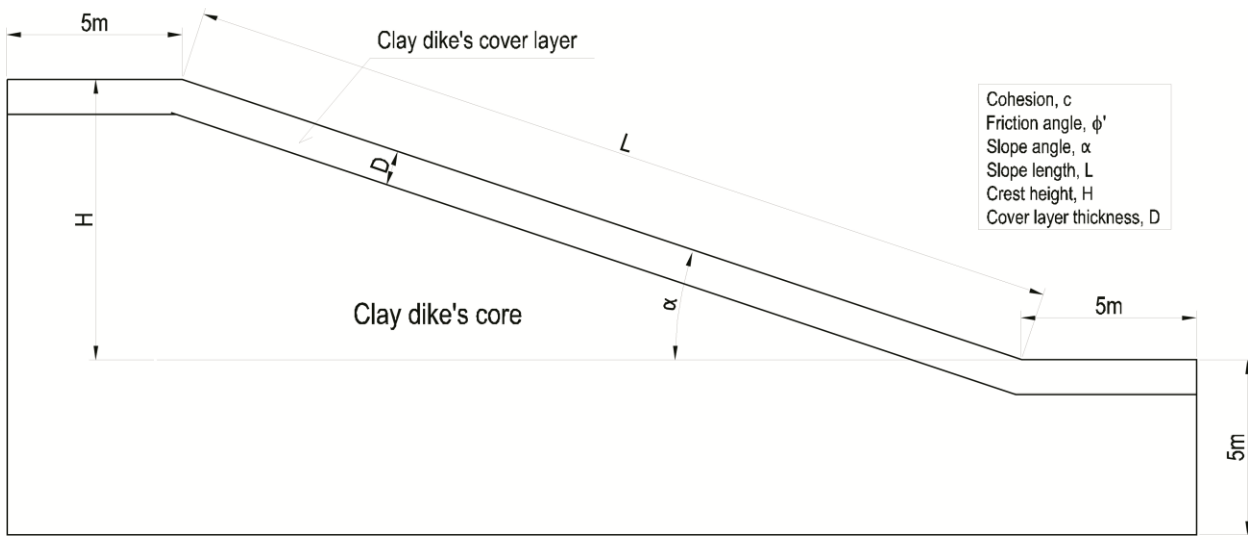

Figure 8. Basic model of inner slope cross section

From this basic model, the factors of safety for 150 different slope geometries are calculated for the purpose stated in the research approach. These cases differ from each other in terms of slope angle, slope height and thickness of the cover layer. The chosen values of the parameters (see Table 2) determine the range of this study, and 150 cases are the result of different combinations (H; D; α) made from those values.

Table 2. Variables range

Crest Height, H (m)	Thickness of cover layer, D (m)	Slope angle[2], α (1:x)
2	0.6	1V:1.5H
4	0.8	1V:2H
6	1.0	1V:2.5H
8	1.2	1V:3.0H
10	1.4	1V:3.5H
		1V:4H

In order to quantify the effect of slope length on the safety factor and avoid as many influencing elements as possible, similar material properties are applied to all 150 cases. The basic soil parameters are shown in Table 3. However, since the study uses three methods with different levels of sophistication, additional properties are carefully assumed and corrected when necessary, ensuring the comparability of those methods.

Table 3. Basic soil parameters

Layer 1: Clay cover layer	
Unit weight of water, γ_w :	9.81 kN/ m^3
Cohesion, c:	4.00 kN/ m^2
Friction angle, ϕ':	20.0 deg
Saturated unit weight of soil:	19.00 kN/ m^3
Layer 2: Clay core of dike	
Unit weight of water, γ_w:	9.81 kN/m^3
Cohesion, c:	15.00 kN/m^2
Friction angle, ϕ':	22.0 deg
Saturated unit weight of soil, γ_n:	21.00 kN/m^3

The clay core of the dike was assumed to be considerably stronger than the cover layer, to prevent deep sliding surfaces becoming critical in stability analyses.

[2] 1:x stands for the ratio of vertical dimension/horizontal dimension

3.2. Infinite Method – Edelman Joustra

With the basic parameters above, infinite method calculated the stability of 150 cases using equation [7] described in Chapter 2. A spreadsheet calculating the factor of safety of different situations is attached in Appendix 1. The equation indicates that the crest height H, therefore the slope length, has no influence on the safety factor in the safety criterion. In other words, different situations that share the same slope angle and cover layer's thickness, but different slope heights will have the same factor of safety. This is not the case when the models work with other limit equilibrium methods.

3.3. Spencer's Method – D Geo Stability

D Geo Stability software calculates the factor of safety of slopes using Spencer's theory of limit equilibrium. This is a convenient and suitable tool since it allows users to define and calculate the safety factor of non-circular slip planes. Although this method has a higher level of sophistication than Edelman Joustra's, strength parameters of the dike core are required for calculation models. However, this did not influence the factor of safety.

One concern is the state of ground water condition. To make the model in D Geo Stability comparable with Edelman – Joustra method, the assumption used in Edelman – Joustra calculation needs to be satisfied. This is done by changing the unit weight of water together with the slope angle in Spencer's models. By doing this, the ground water flow parallel to the slope surface is simulated to some extent. The corrected unit weight of water is presented in the table below. In addition, the phreatic line in these models is also set up to the level at which the soil is fully saturated. A specific calculation procedure with an illustrative example is depicted in Appendix 3.

Table 4. Correction of Unit weight of water

Slope angle, α (1:x)	Unit weight of water (kN/m^3)

1V:1.5H	8.16
1V:2H	8.77
1V:2.5H	9.11
1V:3H	9.31
1V:3.5H	9.43
1V:4H	9.52
Horizontal	9.81

3.4. Finite Element Method – Plaxis

Unlike previous methods, FEM method calculates the safety factor using the technique of shear strength reduction. In order to be able to implement this technique, the model requires the soil stiffness parameters for calculating the overall stability of the models. These stiffness properties are Young's modulus E, Poisson's ratios υ, and dilation angle ψ. The next paragraph will explain how these parameters are chosen as laid in Table 5.

Table 5. Soil parameters used in FEM

Layer 1: Clay top cover layer	
Unit weight of water, γ_w:	9.81 kN/m^3
Cohesion, c:	4.00 kN/m^2
Friction angle, ϕ':	20.0 deg
Saturated unit weight of soil, γ_n:	19.00 kN/m^3
Young's Modulus, E:	2000 kN/m^2
Poisson's ratio, v:	0.3
Gravity loadings, g:	9.81 kN/m^3
Dilation angle, Ψ:	20.0 deg

While there is no discussion about the soil strength parameters, the reasons for choosing the stiffness parameters above have been justified in this part. Because this study uses FEM method to check localized failure whereas the solution produced by Plaxis is always representing the global failure, in some cases the stiffness parameters of the core layer (i.e. Young's modulus E) has to be adjusted to avoid global failure slip planes going through the dike core. In addition, verification shows that Young's modulus E does not have significant influence on the safety analysis, although it accounts for the significant effect on deformations analysis and stress behaviors (Reginald, Thamer, Brent, and John, 2005). Similarly, Poisson's ratios have no influence on the safety factor. Chosen value of 0.3 is suitable for the soil type of clay.

In this soil model, the value of dilation angle is equal to the friction angle so that the infinite slope angle calculation and finite analysis satisfy the same associated flow rule, where the plastic potential is identical to the yielding surface in stress space. This value indicates that the soil mass changes its volume during the loading and reaches the maximum volumetric expansion limited by dilation angle. This also implies that the volumetric strain remains unchanged after the soil reaches the peak failure envelope (Yu-Jie, and Jian-Hua, Teunissen, and Spierenburg, 1995).

Furthermore, appropriate iterations and the magnitude of tolerance need to be figured out so that more precise and reliable results can be obtained. Experience acquired from literature has shown that the predicted factor of safety is insensitive to the form of gravity application when using elastic-perfectly plastic Mohr-Coulomb models (Griffiths, and Lane, 1999). Therefore, the value of 9.81 is used as default. These relevant parameters are used in calculation models of 150 cases. One demonstrative description of its application is in Appendix 4.

In general, the results calculated from finite element method (Plaxis) are more or less equal to that in Spencer's. The factors of safety of 150 situations are discussed in verification section of Chapter 5.

Chapter 4. Comparison and Improved Method

In preceding chapters, we described the implementation of three different methods so that the factor of safety can be determined. This chapter will use the calculated results to make a comparison between Edelman – Joustra method and Spencer method, which shows a clear distinction between the infinite and finite analysis in a function of slope length and the thickness of the cover layer. From this basis, an improved method adapted from Edelman – Joustra equation is formulated.

4.1. Comparison

Our aim is to see how the slope length determines the difference in safety factors between two calculation techniques. As such, we decided to present their difference in the ratio of FOS_S over FOS_{E-J}, of which FOS_S is the factor of safety calculated from Spencer's procedure whereas FOS_{E-J} represents the factor of safety derived from Edelman-Joustra's equation. Five following figures visualize the gap between two methods under different thickness of covers layers. All these 5 figures show a similar trend in which the gap is large when the slope length is relatively short and smaller when the slope length becomes longer. It is likely that they will converge if the slope length reaches a certain critical value.

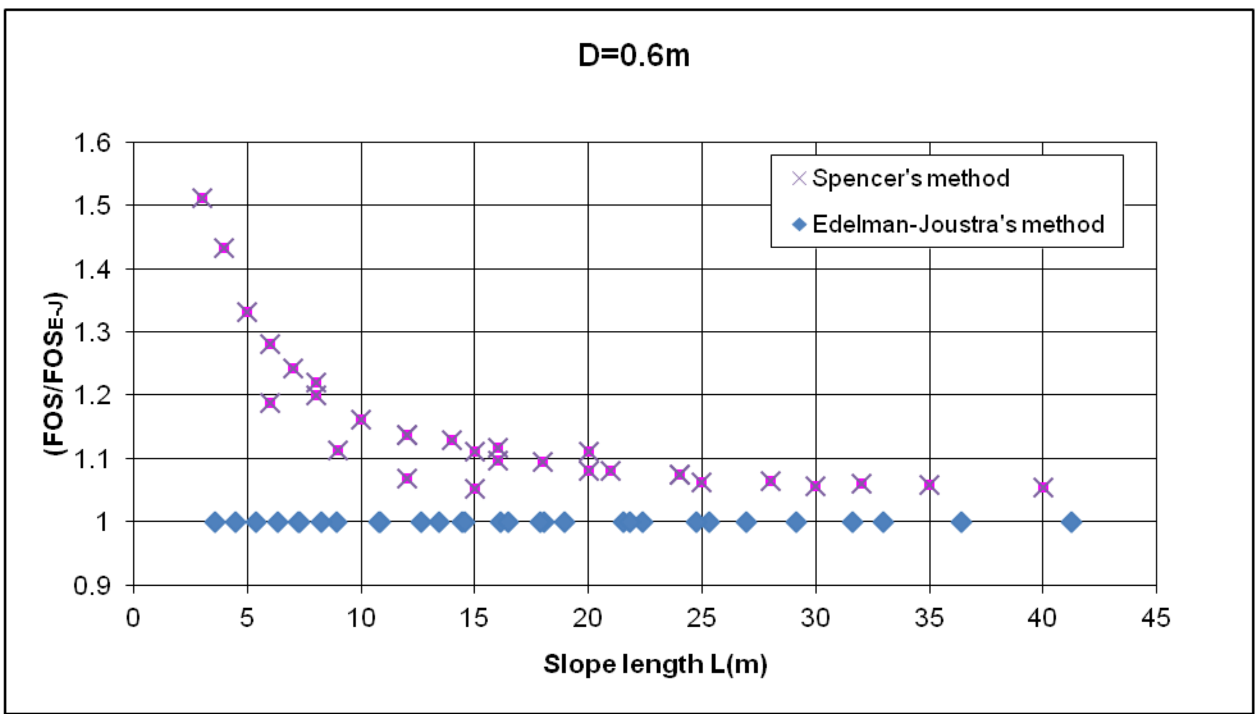

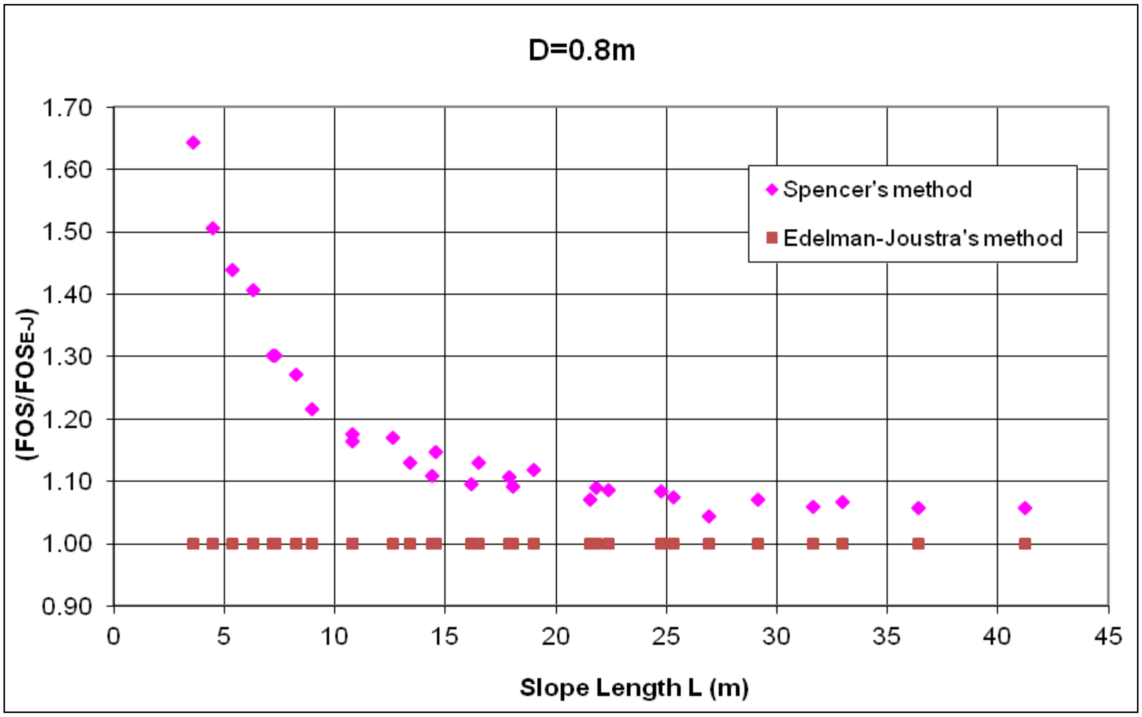
D=0.8m
(FOS/FOS$_{E-J}$)
Slope Length L (m)
Spencer's method
Edelman-Joustra's method
1.70
1.60
1.50
1.40
1.30
1.20
1.10
1.00
0.90
0
5
10
15
20
25
30
35
40
45

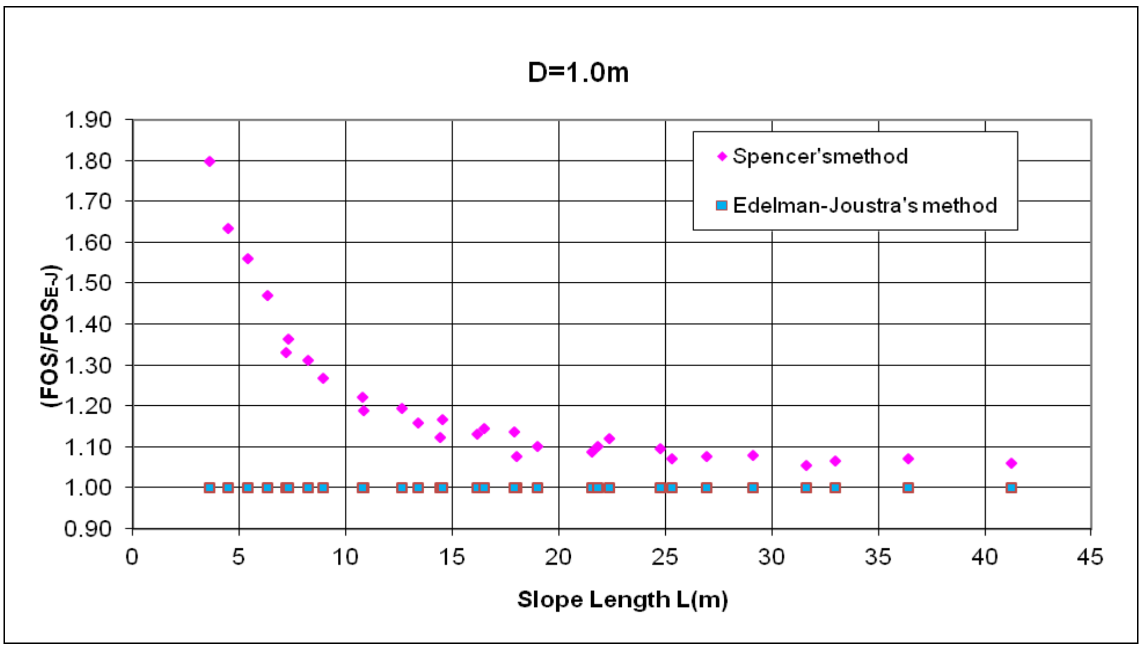
D=1.0m
(FOS/FOS$_{E-J}$)
Slope Length L(m)
Spencer'smethod
Edelman-Joustra's method
1.90
1.80
1.70
1.60
1.50
1.40
1.30
1.20
1.10
1.00
0.90
0
5
10
15
20
25
30
35
40
45

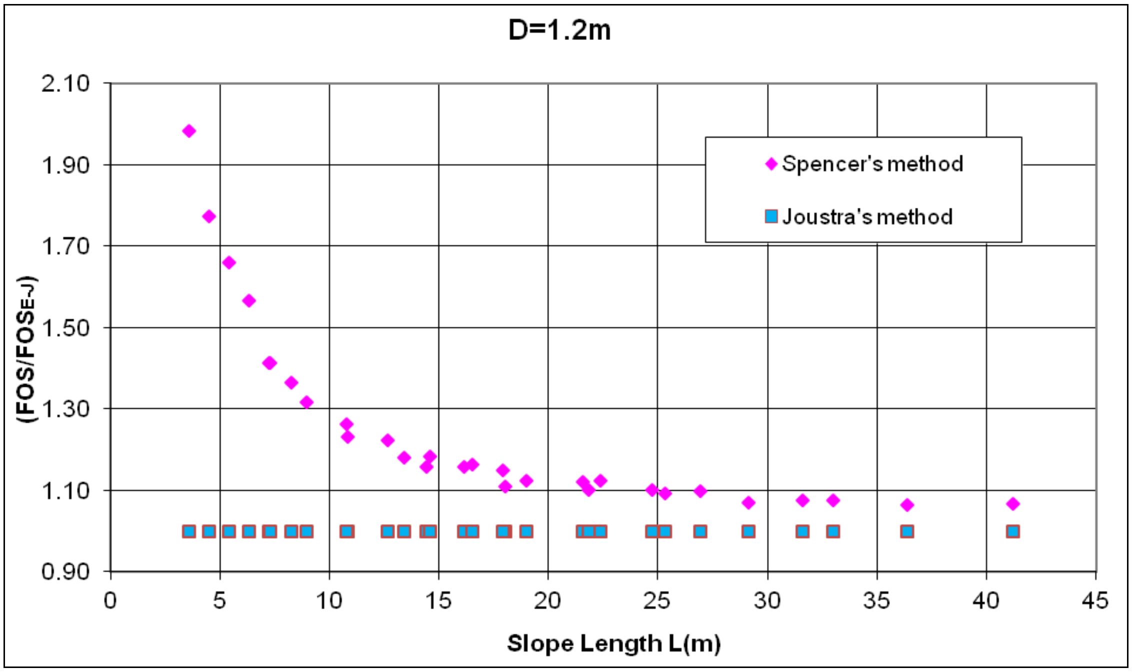

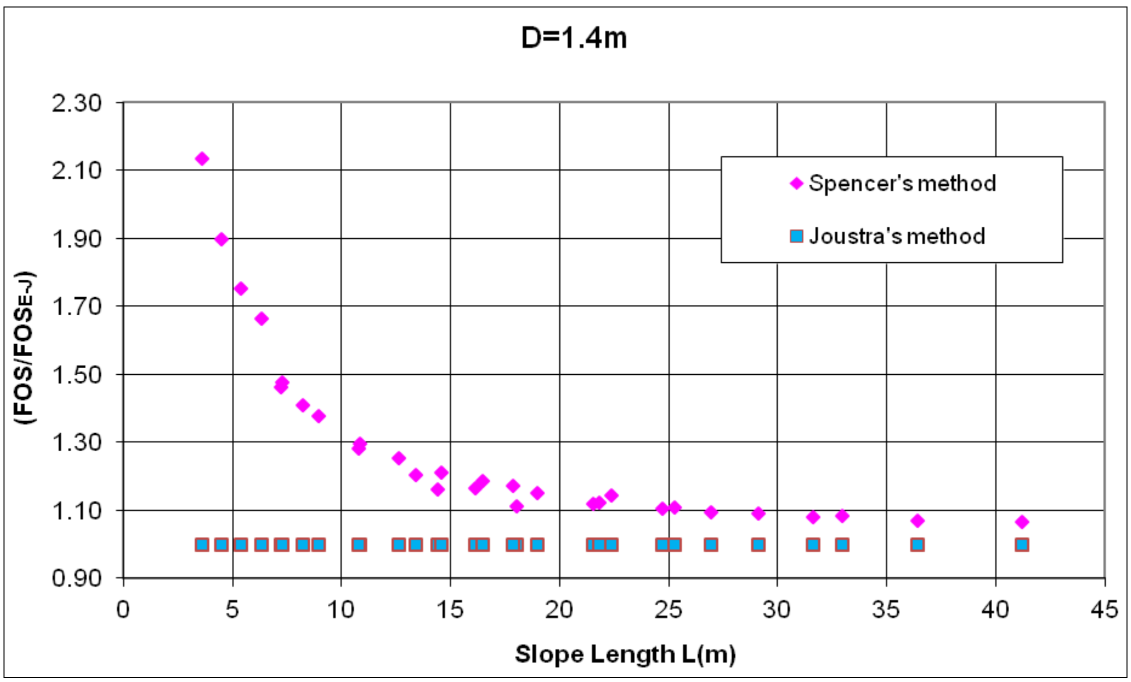

4.2. Improved Method

As seen in the comparison part above, there is always a gap between two types of factor of safety, depending on the magnitude of slope length. We then try to predict a rule for this kind of effect. Generally, Figure 9 shows that the two methods differ by 5% when the value of L/D is larger than 25, and when the ratio of L/D varies from 10 to 25, the difference is fluctuating over 10%. According to this effect, two improved functions are introduced in next paragraphs.

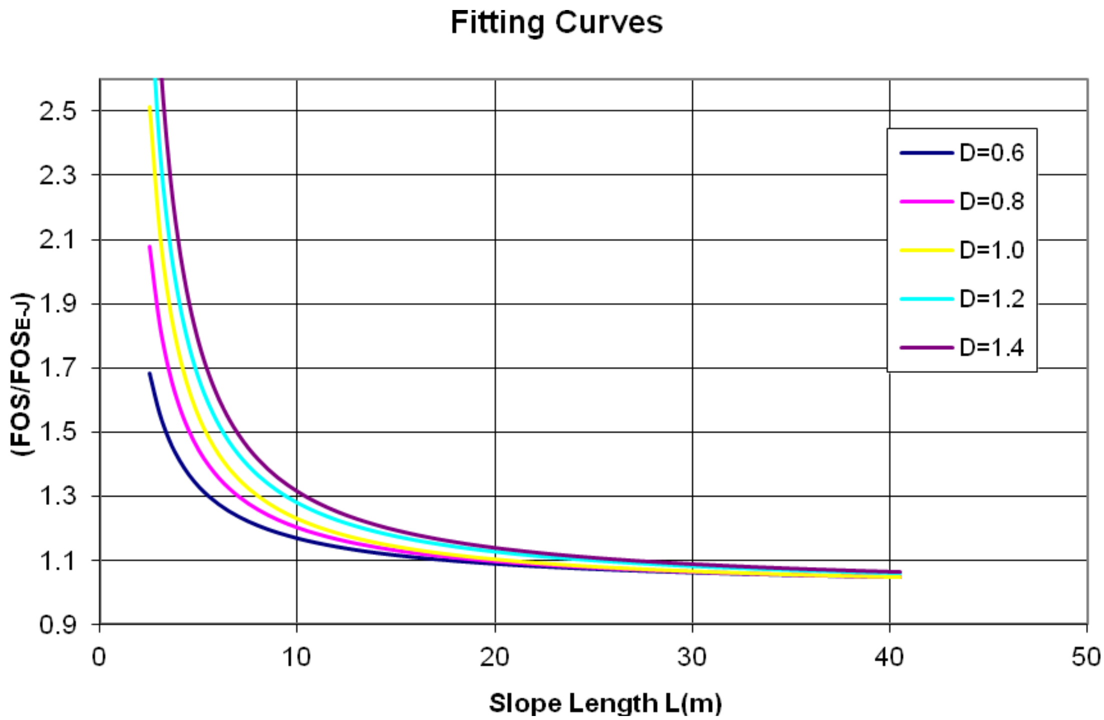

Figure 9. Prediction curves with different thickness of cover layer

4.2.1. Improved function 1

Five lines with different colors in Figure 9 are predicting curves formulated from the previous comparison. They represent five values of layer thickness, which make the relationship between slope lengths L, ratio of safety factor, and layer thickness d likely to be a three-dimensional function (see Figure 12). Therefore, we first identify the pattern of the slope lengths' effect at every value of depth. The second step is determining the effect of thickness of the cover layer through a coefficient a. The predicting function is as follows:

$$FOS_{imp1}=a.f(L).FOS_{E\text{-}J} \quad [15]$$

$$f(L)=10^{(0,5023.L^{-0,874})} \quad [16]$$

$$FOS_{imp1}=a.f(L).FOS_{E\text{-}J}=a.10^{(0,5023.L^{-0,874})}.FOS_{E\text{-}J} \quad [17]$$

a is a coefficient depending on the thickness of the cover layer for a certain slope length. This coefficient can be obtained using the chart below.

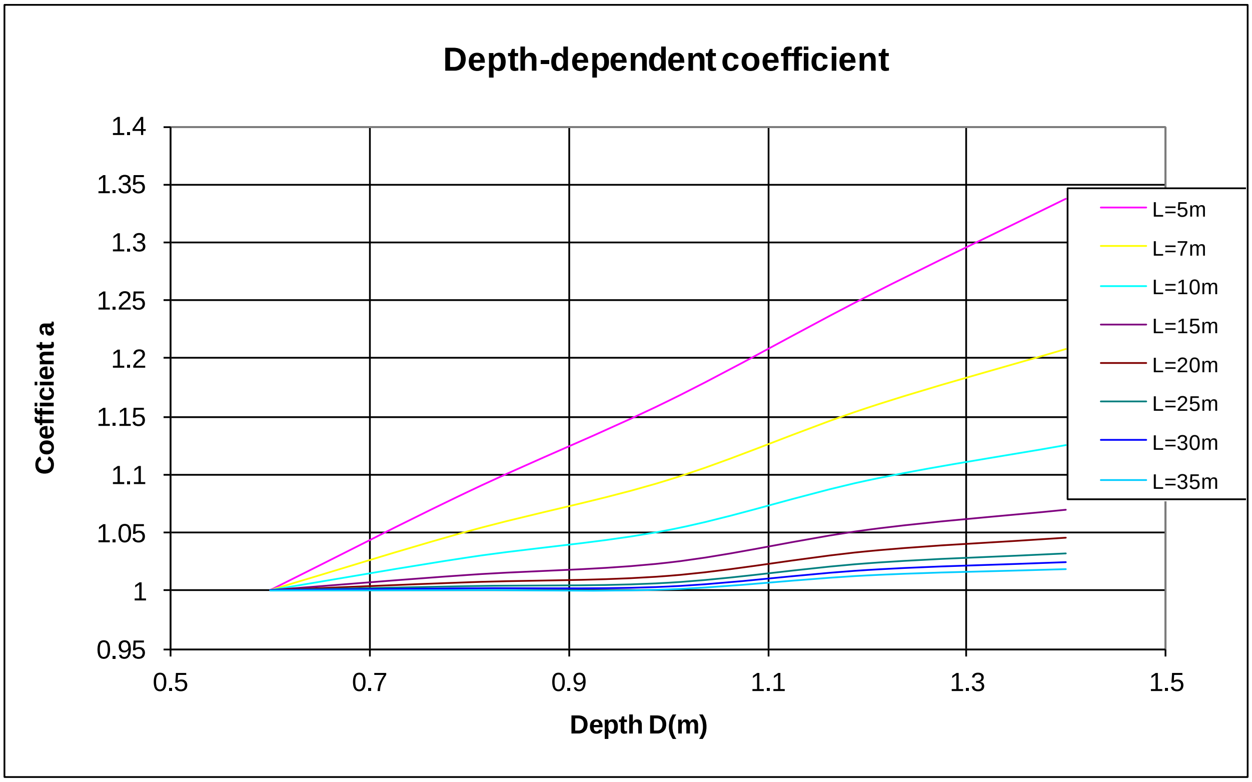

Figure 10. Depth-dependent coefficient a

4.2.2. Proposed function 2

The purpose of this part is to give a shorter predicting function of the effect of slope length and cover layer thickness. As seen in improved function 1, the improved method discussed above is still complicated to some degree because users have to account for slope length and thickness of the cover layer separately. An attempt to incorporate two parameters into the ratio of L/D is made so that the difference between infinite stability and finite stability – correlation ratio, C_r - is determined in only one function. After making a number of trials and errors, the predicting function is realized as follows (Figure 11):

$$C_r = 5.25(L/D)^{-2}+1.38(L/D)^{-1}+1.01 \qquad [18]$$

In this figure, the blue points represent the raw data, which are the ratios of the Spencer 's safety factors to the safety factors calculated from Edelman – Joustra method. The purple line is the predicting curve representing the quantitative effect of (L/D). This function is conservative since it lies below most data points. Some points lying below the line are invalid data (explained in 5.1.).

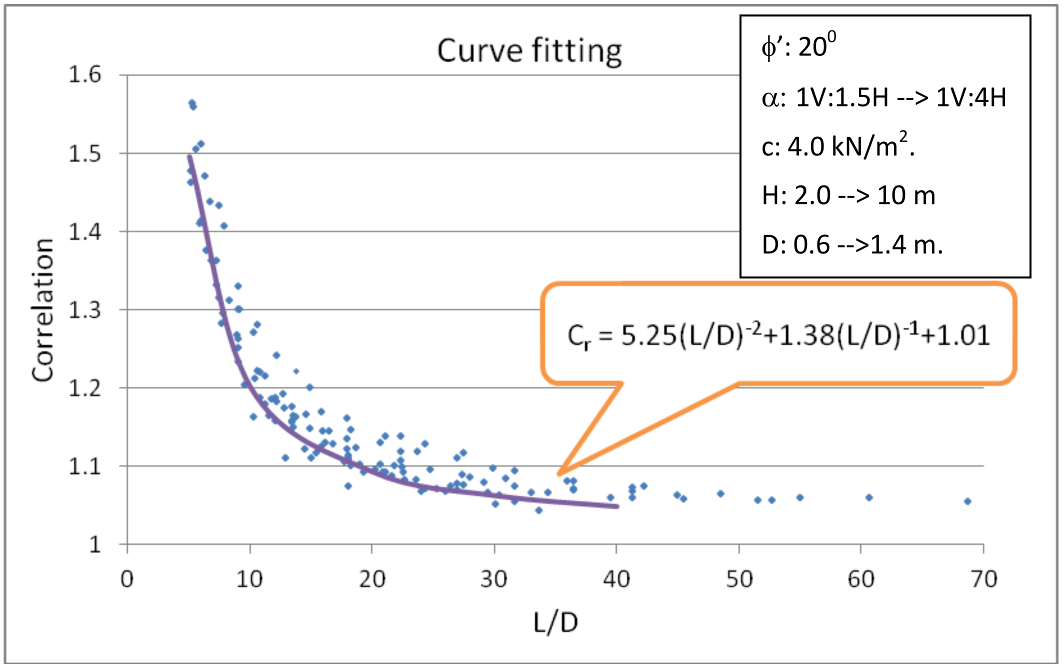

Figure 11. Improved function 2

A similar procedure of validation is done to underpin the predicting function. This results in a reasonable outcome as well, which shows that the function works well on cohesive soil or clay-dominated soil with an error less than 5%. A 10% difference is recognized for c-ϕ' soil considered as sand dominant. The indicator used to distinguish between two types of soil is the ratio of $c/(\gamma'.D.\tan\phi')$ (see Appendix 6). Relatively, if this ratio is larger than 1.05, the soil property is considered as cohesion-dominated.

Furthermore, this function is valid in case of L/D smaller than 25 for all types of soil with a maximum error of 10%. A random parameter exploration showed that when L/D is greater than 25 the infinite stability and finite calculation converge with an error of 5 % (Milledge, Griffiths, Lane, and Warburton, 2010). This is also in line with the findings described in the figure. When the number of random calculations increases to 1000, the smallest difference is just over 2%.

4.2.3. Proposed assessment procedure

- Calculate factor of safety using Edelman – Joustra function

$$FOS_{E\text{-}J}=\frac{\tau_c}{\tau_o}=\frac{c+\left(D.\gamma_n.\cos\alpha\text{-}D.\gamma_w.\cos\alpha\right)\tan\phi'}{D.\gamma_n.\sin\alpha} \quad [19]$$

- Apply the equation [16] or [18] to derive the influence of slope length or L/D on the safety factor,
- In case of using function [16], with the given slope length, the effect of top layer's depth is obtained using the chart of coefficient a.
- Calculate new improved factor of safety:

$$FOS_{imp1}=a.f(L).FOS_{E\text{-}J}=a.10^{(0,5023.L^{-0,874})}.FOS_{E\text{-}J} \quad [20]$$

Or

$$FOS_{imp2} = C_r.FOS_{E\text{-}J} = \left(\frac{5.25}{(L/D)^2} + \frac{1.38}{(L/D)} + 1.01 \right).FOS_{E\text{-}J} \quad [21]$$

Figure 12 gives an overview of how the improved function looks like in 3 dimensional space. The images on the left shows the real pattern representing the difference between Spencer method and Edelman – Joustra method, while the middle visualizes the pattern is smoother when the improved function is used. The last graphs gives the smoothest pattern with high level of correction, which makes the value of R^2 get closer to 1.

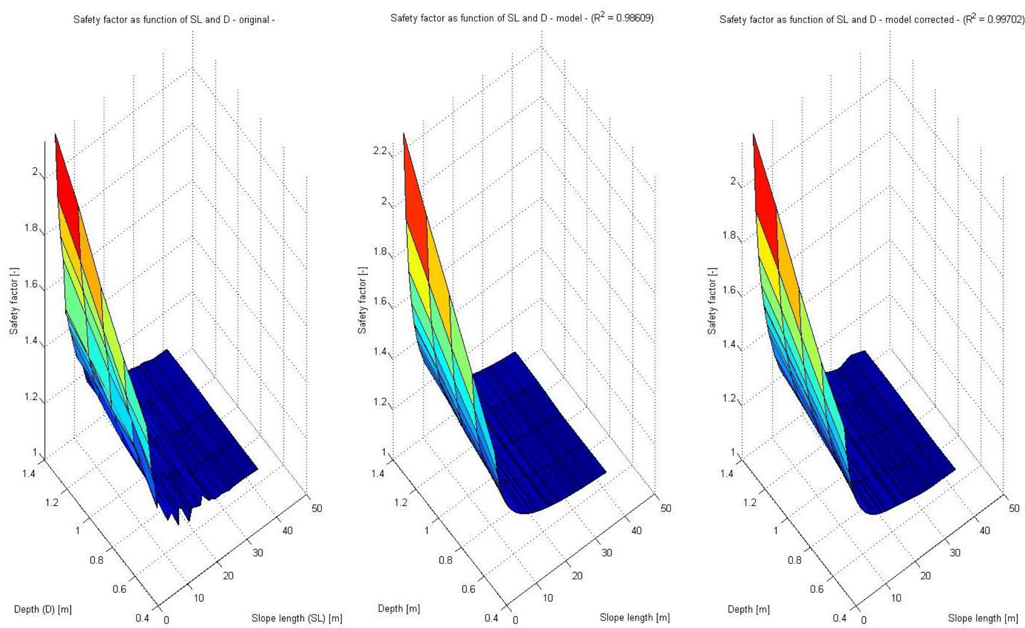

Figure 12. Illustration

4.2.4. Suggestion guidelines for dike safety assessment

For the purpose of application, it is wise to indicate where the improved method can be placed on the current statutory assessment guideline. Figure 13 gives a general guideline for implementing the improved method in practice. This guideline is adapted from the procedure described in TAW 2001. Given a minimum set of soil strength parameters defined for Edelman – Joustra method, safety criterion is checked, based on Edelman – Joustra criterion. Then, the improved method can be executed if the previous criterion is not met. The procedure to implement the improved method is stated in previous section 4.2.3.

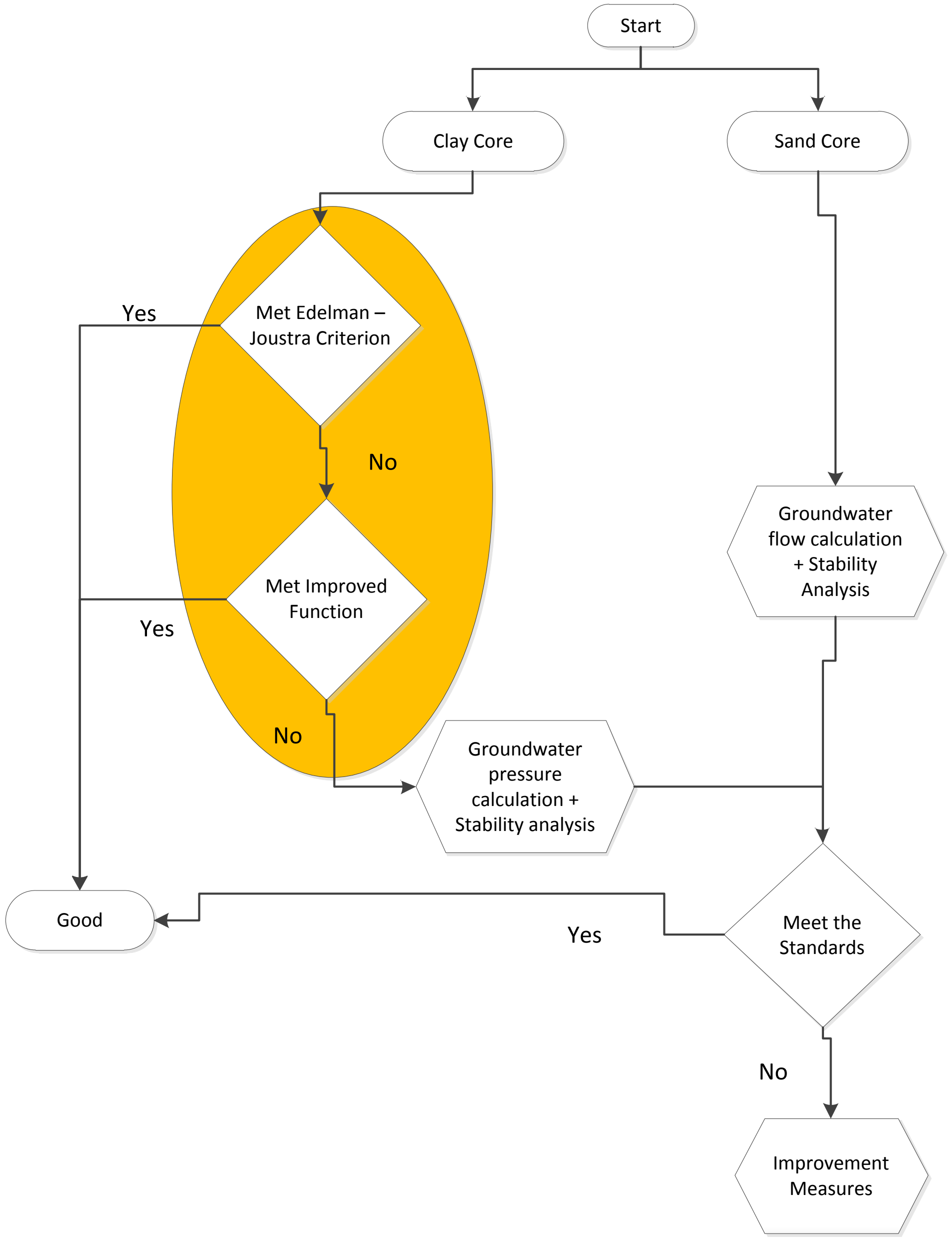

Figure 13. Stability diagram analysis for superficial sliding due to infiltration

Figure 14 specifies the scope of the application in terms of safety criteria. The added criterion is "1V:3H and moderate clay". The term "moderate clay" is defined statutorily in NEN 9997 – Table 2b. Specifically, if given a slope angle of 1V:3H, the soil of the cover layer is characterized as moderate clay, it will be safe to superficial sliding mechanism, irrespective of the thickness of the cover layer. Similar calculations were done with other soil types to figure out possible L/D limitations at which 'detailed analysis' and 'advanced analysis' can be avoided.

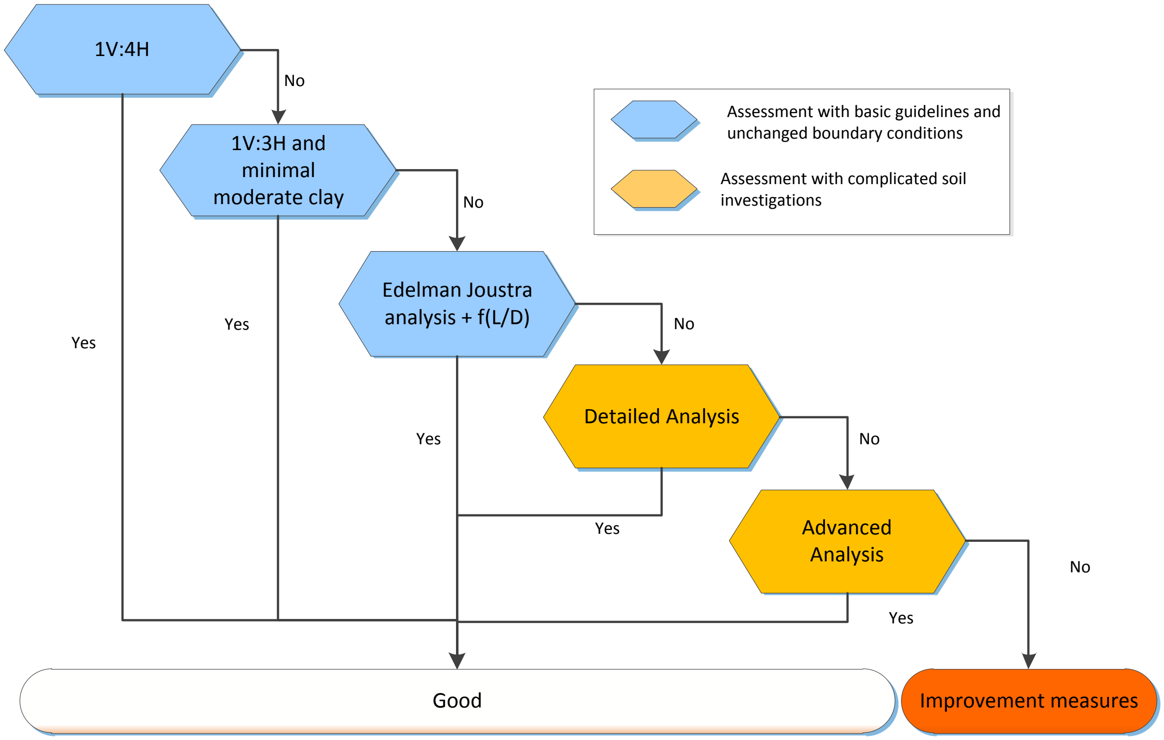

Figure 14. Assessment Sophistication levels

According to NEN 9997, the soil of the cover layer can be classified into seven types. The classification is made based on Atterberg limits. The first limit is the plasticity limit, which indicates the water content required to make a soil change its state from solid to plastic. To determine this water content, a simple test is conducted. First, water is added to a soil sample little by little. Then, a tester will make a thread of soil with length of 4 cm. The thread is rolled between one's two hands until its diameter is about 3mm without any crack or fissure on the surface of the thread. The water content at this point is the plastic limit.

About the liquid limit, this is an important indicator since it makes a distinction between the plastic state and liquid state of a soil. The water content at this point can be identified by using Cassagrande test. The procedure for identifying the liquid limit is as follows. A pat of clay is mixed up with water and placed into a round-bottomed cup, and it is called Cassagrande cup. A groove is cut through the pat of clay with a specialized spatula of 13.5-milimeter width. Then, the cup is dropped repeatedly many times until the groove is closed. The water content at which the groove on the soil sample is closed after 25 drops determines the liquid limit. From these laboratory tests according to ASTM, basic strength parameters are defined as seen in the table below.

No.	*Soil type description*	*Unsaturated unit weight (kN/m^3)*	*Saturated unit weight*	*Cohesion (kN/m^2)*	*Friction angle (deg)*	*Cohesion reliability class (-)*	*Friction reliability class (-)*
1	Clean, soft clay	14	14	0	17.5	1.3	1.6

2	Clean, moderate clay	17	17	5	17.5	1.3	1.6
3	Clean, stiff clay	19	19 – 20	13	17.5	1.3	1.6
4	Loose clay, small proportion of sand	15	15	0	22.5	1.3	1.6
5	Moderate clay, small proportion of sand	18	18	5	22.5	1.3	1.6
6	Stiff clay, small proportion of sand	20 – 21	20 – 21	13	22.5	1.3	1.6
7	Clay, very much sand	18 – 20	18 – 20	0	27.5	1.3	1.6

With these seven types of soil, the Edelman – Joustra equation is used to assess the stability of inner slopes, given a certain slope angle and thickness of the cover layer. If the E – J condition is not satisfied, the improved function of L/D is applied to see which magnitude can bring the situation from unsafe state to safe one. To do this, a number of iterations are done to search for the largest L/D ratio that determines the point at which the slope starts to be unsafe. The procedure worked with three different slope angles (namely, 1:2.5, 1:3, and 1:3.5) and three different thicknesses of the cover layers (0.8m, 1.0m, and 1.2m). The results are shown in the figures below.

The results showed that, for the soil type 1, 4 and 7, the calculated outcomes are unrealistic since the slope length should be quite short to make the dike safe. Soil type 2 and 6 are the scope of possible improvement. From those figures, if the thickness is about 0.8m, a dike with a slope angle of 1V:3H can be safe at rather long slope length. This means that there may be a number of dike sections falling into this category and more complicated stability analyses can be saved. Together with the illustrative example, a statistic of geometry of 53 dike rings (see in section 7.2) gives some arguments for this possibility.

SAFETY CRITERIA FOR LANDWARD SLOPE (D=1.2M)			
Soil Type	Slope angle (1:x)		
	1:2.5	1:3	1:3.5
	L/D	L/D	L/D
1	< 1.09	< 1.23	< 1.37
2	< 3.57	< 4.78	< 6.9
3	With any	With any	With any
4	< 1.47	< 1.69	< 1.92
5	< 4.32	< 6.37	< 11.47
6	With any	With any	With any
7	< 2.25	< 2.73	< 3.32

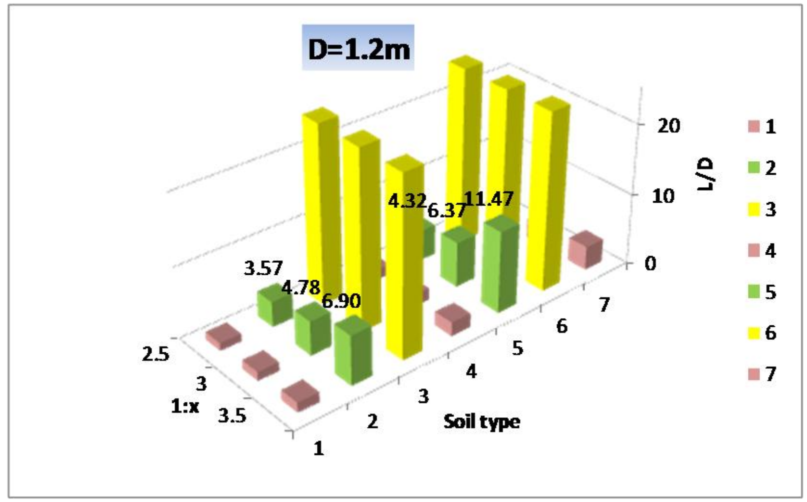

SAFETY CRITERIA FOR LANDWARD SLOPE (D=1.0M)			
Soil Type	Slope angle (1:x)		
	1:2.5	1:3	1:3.5
	L/D	L/D	L/D
1	< 1.09	< 1.23	< 1.38
2	< 4.32	< 6.3	< 11.1
3	With any	With any	With any
4	< 1.46	< 1.69	< 1.92
5	< 5.29	< 8.94	< 29.91
6	With any	With any	With any
7	< 2.25	< 2.73	< 3.33

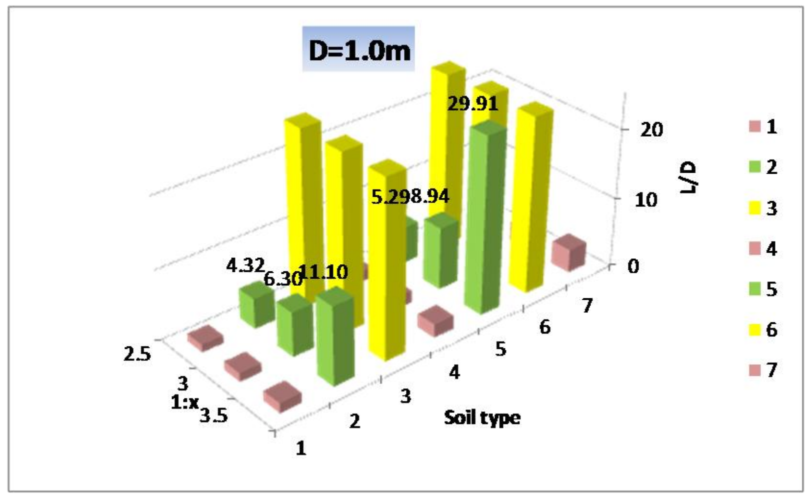

SAFETY CRITERIA FOR LANDWARD SLOPE (D=0.8M)			
Soil Type	Slope angle (1:x)		
	1:2.5	1:3	1:3.5
	L/D	L/D	L/D
1	< 1.09	< 1.22	< 1.37
2	< 6.02	< 11.49	< 37.49
3	With any	With any	With any
4	< 1.46	< 1.69	< 1.92
5	< 7.69	< 23.2	< 37.49
6	With any	With any	With any
7	< 2.25	< 2.74	< 3.32

	Unrealistic as very small L/D
	Safe with acceptable range of L/D
	Safe in any L/D

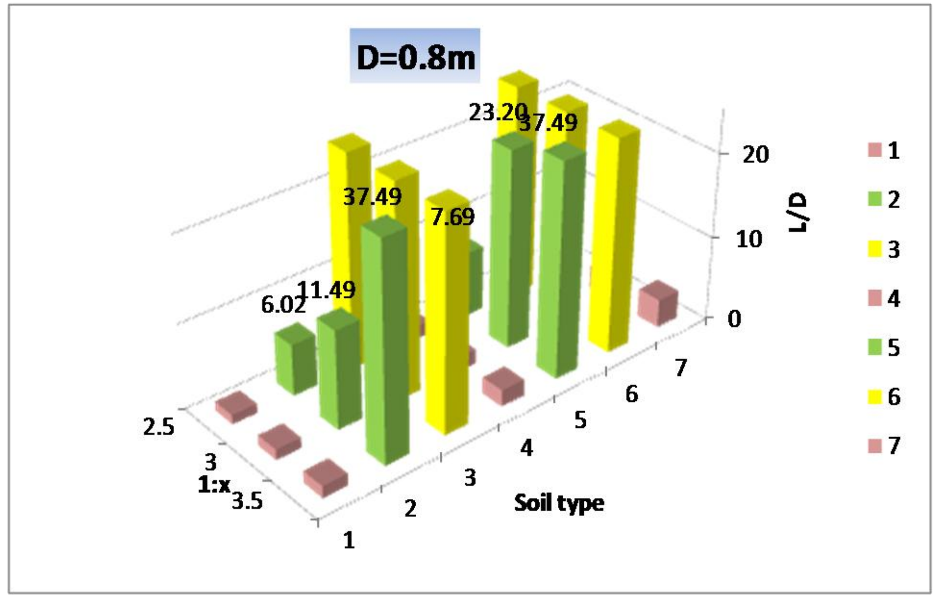

Illustrative example:

Given a slope of a clay dike, the top cover layer is in saturated condition and the factor of safety needs to be calculated. Site investigation supplies shear strengths and soil parameters as follows: H= 7; c =4.00 kN/m^2, phi =25.0^0, D = 1.0 m, alpha = 1V:3H; γ_n = 20.00 kN/m^3, γ_w = 9.81 kN/m^3.

Calculate the factor of safety of this slope.

Solution:

The factor of safety calculated using the function of Edelman – Joustra method is:

$$FOS_{E\text{-}J}=\frac{\tau_c}{\tau_o}=\frac{c+\left(D.\gamma_n.\cos\alpha\text{-}D.\gamma_w.\cos\alpha\right)\tan\phi'}{D.\gamma_n.\sin\alpha}$$

$FOS_{E\text{-}J}$ = 1.13

L= 22.13m

$$f(L)=10^{(0{,}5023.L^{-0{,}874})}=10^{(0{,}5023*22.13^{-0{,}874})}=1.082$$

$$f(L/D)=\frac{5.25}{(L/D)^2}+\frac{1.38}{(L/D)}+1.01 = 1.084$$

Coefficient a =1.01

Factor of safety improved:

FOS_{imp1} = 1.13*1.08*1.01 = 1.23

FOS_{imp2} = 1.13*1.084 = 1.22

These factors of safety meet the required safety for the Edelman – Joustra method (namely, 1.21) using design values of shear strength parameters. It proves that the upgraded result turns out to be an acceptable safety assessment. . From now on, the term “improved method” implies the use of the improved function [21].

Chapter 5. Verification and Validation

5.1. Verification

The purpose of verification is to prove the study conclusion to be reliable. In this part, the improved function is verified in two steps: checking the accuracy of the results calculated by Spencer itself; and the comparison in safety factor between Spencer method and finite element method.

With respect to the first step, the predicting line in Figure 11 lies above some raw data points, which show that, predicted safety factors can be higher than real solutions. This can happen in reality when this predicting function is applied (discussed in section 7.2.). However, in the sense of formulating the predicting line, this does not mean that the proposed function does not work on safe side. These data points are ignored since they are unreasonable solutions of the Spencer calculation. The geometrical information of these points is presented in Table 6. The cases show that when the slope angle is high, care should be taken into the safety factor since Spencer method due to calculations may not give acceptable solutions. According to the method of generic algorithm used in Spencer's method, the thrust line should be inside the collapsed soil body to give a sound solution; otherwise, the result is questionable (Trompille, and Eerninck, 2011). A check of physical slip planes of these situations is unlikely to show good solutions. This is also a limitation associated with convergence problems in Spencer-like calculation. Therefore, the prediction lines excluded these data points in the formulated function, and these cases should be excluded when using the improved method. It is noted, however, slopes of 1:1.5 are extremely rare in primary dikes in The Netherlands and the improved method limitation for 1:1.5 slopes has therefore little effect on the improved method efficiency and effectiveness.

Table 6. Situations give questionable solutions

Slope length (L)	Safety factor (-)	Slope angle (1:x)	Slope Height (m)	Depth (m)
7.21	1.19	1.5	4.0	0.6
10.82	1.14	1.5	6.0	0.6
14.42	1.07	1.5	8.0	0.6
18.03	1.05	1.5	10.0	0.6

About the second step, a comparison between finite element method and analytical method showed that data used to upgrade Edelman – Joustra method is reliable enough. Resultant tables (seen in Appendix 5) points out that the difference in value between two types of calculation varies from -6% to 9% (see Figure 15). The reasons for this difference are elaborated in section 5.2.3; and it indicates a significant value for ensuring the reliability of FOS formulated from Spencer method.

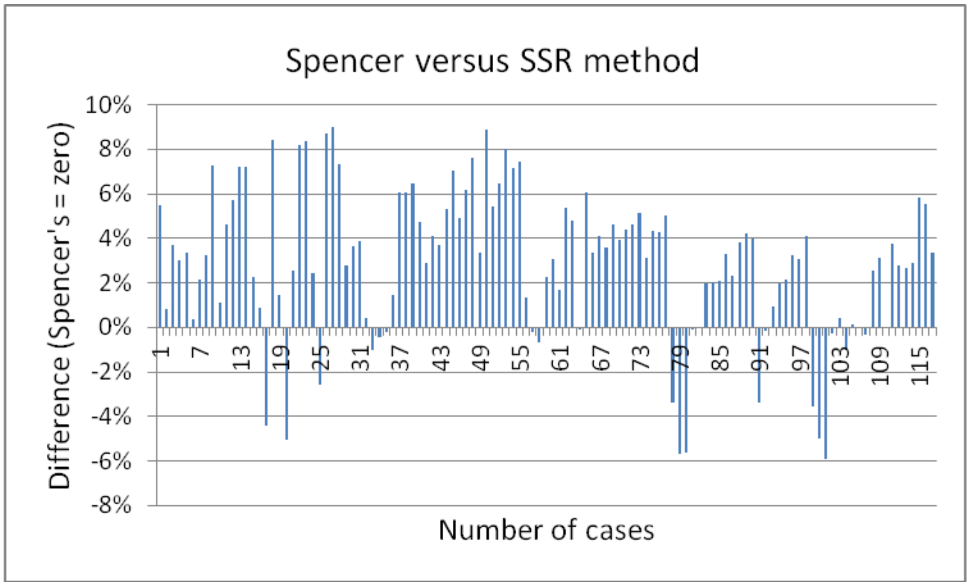

Figure 15. Difference between SSR method and Spencer method

To conclude, a dike with a slope angle of 1V:1.5H usually gives large differences in factor of safety between methods. These solutions are unreasonable when being combined with thin cover layers. As implicitly stated in section 4.2, this limit is not considered as relevant since it yields large divergence with low ratio of L/D.

5.2. Validation

Along with verification, validation contributes for an important part to the value of the research findings that facilitate the application of the improved method in practice. By definition, the validity gives an indication that the methodology has measured exactly what was intended to measure (Paul, and Jeanne, 2010). Up to now, the work of quantifying the L/D effect on the stability is finished. Therefore, the remaining issue relates how accurate the result produced by the method is, compare to other existing methods. This part tackles the issue in three following aspects, respectively: the agreement between the improved method with experiments results; the agreement between the improved method and current analytical method – Spencer method; agreement between the existing Spencer method with finite element method.

5.2.1. The agreement between the improved method with experiments

Since validity can take different forms depending on the importance of situations, the three aspects mentioned above can be regarded as the multitrait-multimethod approach (Paul, and Jeanne, 2010) where only one characteristic of the improved method (the factor of safety) is measured using three different ways. In this first aspect, the factors of safety calculated by the proposed assessment are compared with the real experiments' results derived from back analysis cases in geotechnical literature (Crabb, and Atkinson, 1991). The data from these back calculations (see in Table 7) imply that such soil parameters as cohesion, friction angle lead to the safety factor of 1. Case 1 and Case 2 were landslides occurring in UK due to rainfalls. Laboratory tests simulated similar failure condition on the soil at those locations of to find out the strength parameters. Case 3 is a field test conducted in California and Case 4 was a field experiment conducted by Deltares in the Netherlands. The improved method then uses these material properties to re-calculate the safety factors using the proposed procedure. The results are plotted in Figure 16.

Table 7. Experiment profiles

Parameter	Unit	Case 1: Cambridge – A45	Case 2: M26-Wrotham	Case 3: Santa Cruz County, California	Case 4: Afsluitdijk
Cohesion	kN/m^2	0.0	0.0	0.2	3.5
Friction angle	deg	23.0	23.0	25.0	30.0
Crest height	m	7.8	6.7	8.0	2.8
Slope angle	deg	27.00	17.00	16.00	21.04
Layer thickness	m	1.5	1.3	1.4	1.1
Density of soil	kN/m^3	18.50	18.50	20.00	21.50

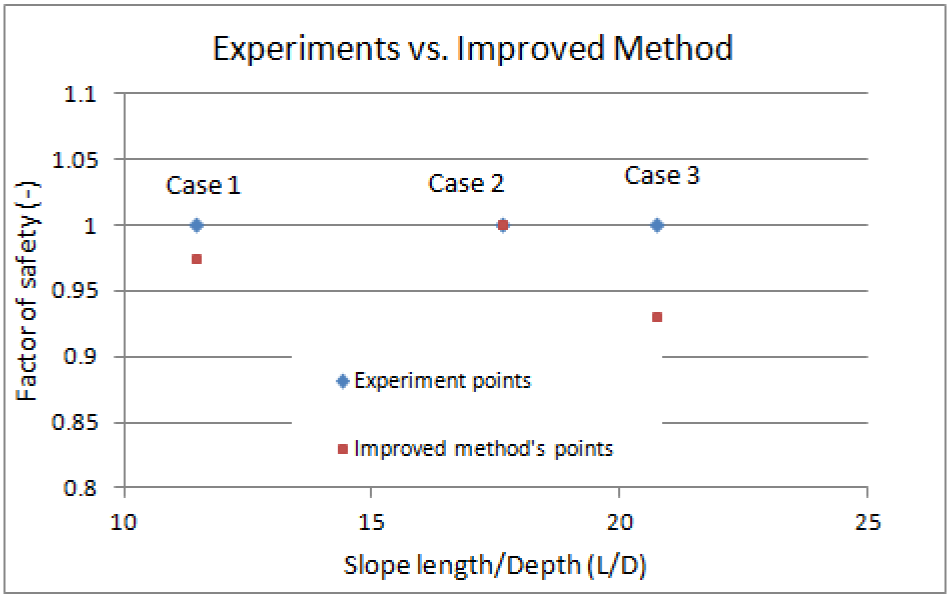

Figure 16. Difference between Experiment and improved method

Although there are a limited number of experiment results, the safety factors of improved method are relatively close to unity. This indicates that the error margin of the proposed method is fluctuating less than 10% around the right solution. This difference can account for the measurement of pore water pressure in those situations and the conservative prediction in the proposed function. For instances, the magnitude of pore water pressure was not constant when being measured at different positions. Average value was calculated from those data. In addition, Case 4 – the experiment of Afsluitdijk – is not plotted here due to the slope did not fail at the end of the experiment. Chapter 6 will be spent to study this case in details.

5.2.2. The agreement between Improved method and Spencer method

The improved method is originally formulated based on fixed shear strength parameters (the same c – ϕ' values), which mainly represent clay soil properties. Therefore, a major question is that to what extent the improved method or function works properly under various of cohesion and friction angle values. This concern is well-grounded from the result of a sensitivity analysis shown in Figure 17. As seen in the figure, changes in cohesion gives a higher influence on the safety factor than changes in friction angle. If so, the improved method may encounter a limitation when it is applied to different situations for the purpose of generalization. For instances, the limitation associated with large ranges of cohesion can be one of major concern since it can amplify the divergence between the improved method and Spencer method.

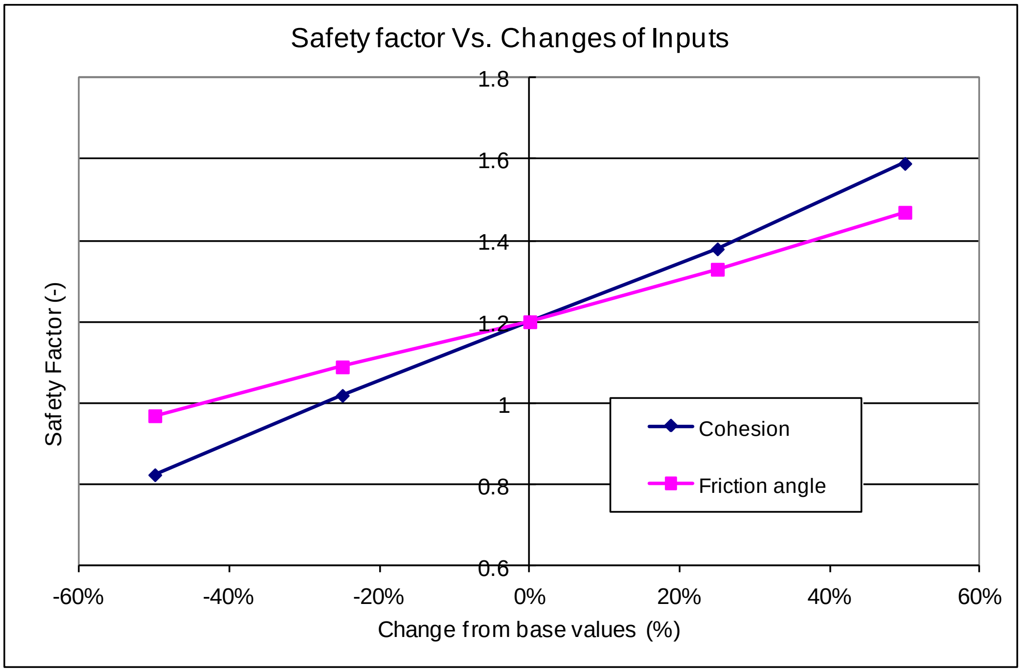

Figure 17. Sensitivity of Inputs on Stability

In order to check the limitation above, more than 60 cases are formulated, which focus only on the variability of cohesion and friction angle values. Their safety factors are calculated using both improved method and Spencer method (results plotted in Figure 18). This figure shows that the difference between two methods increases with a decreasing cohesion value. In other words, if the soil has less cohesion, the improved method gives a less accurate value compared to Spencer method. The relative difference in form of percentage is compared in

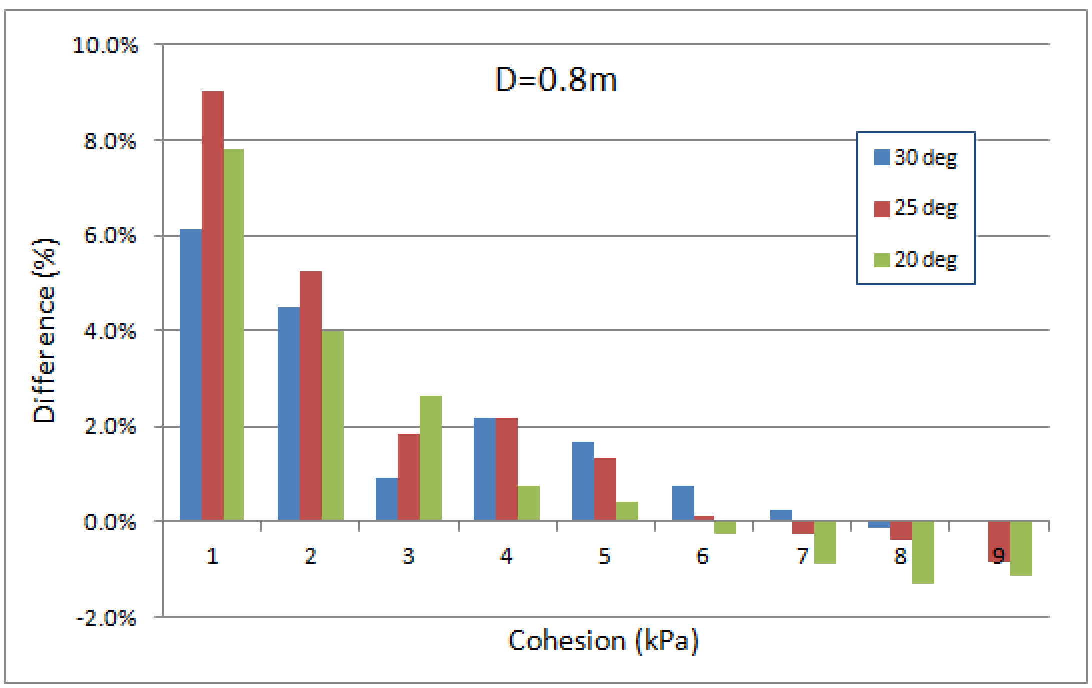

Figure 19, Figure 20. In these two figures, the factor of safety of the improved method is considered as the reference and lies on 0%. The difference is then calculated using the following function:

$$\%=\frac{(FOS_{imp}-FOS_{Spencer})*100}{FOS_{imp}} \quad [22]$$

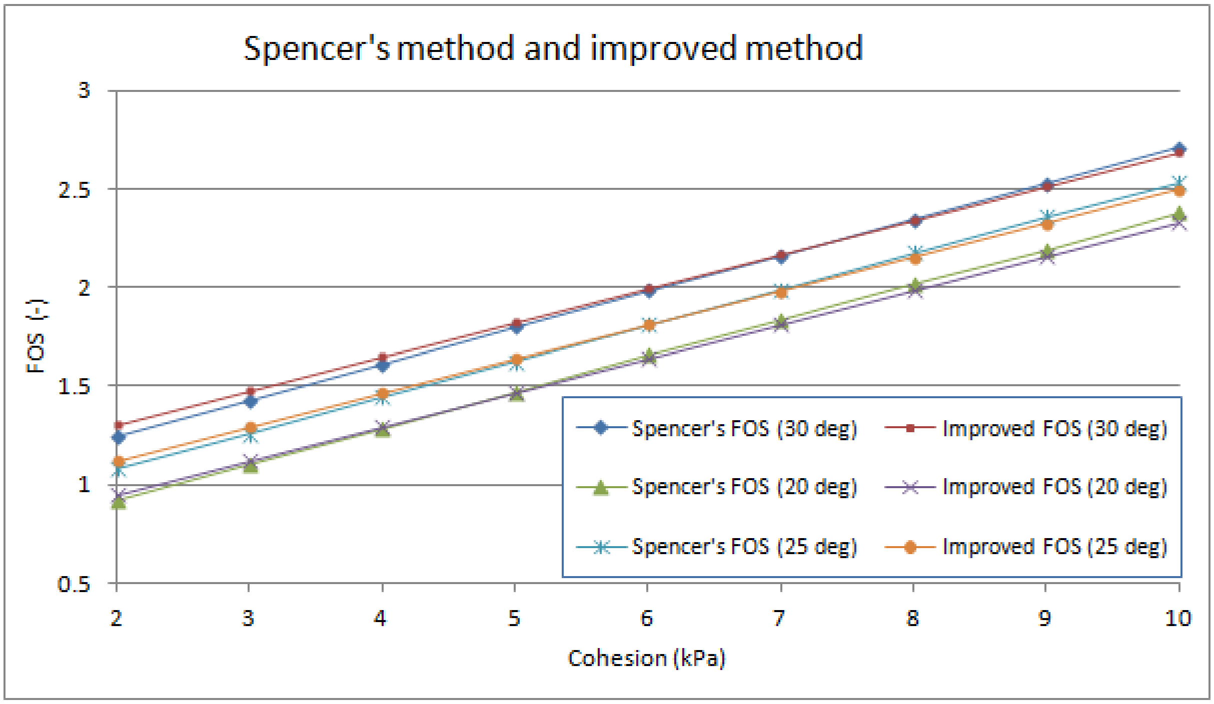

Figure 18. Factor of safety of Spencer's method and improved method

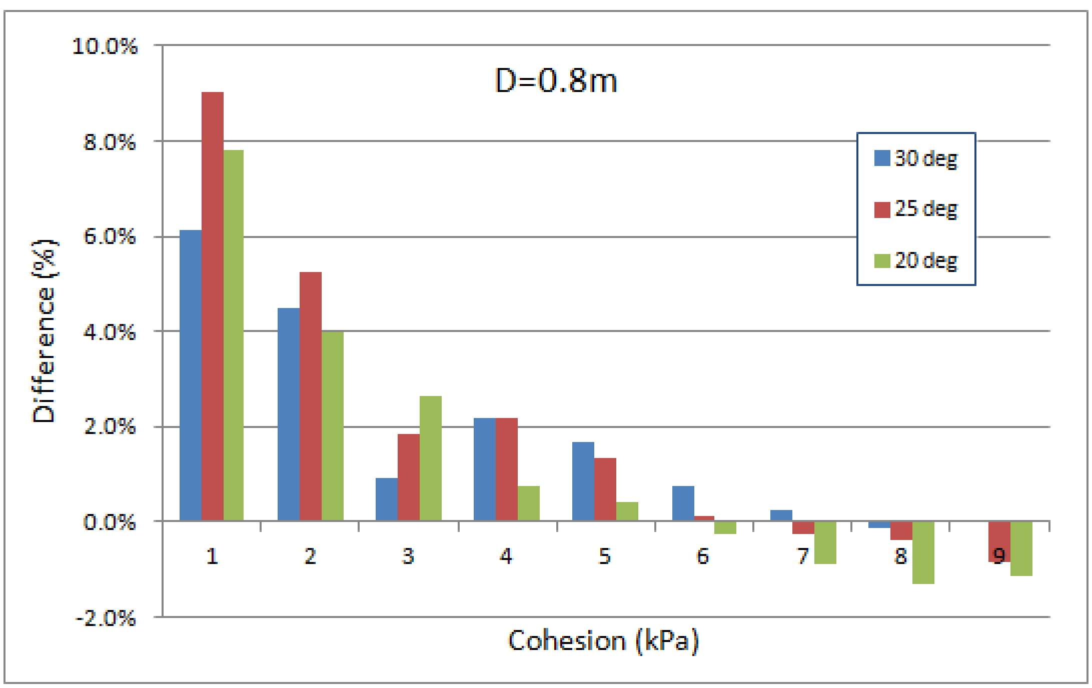

Figure 19. Difference between Spencer's and improved method (D=0.8m, improved method - 0% as reference)

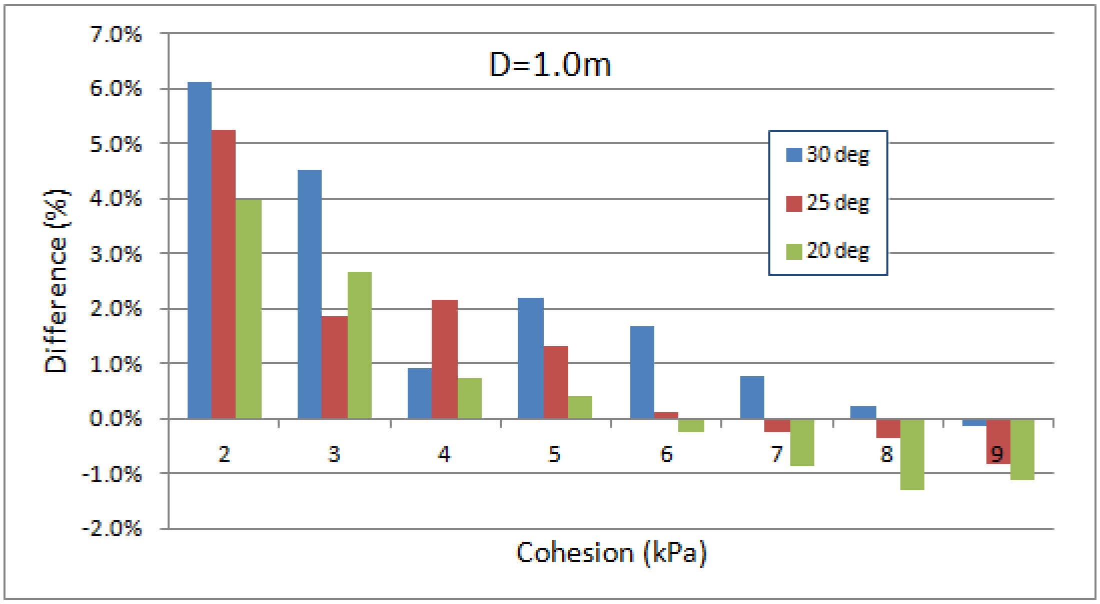

Figure 20. Difference between Spencer's and improved method (D=1.0m, improved method - 0% as reference)

These figures show that the improved method is in line with Spencer method in case of cohesion-dominated soil, with a cohesion larger than 4.0 (kN/m^2). This is because the difference is only about 2% from this value onwards. Another way of expressing this remark is depicted in Figure 21. It is mentioned that low cohesion will cause the improved method's FOS to be higher than Spencer's. This makes the improved method work on the unsafe side whereas clay-dominated soil with higher cohesion keeps the improved method a little bit smaller than Spencer method in terms of FOS.

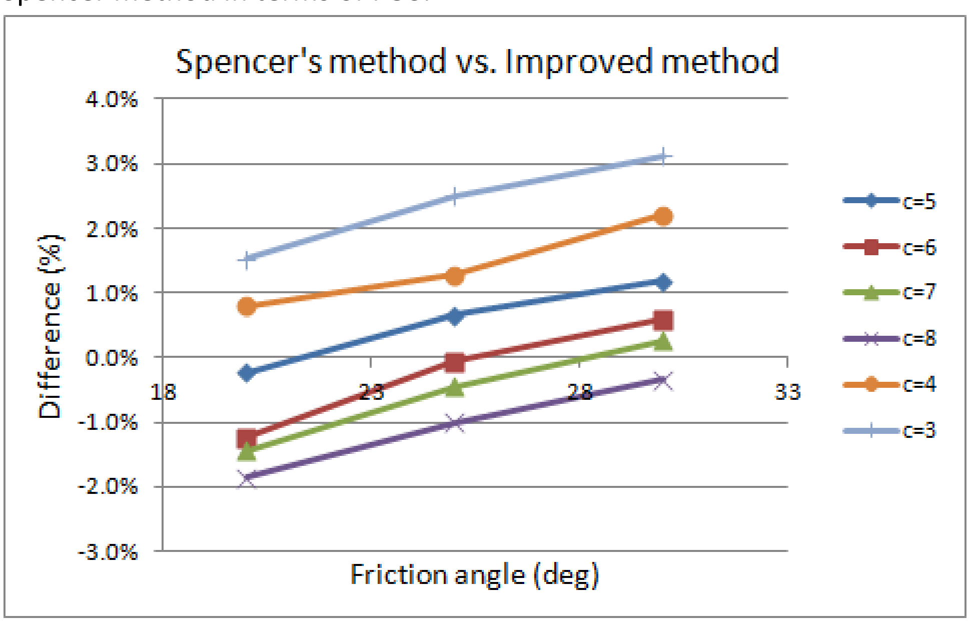

Figure 21. Difference between Spencer's and improved method (improved method - 0% as reference)

To conclude, the improved function can be applied without any adjustment to clay cover layer, based on the current findings. However, very small cohesion values (smaller than 3) make the safety factor of improved method higher than that of Spencer. This is unsafe to some extent and will be one of the discussed objects in Chapter 7.

5.2.3. The agreement between Spencer method and finite element method

In the previous section 5.1, the verification showed a difference between Spencer and FEM method in terms of stability. This section aims at figuring out possible explanations to such difference. Up to now, two particular situations are investigated, in which such quantities as pore water pressure and shear stress are compared in terms of safety analysis. In this validation test, FEM method and analytical method are identical with respect to dike geometry, shear strength parameters, and water conditions (as seen in Table 8).

Table 8. Finite element method vs. Analytical method

Situation	Cohesion (kN/m^2)	Friction angle (deg)	Crest height (m)	Slope angle (deg)	Slope length (m)	Thickness (m)	FEM' FoS	Spencer's FoS	Difference
1	4.00	20.0	6	18.43	18.97	1.0	1.277	1.310	-3%
2	4.00	20.0	8	18.43	25.30	1.0	1.252	1.270	-1%

Generally, a pattern representing the correlation between the finite element method and analytical method is improved in accordance with their level of sophistication. In other words, by improving the accuracy of simulation in both methods in calculated models (i.e. incorporating the interface element between two soil layers), the FOS calculated from finite element method is a slightly lower than that of analytical method. The remaining issue is the reason for their difference. Another comparison is made between two methods in a higher level of details. Since FEM and analytical methods use different calculation process to produce factors of safety, it is wise to compare how different they are in terms of pore water pressure distribution and effective stresses.

With respect to pore water pressure, although the method of slices works with an assumption and vertical inter-slices whereas FEM use shear strength reduction techniques, they seems to have equal pore water pressure distribution along the slip planes (see in Table 9). Therefore, the reason for difference is now lying on shear stresses generated from two methods. In fact, the shear stress of FEM calculation is higher than that of Spencer's. This can be justified using the forces model used in two calculations in next paragraphs.

First, Spencer method assumes a number of vertical slices and does not consider the inter-slices side stress. As can be seen in the Figure 43 (in Appendix 2), only shear stress at the base of inter-slices is attributed to the force and moment equilibrium conditions. On contrary to theory of Spencer, finite element methods take the side stresses between soil elements into consideration, and therefore give higher shear stress magnitudes.

Table 9. Shear stresses comparison.

Situation	Coordinates (equivalent to 1-m depth)		Pore water pressure (kN/m^2)		Shear Stress (kN/m^2)	
	X	Y	FEM	Spencer	FEM	Spencer
1	9.087	3.571	9.926	9.928	5.76	5.36
2	10.215	5.195	9.926	9.93	5.93	5.51

The second explanation concerns how accurate the soil behavior is modeled when stress-strain dependence is taken into account. During the calculation process of finite element methods, there can be some local positions where increasing strains can develop without any increasing changes in stresses of soil elements. These volume changes or displacements then redistribute the stresses of neighbor soil elements, and thereby increase shear stresses as a whole. Another point relates to the difference in principal effective stress directions. Figure 22 shows that the two methods work with different calculated models of principal effective stress directions. In this way, the difference in the angle of principal stress directions leads to a sense of how shear stresses along the slip planes are mobilized differently.

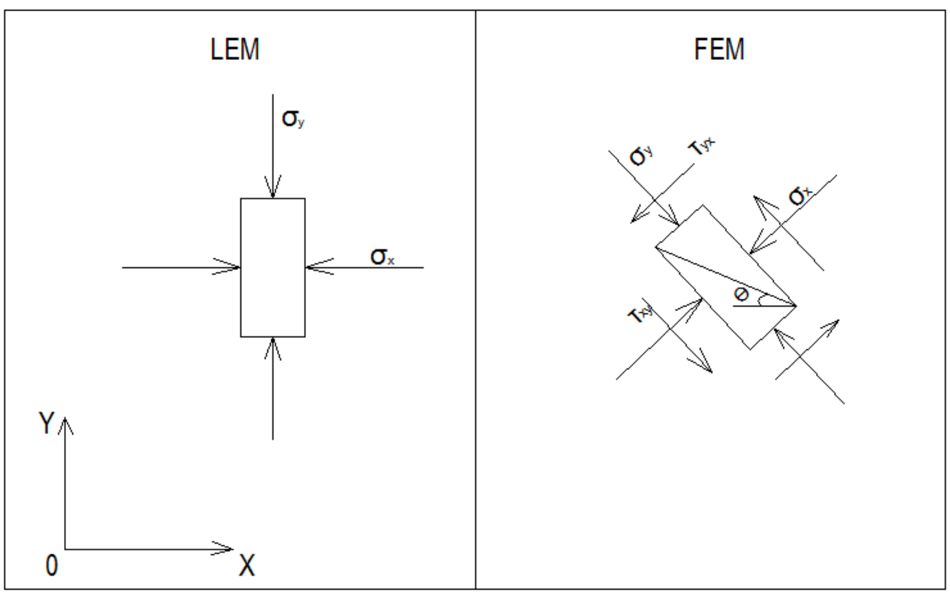

Figure 22. Principal effective stress directions

Another possible concern is associated with upper bound and lower bound solutions in limit analysis (Fredlund, 1984). For calculating the safety factor, Spencer method employed upper bound procedure whereas FEM works with lower bound condition. Mathematically, lower bound solutions result in lower factors of safety than that of the exact solutions while upper boundary condition gives solutions higher in magnitude than exact solutions. The reason for it concerns the following assumptions used in the two methods.

Generally, different methods of slices have different assumptions with respect to inter-slices force inclinations. They satisfy either certain conditions of equilibrium or all equilibrium conditions to come up with intended solutions. Therefore, upper bound solutions only satisfy the equilibrium equations, velocity boundary conditions, and failure criterion conditions. It makes use of the equilibrium of forces associated with kinematically admissible failure mode. The stress conditions are not necessarily the most important condition in equilibrium. It does not pay attention to the stress field condition. In this type of limit analysis, an admissible displacement yield is ensured while the stress equilibrium is ignored.

On contrary to the upper bound solutions, lower bound solutions satisfy stress boundary conditions, the yield criterion for the soil. This considers statically admissible stress discontinuities, which means that an admissible stress field is searched to maximize either a collapse load over some part of the boundary or the magnitude of forces acting within a region. Therefore, lower boundary condition provides lower values of safety factor in this case. However, there is still an ongoing debate whether or not limit equilibrium analysis always is on the realm of upper bound solutions (Yu, Salgado, Sloan, and Kim, 1998) because limit equilibrium method is an approximate and arbitrary nature.

5.2.4. Difference between improved method and Spencer method

In order to check the uncertainty of the improved method, difference between improved method and Spencer method is considered. This uncertainty is concerned with the probability, which shows how far a factor of safety calculated using improved method is from detailed analytical method - Spencer. One hundred cases were set up with a slope angle of 1V:3H and randomly different soil parameters to see how far the Spencer's FOS is from the predicting line. The result indicated that the predicting function is acceptable with a value of R^2 equal to 0.97 (see Figure 23).

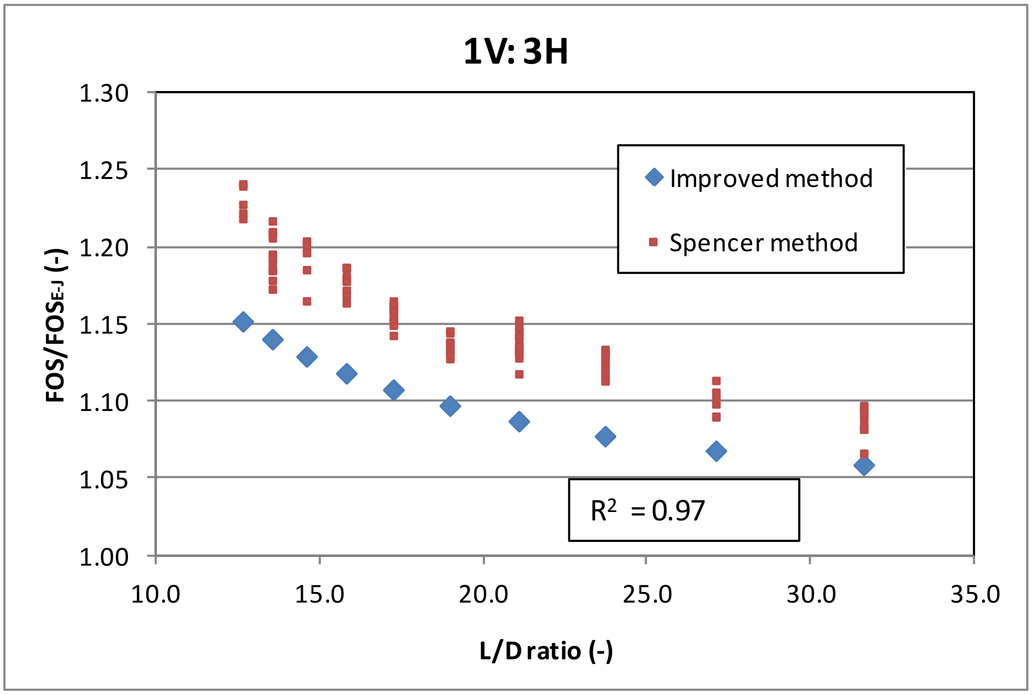

Figure 23. Uncertainty check for improved method

5.2.5. Generalization – Meaningful range of L/D ratio

As stated in section 4.2.4., the relevant range of L/D ratio is from 10 to 25, while only 5% improvement occurred if L/D is larger than 25. Moreover, the conclusion of section 5.2.2 indicated the range of soil strength parameters could work well with the improved method. This section then looks for possible approaches to extend the use of the improved method.

It is said that the improved method works well with clay-dominated soil while a little overestimation can happen in case of sandy-dominated soil. However, there is still now a quantitative indicator that can make a distinction between two types of soil here. From the study of 10 random situations (Table 10) and 63 cases (see 5.2.2. and Appendix 6), we proposed a ratio of c/(γ'.D.tanϕ') as the intended indicator.

Table 10. Difference between Improved method and Spencer's method

Situation	Cohesion (kN/m2)	Friction angle (deg)	Crest height (m)	Slope angle (deg)	Slope length (m)	Thickness (m)	Improved FoS	Spencer's FoS	Difference
1	1	30	7	18.43	22.14	1	1.160	1.102	5%
2	2	30	7	18.43	22.14	1	1.314	1.275	3%
3	2	35	7	18.43	22.14	1	1.525	1.472	3%
4	3	10	7	18.43	22.14	1	0.787	0.806	-2%
5	4	12	7	18.43	22.14	1	1.011	1.037	-3%
6	5	25	7	18.43	22.14	0.8	1.856	1.840	1%
7	8	22	9	26.57	20.12	1	1.477	1.470	0%
8	6	18	5	21.81	13.46	1.2	1.294	1.310	-1%
9	3	20	8	15.95	29.12	1.3	1.175	1.143	3%
10	7	16	10	33.69	18.03	0.6	1.442	1.420	2%

As can be seen in the Appendix 6, the ratio of c/(γ'.D.tanϕ') varies from 1.05 to 1.3 where the improved function and Spencer's calculation give similar results. In order to extend the method to a wider range of soil parameter and make the assessment tool lie on the safe side, a 5% reduction of the results calculated from improved method should apply to situations whose material properties are sand-dominant. Therefore, if the ratio is smaller than 1.05, the soil property is considered as sandy soil in this method, and 5% reduction is valid in this case.

In conclusion, about 15% improvement seems to work well in case of cohesion-dominated soil while a certain degree of overestimation occurs in case of (less-cohesive) sandy-dominated soil. This is because the improved method developed based on the clay soil parameters. To solve this limitation, in an ideal scenario, a corresponding function should be made for sandy-dominated soil. However, recently a suggestion was made using the non-dimensionless ratio of $c/(\gamma'.D.\tan\phi')$ to distinguish between the two types of soil, and then 5% reduction is applied for the result calculated from the existing function. With this consideration, the meaningful range of L/D ratio is justified.

Chapter 6. Case Study - Afsluitdijk

6.1. Introduction

So far, the Netherlands as well as other countries facing high risk of flooding such as Germany, Denmark and Belgium are using return period as the most important criterion for designing and determining the safety level of a dike section (Jorissen, Van Loon, and Lorenzo, 2000). However, actual safety levels are practically calculated using applied data, design procedures, criteria, and safety margins. Moreover, one disadvantage of expressing the safety level in terms of return periods is that the actual risk of flooding is unknown. Actually, the probability that a water level is exceeded in a particular year is different from the probability that an area will be flooded. Another disadvantage of using return periods as primary safety standards is that safety against flooding can only be improved by raising the crest height of flood protection structures. In contrast, if safety standards are stated as risk of flooding, which means the combination of probability of failure and its consequences, there will be more room for measures improving the flood protection structures. Therefore, development and research activities in probabilistic techniques have raised much attention in designing flood defense structures. Wave overtopping discharge is also one of significant parameters involving design procedures. This part of report will focus on the effect of different overtopping discharges.

At the present, the average overtopping discharge of 0.1 l/s per m is a critical design criterion, which ensures a dike is safe from failing by wave-overtopping-related mechanisms such as erosion and superficial sliding of the inner slope. For any type of dikes, this overtopping phenomenon does not cause any significant damages on inner slopes irrespective of the type of soil of the cover layer. However, not many sea dikes in the Netherlands conform this criterion since it generates very high of crest levels which are costly to build and maintain, but somehow conservative.

In order to contribute to extend this criterion in a positive manner, this part of report discusses the influence of different overtopping conditions on the stability of inner slopes of sea dikes. A brief content of this part is given as follows:

Hydraulic Loadings

- Overtopping wave theory
- Overtopping wave simulating under five overtopping discharges
- Calculating infiltration time
- Infiltration volume

Soil investigation

- Flow Parameters
- Soil shear strength parameters

Finite element method simulation

Results and discussion

6.2. Hydraulic Loading

6.2.1. Overtopping wave theory

6.2.1.1. Wave run-up

By definition, wave run-up is the up rush of water from a wave action on a shore barrier intercepting the still water level (Sorensen, 2006). In other words, wave run-up is the maximum vertical extent of a water up rush on the beach or barrier above still water level. The definition is depicted in the figure below, where R is the vertical water rush up.

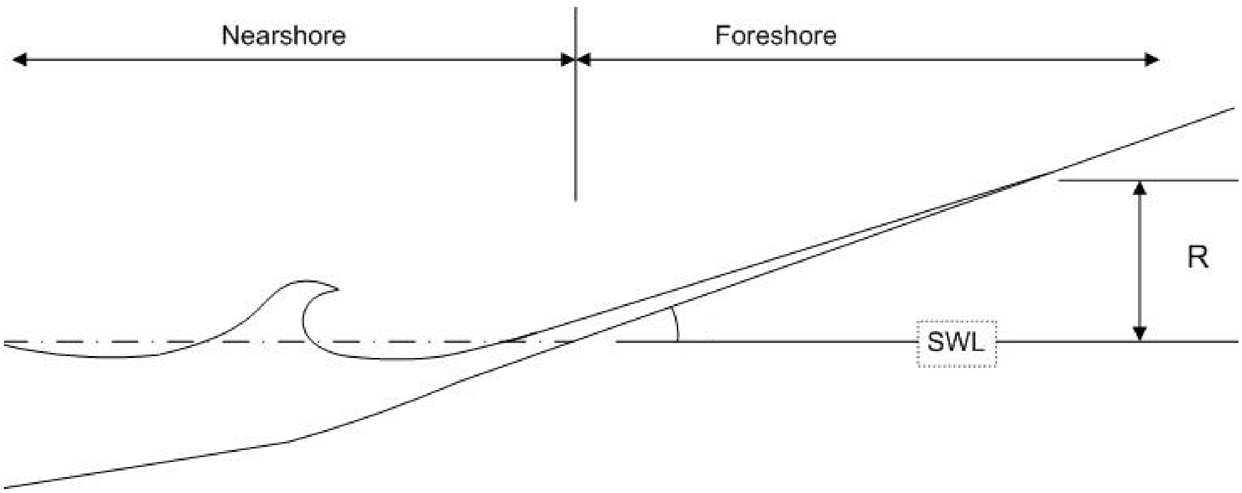

Figure 24. Wave run-up sketch

Wave run-up has two definitions in use, namely mean wave run-up and 2% wave run-up. Mean wave run-up is simply the averaging run-up of all coming waves while 2% wave run-up indicates that only 2% of incident waves will overtop the crest height of slopes. The later definition is relevant to the overtopping wave phenomenon, which leads to the consideration of erosion and sliding mechanism on the inner slopes of sea dikes.

Wave run-up is characterized by breaker parameter, which will be specified in next paragraphs. Theoretically, wave run-up depends on a number of parameters associated with slope geometry and wave characteristics. Firstly, the breaker parameter is an important element influencing the wave run-up, which is then dependent on the angle of the outer slope, the wave height and the wave period. The second parameter relates the roughness of the outer slope, which is usually considered as smooth or rough due to the presence of surface materials (grass, asphalt, rock, etc). For instances, a smooth surface of outer slopes will lead to a higher level of wave run-up than a rough surface. Another important parameter is the effect of the berm of the outer slope. Finally yet importantly, the angle of the incident waves is significant for a determination of the run-up. In the Netherlands, the 2% wave run-up is used in design guidelines of dikes, determined as follows:

$$\frac{R_{u,2\%}}{H_{m,0}} = 1.75.\gamma_b.\gamma_\beta.\gamma_f.\xi_0 \qquad [22]$$

If the value of the breaker parameter is larger than 1.75, the maximum value of the 2 % wave run-up is:

$$\frac{R_{u,2\%}}{H_{m,0}} = 1.75.\gamma_\beta.\gamma_f\cdot\left(4.0 - \frac{1.5}{\sqrt{\xi_0}}\right) \quad [23]$$

Where:

$R_{u,2\%}$: run-up level exceeded by 2% of the incoming waves (m)

γ_b : reduction factor for a berm effect, called dike coefficient (-)

γ_f : reduction factor for the roughness of the outer slope, or friction coefficient (-)

γ_β : reduction factor for the angle of wave attack (-)

H_{m0} : spectral wave height (m)

6.2.1.2. Breaker parameter

The parameter that, importantly characterizes the wave run-up or overtopping phenomenon, is breaker parameter. This concerns other different parameters such as the angle of outer slope, the wave height, and the wave period. This parameter is defined as the function of the steepness of the outer slope and the wave steepness (Eq. 24). In this function, the value of breaker parameter is the ratio of the steepness of the outer slope over the root mean square of the wave steepness that, in turn, is defined by the wave height divided by wavelength (Eq.25). The wave height is the highest one third of all incoming waves, and called significant wave height, H_s, if the wave height is determined by measurements. When being based on the zero moment of a wave spectrum (Bosman, 2007), this value is called H_{m0}. In the case of deep-water waves, these two values are identical, while a difference varying from 10 to 15% is realized in the case of shallow water.

Beside the angle of the outer slope, the other part is the wavelength, which is dependent on the wave period. In this sense, the spectral mean period, $T_{m-1,0}$ is used. It is used since it is more significant for longer waves, which are very important for overtopping. From the description, the breaker parameter is written as follows:

$$\xi_0 = \frac{\tan\alpha^*}{\sqrt{s_0}} \quad [24]$$

With $s_0 = \frac{H_{m,0}}{L_0}$ and $L_0 = \frac{g.T^2_{m-1,0}}{2\pi}$ [25]

Where:

ξ_0 : breaker parameter (-)

α^* : angle of the outer slope (deg)

s_0 : wave steepness (-)

H_{m0} : significant wave height or spectral wave height (m)

L_0 : deep water wave length (m)

g : acceleration due to gravity (m/s^2)

$T_{m-1,0}$: spectral wave period at toe of dike (s)

$$T_{m-1,0} = T_p / 1.1 \quad [26]$$

The significant wave height is a quantity that is used to describe the strength of wave-field. This is the average height of the highest 1/3 of the waves. It is closely associated with moments, which describe the intensity of wave-field, and then the zero moment of a wave spectrum, which is the distribution of wave energy as a function of wave frequency.

6.2.1.3. Overtopping discharge

Overtopping discharge is the mean discharge per linear meter of width (l/s per m). It is commonly used to characterize the magnitude of storms. Generally, overtopping discharge is predicted using an exponential function as follows:

$$Q^* = \frac{q}{\sqrt{g.H_s}} = A.\exp\left(-B\frac{R_c}{\gamma.H_s}\right) \quad [27]$$

According to TAW 2001, the values of coefficients A and B are defined:

$$\frac{q}{\sqrt{g.H^3_{m,0}}} = \frac{0.067}{\sqrt{\tan\alpha^*}}\gamma_b.\xi_0.\exp\left(-4.3\frac{R_c}{H_{m,0}}.\frac{1}{\xi_0.\gamma_b.\gamma_f.\gamma_\beta.\gamma_v}\right) \quad [28]$$

With a maximum of:

$$\frac{q}{\sqrt{g.H^3_{m,0}}} = 0.02\exp\left(-2.3\frac{R_c}{H_{m,0}}.\frac{1}{\gamma_f.\gamma_\beta}\right) \quad [29]$$

Where:

Q^* : dimensionless overtopping discharge (-)

q : average wave overtopping discharge per meter (m^3/s per meter)

R_c : crest freeboard relative to still water level (m)

γ_υ : influence factor for a vertical wall on slope (-)

Although average overtopping discharge is a practical and commonly used parameter, it has a drawback in depicting the wave conditions. In fact, it does not successfully simulate the effect of overtopping waves on the structures stability since the parameters of individual overtopping waves such as volumes and velocity are not considered. For example, a discharge of 1 l/s per m caused by several small waves might have a different effect on the dike than the same discharge caused by only one single wave of 3600 liter in one hour.

6.2.1.4. Overtopping volume per wave

Overtopping volume per wave is very significant in terms of safety of inner slopes since it manifests specific influence of wave conditions on the slopes. The different overtopping volumes during a storm can be described by a Weibull distribution.

$$P_v = 1-\exp\left[-\left(\frac{V}{a}\right)^{0.75}\right]$$ (Eurotop, 2007) [30]

With

$$a=0.84.T_m \frac{q}{P_{ov}}=0.84.q\frac{T_s}{N_{ov}}$$ (Van der Meer, 2006a) [31]

Where:

P_v : probability of the overtopping volume being smaller than V

V : overtopping wave volume

N_{ov} : number of overtopping waves

P_{ov} : probability of an overtopping event

$$P_{ov}=\exp\left[-\left(\sqrt{-\ln(0.02)}\frac{R_c}{R_{u,2\%}}\right)^2\right]$$

[32]

6.2.2. Simulation of overtopping wave

6.2.2.1 Typical wave condition

Information about hydraulic conditions at the location of the experiment is used to simulate wave overtopping. A significant wave height is 2m and the wave steepness is taken to be 5%. A virtual storm will last for 6 hours and generating overtopping waves towards a seaward slope of 1:4. Furthermore, the peak wave period is chosen to be 5.7 seconds under various average overtopping discharges. These conditions represent typical conditions for Dutch coast (Steendam, Van der Meer, Hardeman, and Van Hoven, 2010).

With the sea state parameters discussed above, five different overtopping discharges are simulated in terms of overtopping volume. The probabilistic calculation of detailed procedure is presented in Appendix 8. The resultant simulation is depicted below (Figure 25). These curves show how the overtopping waves are distributed under different storm conditions characterized by average overtopping discharges. These lines indicate the accumulative number of overtopping waves, which pinpoint that the probability of high-volume overtopping wave is smaller than that of lower-volume ones. Their relevance to the study is difference in infiltration time, which is specified in next sections.

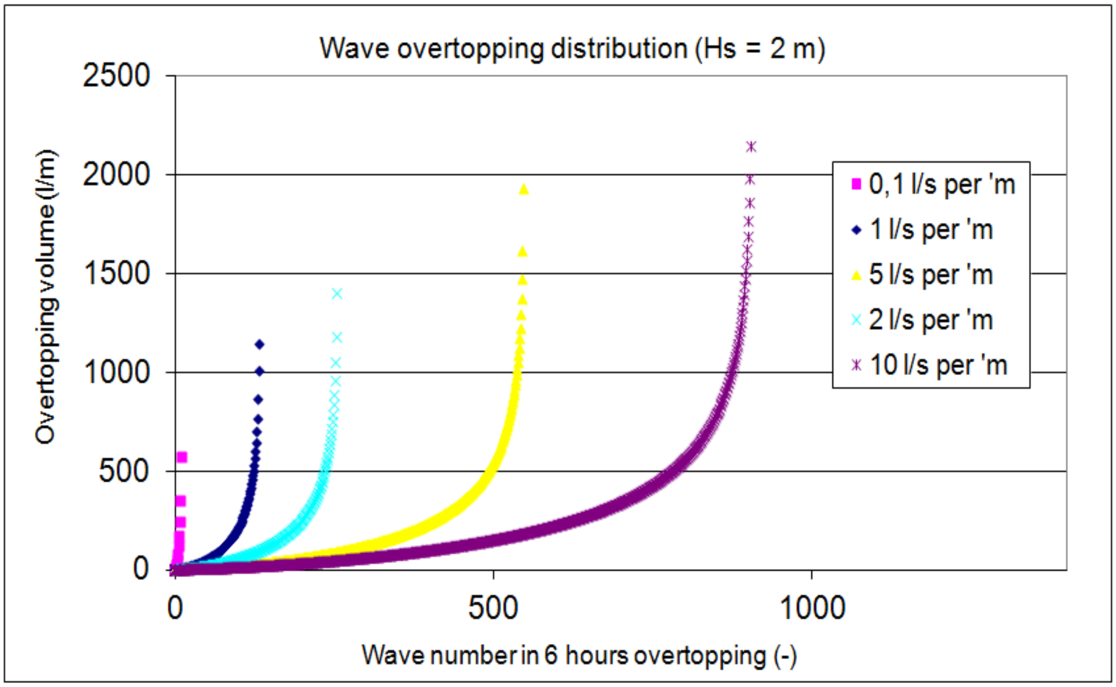

Figure 25. Overtopping wave simulation

6.2.2.2. The infiltration time

The idea of infiltration time generates from the fact that an overtopping wave will be able to stay on the slope surface for a period (i.e. 40 seconds, in this report) and make the slope wet within this amount of time. Therefore, if the time between two consecutive overtopping waves is longer than 40 s, the slope can be dry for the time left over. Summing up the total dry time and wet time during the storm duration results in infiltration time as listed in Table 11. The difference between different overtopping discharges is the amount of time that the slope gets wet. For example, a 6-hour storm with an average overtopping discharge of 0.1 l/s per m will caused the inner slope to be wet for 0.026*21600= 562 s ≈ 9.36 (minutes). In the meantime, another 6-hour storm with an average overtopping discharge of 10 l/s per m will make the slope wet for 0.945*21600 = 20421 (s) ≈ 340.20 (minutes)

Table 11. Infiltration time

Overtopping discharge (l/s per m)	Number of overtopping waves	Timeline of infiltration (hour)	Overtopping volume (l/m)	Infiltration time (%)
0.1	9	1	25.99	3.0
		2	0.00	
		3	241.18	
		4	395.91	

		5	289.66	
		6	74.48	
1.0	132	1	3380.22	22.0
		2	5278.99	
		3	3903.61	
		4	2654.16	
		5	2741.25	
		6	2591.77	
2.0	254	1	9649.06	45.0
		2	5244.89	
		3	8636.88	
		4	7178.92	
		5	6698.65	
		6	8349.97	
5.0	547	1	11729.66	67.0
		2	16190.53	
		3	22317.54	
		4	22211.83	
		5	18974.01	
		6	16148.67	
10	905	1	30717.23	85.0
		2	33948.30	
		3	29364.64	
		4	32347.51	
		5	36584.20	
		6	33032.86	

This table is the result of a probability calculated, using the theory described in preceding sections. In general, storm duration of 6 hours is simulated with a number of incoming waves, according to its overtopping discharge required. Among these incoming waves, called incident waves, there are a proportion of waves exceeding the crest of dike, causing the overtopping phenomenon. Every single overtopping wave makes slope wet for 40s, and they are distributed randomly within 6 hours. The water overflowing within every hour is calculated accordingly, together with the calculation of infiltration time described above.

6.2.2.3. Infiltration capacity and infiltration volume per square meter (l/m^2)

Even though the infiltration time and overtopping volume calculated above are important elements in simulating the wave overtopping, they do not give sufficient data for simulating the water boundary condition on the surface of the slope. In order to overcome this, infiltration capacity has to be acquired and infiltration volume should be calculated. From the flow parameters, the infiltration capacity of the clay layer is 2.8E-05 m/s (from 6.3. Soil Investigation). With the void ratio and the porosity, the water required to make the soil saturated is calculated and the infiltration volume of different overtopping discharges is generated in Table 12. The graph is valid in case of the thickness of the clay cover layer is 0.4 m.

Table 12. Infiltration volume

Overtopping discharge (l/s per m)	Storm duration T_s (hour)	Infitration time I_{fil} (%)	Time of infiltration, t_s (s)	Average permeability k_{ave} (m/s)	Infiltration depth d_{fil} (m)	Void ratios, e (-)	Porosity, n (-)	Infiltration volume, V_{fil} (l/m^2)	Saturated volume threshold, V_{thr} (l/m^2)
(1)	(2)	(3)	(4)	(5)	(6))	(7)	(8)	(9)	(10)
	T_s	I_{fil}	$t_s=T_s*I_{fil}*3600$	k_{ave}	$d_{fil}=k_{ave}*t_s$	e	n=e/(1+e)	$V_{fil}=100*n*d_{fil}$	$V_{thr}=1000*n*0.4$
0.1	6	3%	561.6	2.80E-05	0.016	0.09	0.08257	1.30	33.03
1	6	22%	4788.7	2.80E-05	0.134	0.09	0.08257	11.07	33.03
2	6	45%	9720	2.80E-05	0.272	0.09	0.08257	22.47	33.03
5	6	67%	14472	2.80E-05	0.405	0.09	0.08257	33.46	33.03
10	6	85%	18360	2.80E-05	0.514	0.09	0.08257	42.45	33.03

Where:

T_s : Storm duration (hour)
I_{fil} : Infiltration time (%)
t_s : infiltration time (second)
k_{ave} : average permeability (m/s)
d_{fil} : depth of infiltration (m)
e : Void ratio (-)
n : porosity (-)
V_{fil} : infiltration volume (l per m^2)
V_{thr} : saturated threshold (l per m^2)

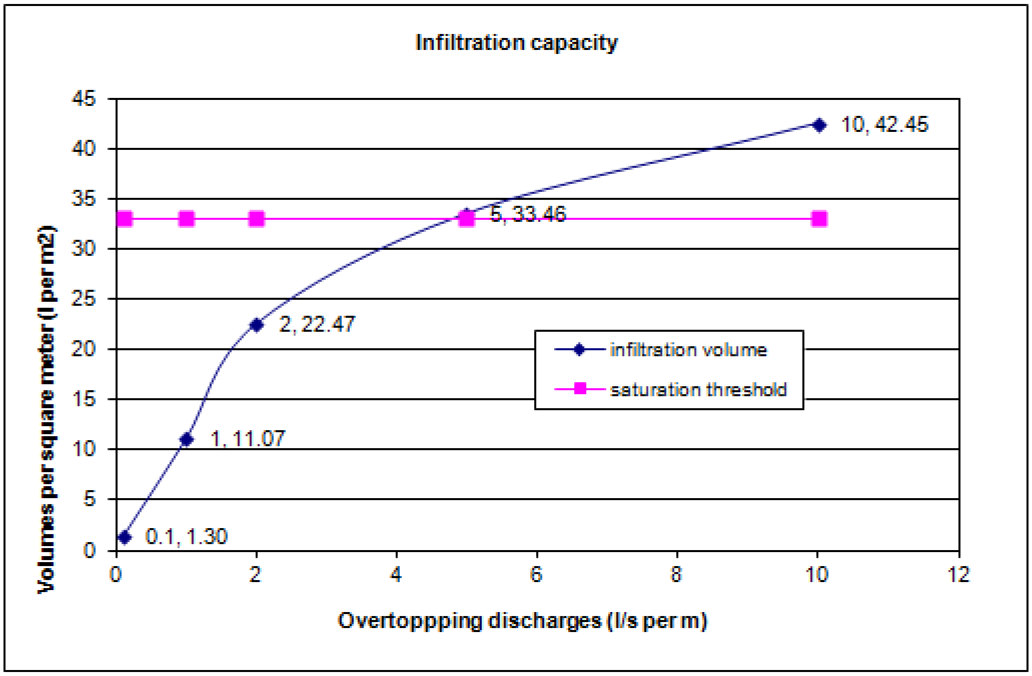

Figure 26. Infiltration volumes versus overtopping discharges

These calculated curves will be used to check against the infiltration process simulated on the finite element method. For example, the cover layer should be saturated after about 5 hours of infiltration.

6.3. Soil Investigation

The hydraulic part gives a description of overtopping simulation varying from calculating number of overtopping wave, infiltration time to infiltration capacity and infiltration volume. The purpose is to supply data for creating the water boundary condition for simulation model of Afsluitdijk. Similarly, this part of the report retrieves data about the geometry, soil strength parameter, and flow parameters which are essential to execute the stability analysis using finite element method.

The information laid out here is derived from the previous documents (DHV 2005, Grondmachanica 1987), laboratory tests and field tests in soil investigation reports. They are combined and discussed in three different parts: Testing locations, soil strength parameters, and flow parameters.

6.3.1. Location of the testing section

The soil investigation tests were made on the inner slope of Afsluitdijk, situated between Knornverderzand and Friesevasterland, nearby km 28.6 (kilometering Afsluitdijk). This section lies beside A7 road parallel to two parking lots. Figure 27 gives an overview of the test location where experiments were carried out.

Figure 27. Experiment location

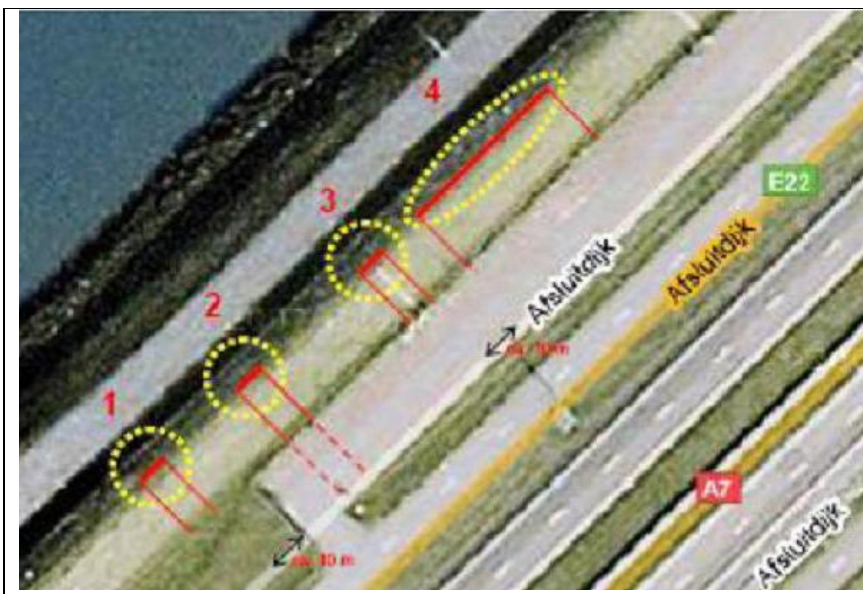

Figure 28. Test positions

Position 1:

Erosion test – Grass-covered slope and horizontal transition

Position 2:

Erosion test – transition embankment with horizontal brick pavement

Position 3:

Erosion test – Slope and stair fences at the bottom of the slope.

Position 4: Sliding test

To be able to build up a simulating model, relevant input data is specified as follows:

The crest height with respect to NAP: +7.2 m

The crest width: 2.0 m

The dike toe elevation with respect to NAP: +4.4 m

The inclination of the inner slope: 1:2.6

The slope Height: 2.8 m

The slope length: 7.28 m

6.3.2. Geological description

Afsluitdijk was composed of sand core at the inner side under a boulder clay layer, which is covered by brick pavement at the seaward sides and a clay layer at the landward side. Regarding to the geology of the inner slope, the clay layer has an average thickness of 0.4m, underlining by 1.1-meter boulder clay layer. Beneath the boulder clay is the sand core of the dike.

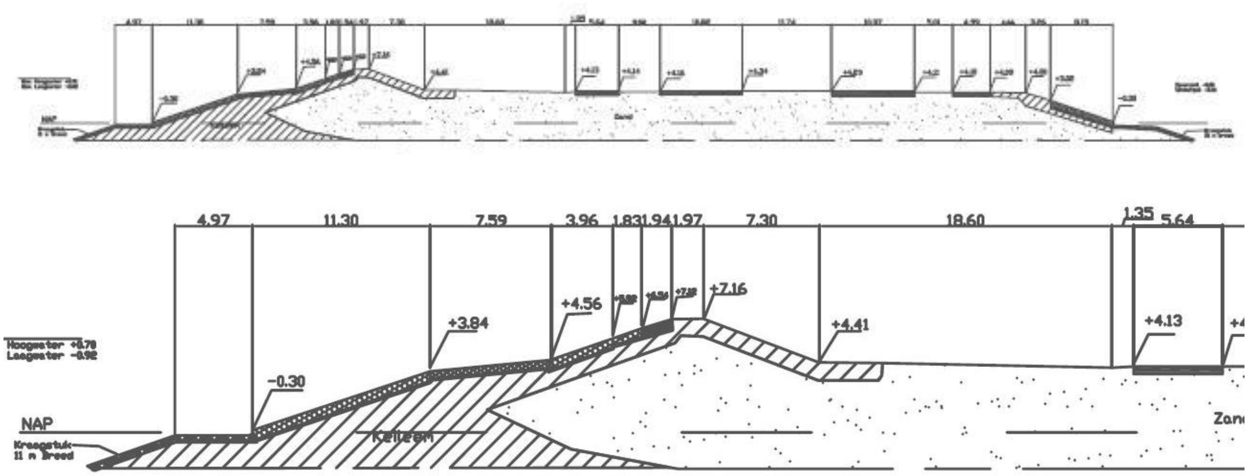

Figure 29. Dike's cross section

6.3.3. Strength parameters

The strength parameters used in this report are derived from relevant soil investigation reports such as Grondmechanica Delft 1987, DHV 2005, tests of Deltares 2009. Detailed discussion is depicted in Appendix 7. In the purpose of this study, clay layer and the boulder clay are two important components.

The cohesion and friction angle of the clay cover layer are c= 6.2 kPa and ϕ'= 23.4^{o}, respectively. These values are derived from five triaxial tests in Deltares, 2009. A detailed procedure to come up with this design value is explained in Appendix 7, including shear direct shear stress tests, relevant tests reported previously.

The friction angle and cohesion values of the boulder clay are obtained from laboratory tests (Grondmechanica Delft 1987) with average values: c=3.5 kPa, and ϕ'= 30.1^{o}. The shear strength parameters of the sand core were not measured by laboratory tests. Instead, for this study, they are assumed based on experience with c=0.1 kPa and ϕ'= 30^{o}. The assumed value of cohesion is to avoid the numeric problems happening in FEM method (PLAXIS) in stability analysis (Van Hoven, Verheij, and Van der Meer, 2009). At the bottom of the slope, there is a small part of brick pavement, which plays no influence on the stability analysis. The values in Table 13 are adapted to this kind of material.

Table 13. Soil Parameters of Afsluitdijk

Parameter	Unit	Cover clay layer	Cover boulder clay layer	Sand	Brick Pavement
γ_{dry}	kN/m^3	15.3	19.5	17.5	20
γ_{wet}	kN/m^3	17.3	21.5	18.5	20
ϕ'	(^{o})	23.4	30	30	35
c	kPa	6.2	3.5	0.1	1

6.3.4. Flow parameters/ permeability

The permeability of the sand core was determined by making laboratory tests on four samples at desired test locations. The permeability was measured in terms of three categories: fixed, medium, and loose packing. The results are shown in Table 17 (Appendix 7).

For the fixed packing, with an average porosity of n=0.36 (-), the average permeability is 1.0x10^{-4} m/s. While the permeability of the medium packing (n=0.38) is 1.3x10^{-4} m/s, the figure for loose packing is 1.7x10^{-4} m/s. The influence of the packing type is small somehow. Therefore, in this report, the value of 1.4x10^{-4} m/s is used for the sand core.

The permeability of the clay cover is calculated based on 4 in-situ infiltration tests. The tests lasted on the slope for several hours. There are tubes with a diameter of 40 cm, being pressed vertically into the slope to the depth of 0.6 and 0.7m. Then, water is poured into those tubes from the top, where the decrease in water columns is monitored. This is important to measure the saturation of the soil layer as well. The used value is 2.8x10^{-5} m/s, which is the result of the first part of infiltration. The value of the second part of infiltration test is not used since it results in a value of 1.2x10^{-5} m/s, over 2 times smaller than the former.

The permeability of the boulder clay is derived from Grondmechanica Delft 1987 with a value of 1x10^{-6} m/s.

6.4. Simulation results

6.4.1. Safety factor versus overtopping discharges

The content of this part is the results of two analyses, namely groundwater flow (transient) analysis and safety analysis. The purpose is to show the relationship between the stability level of the inner slope and the change of the groundwater flow due to different overtopping discharges.

- Safety analysis: monitor the change of stability under 5 different overtopping discharges
- Groundwater flow analysis: the development of parallel groundwater flow

At this stage, all information from hydraulic part and soil investigation are used to create the model (see in Figure 30) and boundary conditions in two analyses. On the inner slope surface, the infiltration process is simulated as head pressure p=0 during the infiltration time, which means that the surface is guaranteed to be wet.

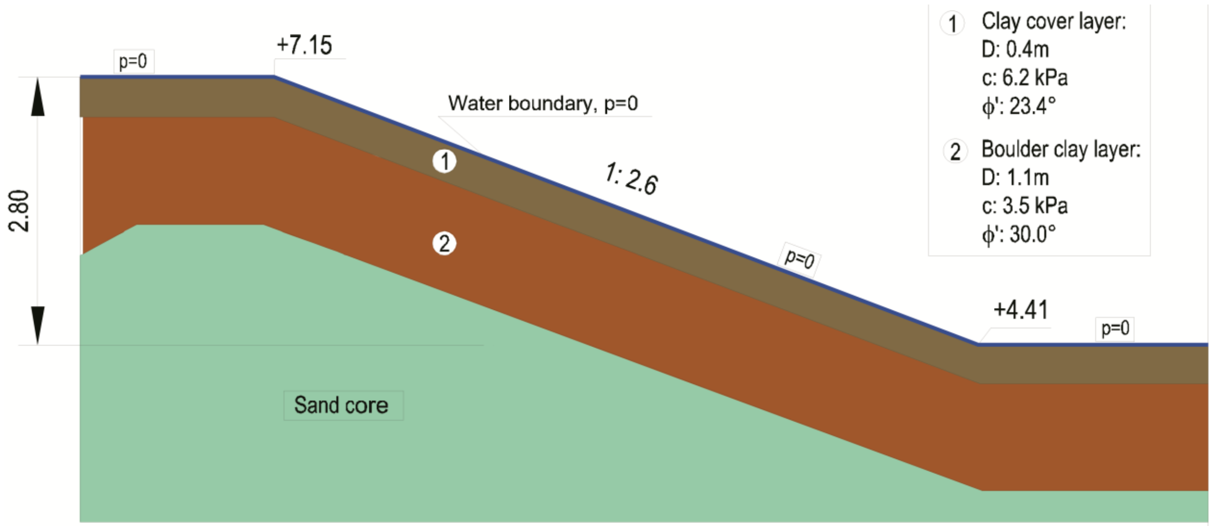

Figure 30. Model sketch

This results in the reduction of the global stability of the inner slopes under different overtopping discharges. Figure 31 depicts the relationship between overtopping discharges and the safety factors in two axes. As shown in the figure, the stability of the inner slope decreases slightly from 0.1 l/s per m to 5.0 l/s per m causing the infiltration from about 9 minutes to 242 minutes. During these periods, the potential slip planes completely stay in the deeper layer. With the overtopping discharge of 10 l/s per m, a considerable decline occurs with the potential slip plane lying on the interface between the top cover layer and the boulder clay. This is visualized in some following pictures.

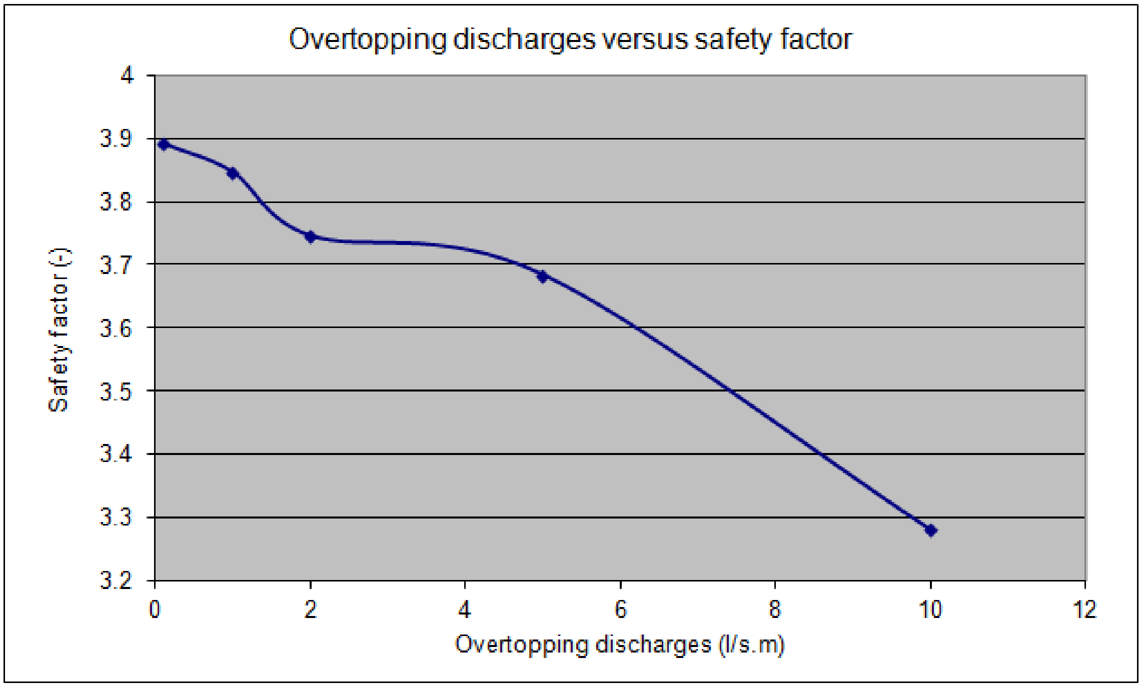

Figure 31. Safety factor versus different overtopping discharges

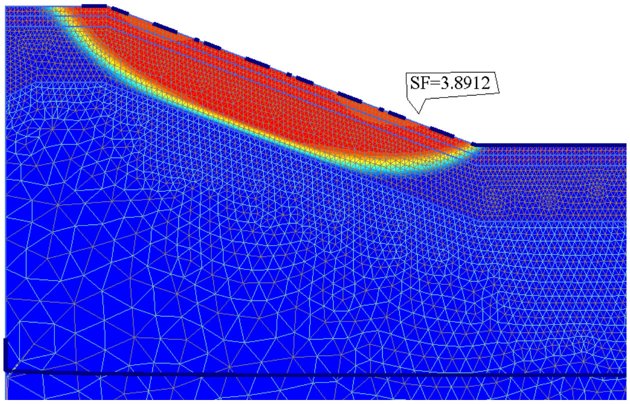

a. 9.3 minutes (0.1 l/s per m)

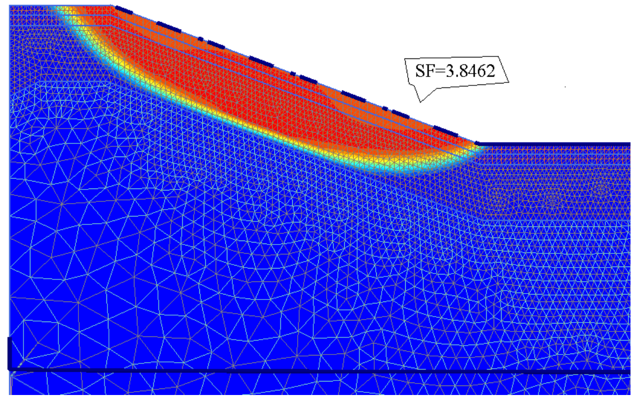

b. 80 minutes (1.0 l/s per m)

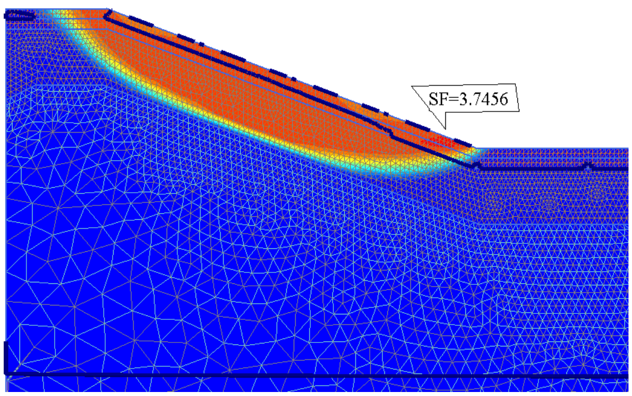

c. 162 minutes (2.0 l/s per m)

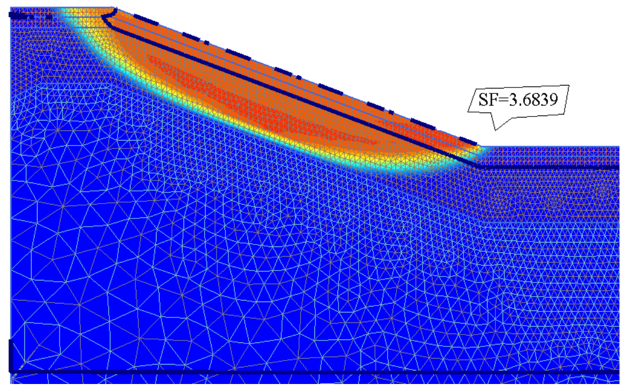

d. 241.6 minutes (5.0 l/s per m)

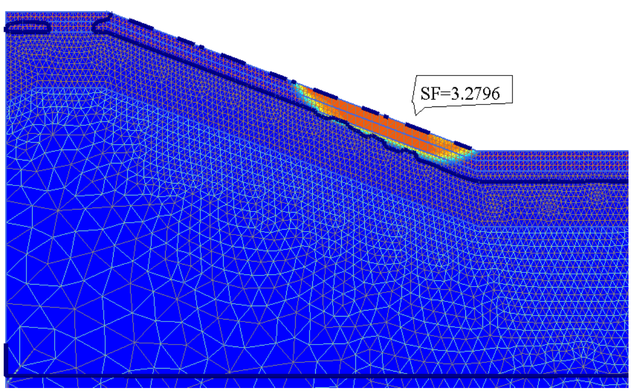

e. 306 minutes (10 l/s per m)

Legends:

: unsafe zone,

above the potential slip plane

: safe zone

Figure 32. Change in stability of the inner slope

6.4.2. Pore water pressure development

The flow analysis also gives a check on the development of the saturation and groundwater flow discharges during these stages. From the result visualized in Figure 33, the saturation degree increases with time of infiltration (red color zones).

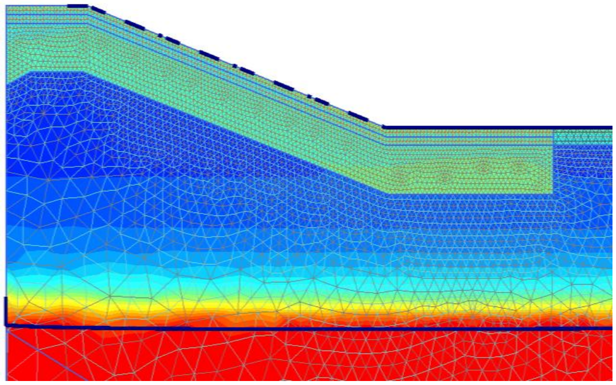

a. 9.3 minutes (0.1 l/s per m)

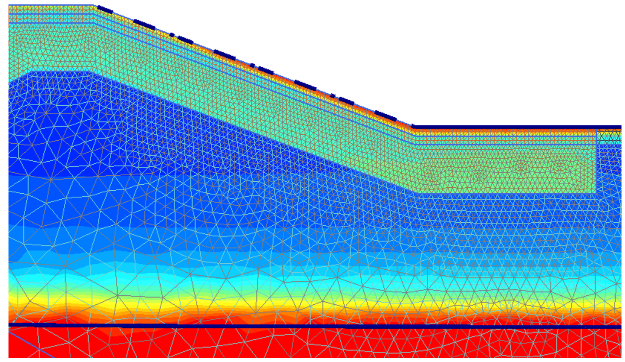

b. 80 minutes (1.0 l/s per m)

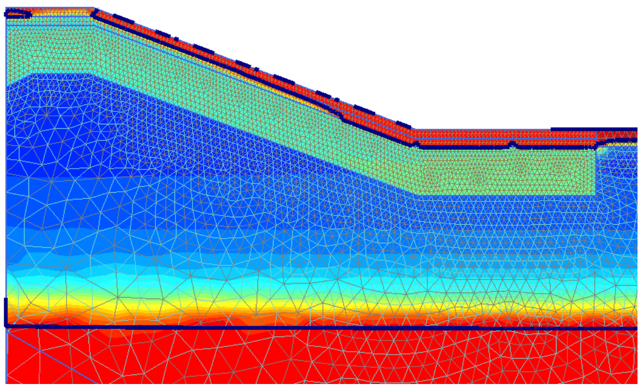

c. 162 minutes (2.0 l/s per m)

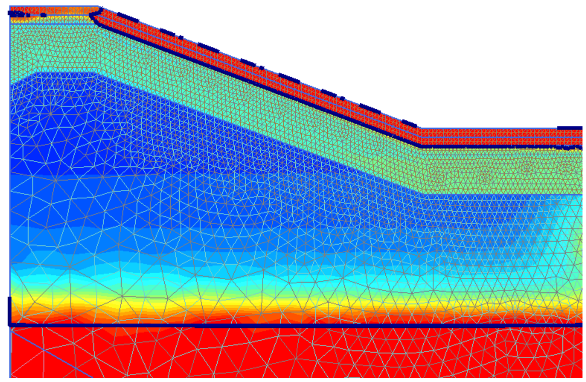

d. 241.6 minutes (5.0 l/s per m)

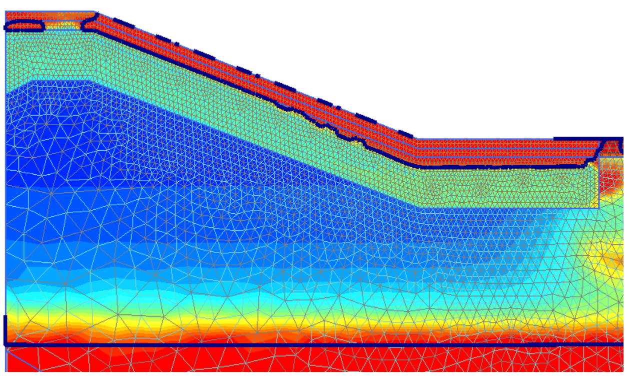

e. 306 minutes (10 l/s per m)

Legends: saturation

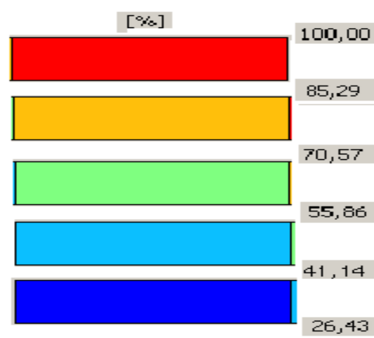

Figure 33. Saturation change

With respect to the saturation issue, it is essential to refer to the infiltration capacity, which is calculated in section 6.2.2.3. The section predicted that the slope would be saturated after suffering the infiltration time of overtopping discharge of 5.0 l/s per m (equivalent to 241.6 minutes of infiltration or 33.03 l/m^{2}, see Figure 26). This is in line with the saturation process presented in the figures above (Figure 33.d), which shows the cover layer is saturated at the time that the overtopping discharge of 5 l/s/m occurs.

In addition, a groundwater flow analysis indicates the development of the parallel flow, which is shown in the following images. This contributes to the argumentation for the use of assumptions stated in Edelman – Joustra method.

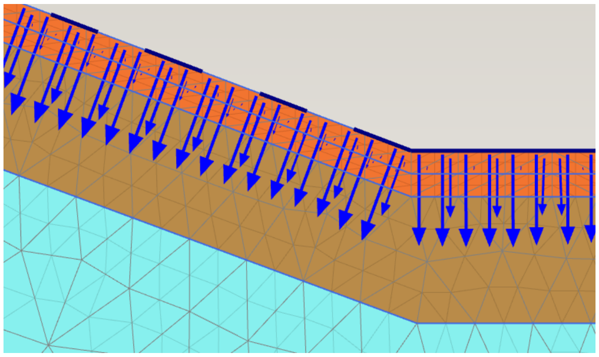

a. 9.3 minutes

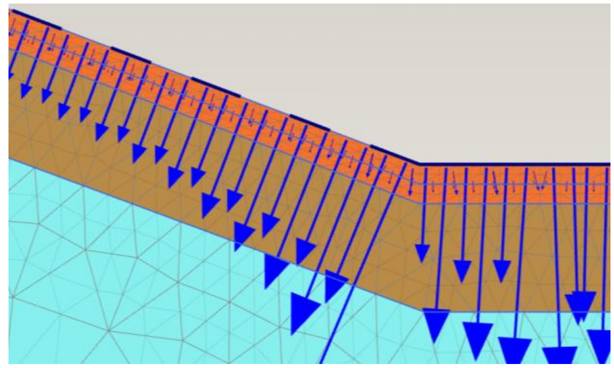

b. 82 minutes

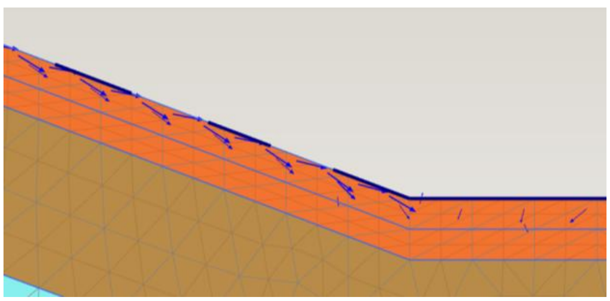

c. 162 minutes

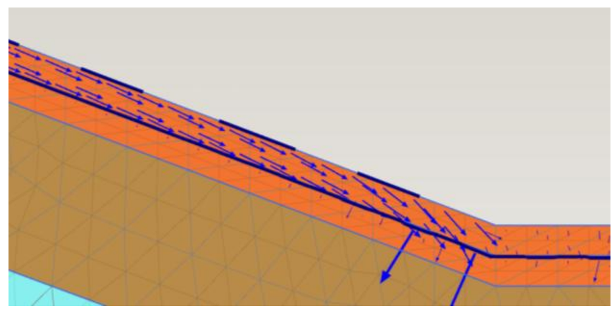

d.241 minutes

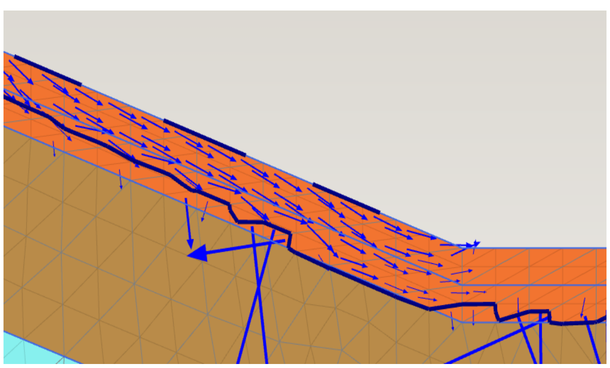

e. 306 minutes

Legend:

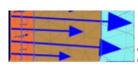
: groundwater flow direction

* Maximum values

a. $0.335.10^{-6}$ (m/s)

b. $1.550.10^{-6}$ (m/s)

c. $0.301.10^{-3}$ (m/s)

d. $0.027.10^{-3}$ (m/s)

e. $0.389.10^{-3}$ (m/s)

Figure 34. Groundwater flow development

Safety factor is also calculated using Edelman Joustra and improved method to underpin the calculation. The difference between the Plaxis and improved method is comparable and reasonable because the improved method was formulated from Spencer with a conservative degree.

Methods	*Edelman Joustra*	*Finite Element Method*	*Improved method*

	Method	*(Plaxis)*	
Factor of safety	2.85	3.27	3.14

Another issue is that the built-up potential of pore water pressure at the interface between two layers. First, ground water head changes over time under different infiltration period. Then, a graph (see in Figure 35) describes how the pore water pressure built up over time. The results indicate that after 6-hour infiltration, the pore water pressure did not reach the critical pressure to initiate the sliding mechanism. According to the assumption, pore pressure should be equal to $9.81*0.4*\cos(21.6^0) = 3.66$ kN/m^2 to be able to cause the sufficient ground water flow. However, after 6-hour infiltration, the pore water pressure at the middle of slope is 1.90 kN/m^2. The difference between these values can be justified by some following ideas. First, this difference involves the difference between hydrostatic pressure and pore water pressure due to seepage. The former value indicates the state of saturated soil, while the latter represents the pressure of groundwater flow. Second, due to the unsaturated zones during the infiltration, the capillary and suction effect contributes to the difference by reducing the positive pore water pressure in the cover layer.

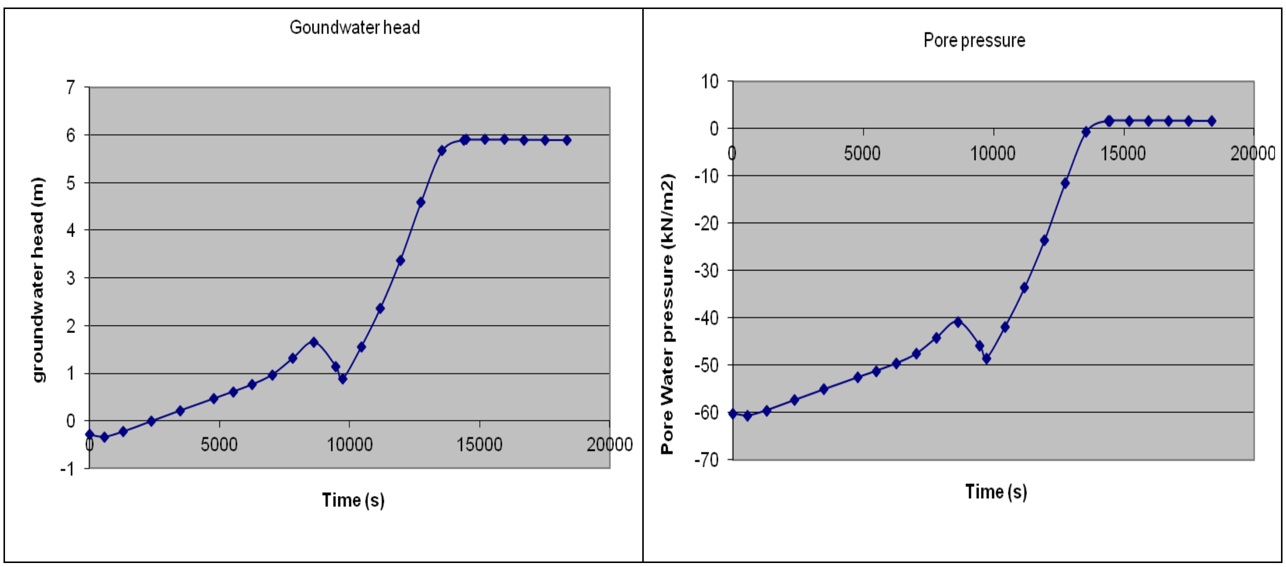

Figure 35. Pore water pressure built-up

In conclusion, for Afsluitdijk case, the relationship between overtopping discharges and safety factor is determined, which shows that small overtopping discharges (especially, 0.1 l/s per m and 1.0 l/s per m) have no significant influence on the inner slope stability. The saturation was reached and the parallel-surface ground water flow is in line with the research assumption.

The analyses for the Afsluitdijk case shows the possibilities to use readily available methods to determine relation between wave overtopping duration and intensity (characterized by q and H_s), and the slope stability. However, the analyses did not lead to a generally applicable simple method to describe this relation.

Chapter 7. Discussion

This chapter aims to discuss the results of the thesis and associated issues such as research questions, methodology, and the significance of the results. The chapter is structured as follows: first, the result of each chapter is briefly summarized and discussed together with the research questions and methodology. Then, the significance of the improved method and the case study are justified.

7.1. Main results, research questions and methodology

This thesis started with problem statement in Chapter 1, which was initiated from basic objectives. Next, research questions were put forward to specify the objectives. Then, the research approach was sketch out to solved the problem and achieve the targets. In addition, some assumptions were essential to shape the thesis boundary.

The research questions stemming directly from the objectives were checked carefully. One thing that needs to be discussed here is the appropriateness of the objectives and the research questions. The utmost objective of the research was to upgrade current assessment tool to a certain degree at which the simple assessments could extend their applicability. One may simply focus on the difference between different assessments methods with different levels of sophistication and gives suggestions. However, the difficulty was that how to upgrade simple methods and enhance the use of them without adding much detailed inputs. Acknowledged this issue, the research questions were formulated carefully, focusing on improving the accuracy of the current assessment tool – Edelman Joustra equation - in predicting slope stability. This ensures that the objectives would be achievable once the research questions are correctly answered. In order to make sure to have good answers, the methodology was planned, connecting the questions to the expected outcomes. Comparing three different methods with different levels of complexity seems to be a sound tool for obtaining the answers. Detailed knowledge about these three methods was elaborated in Chapter 2.

Chapter 2 concentrated on the theoretical explanations used in three methods. The first one was stated in design standard that is the subject of the improvement – Edelman Joustra method. The second was an analytical analysis, which is less advanced than the third one – finite element method. Their advantages and limitations were explained. The methods turned out to be suitable options for making comparisons since the limitations do not have influence on the set-up simulations. Referring to the methodology, finite element method can be seen as the best tool in assessing the stability of the slope. Therefore, using it as the reference tool to check the accuracy and acceptability is the right choice. The detailed verification can be traced back in Chapter 5, section 5.1. The improved method and functions are the result of the comparison between Spencer method and simple method. Choosing Spencer method as one of the detailed analytical analysis is appropriate because of not only the accuracy in iteration calculation, but also the precision of simulating the sliding mechanism (potential slip planes). In short, this methodology is similarly an instrument, which is used to measure the effect of slope length on the stability, and therefore the difference in factor of safety. This gives a sound foundation for implementing these methods in Chapter 3.

Chapter 3 described how safety factor of the downstream slopes were calculated using three different methods. Relevant issues were explained in terms of calculated models so that the comparability between these methods was guaranteed. Since this chapter worked with the question of accuracy, one has to make sure that this reliable instrument should be used correctly to give right and precise answers. To this end, 150 cases were used to generate the improved function. To some extent, this could not represent the entire picture. However, relevant steps of validation mentioned in chapter 5 did argue for the acceptability of the function at a certain degree. For instances, some experiment results were used in the application of the improved function and relatively show the consistency in the accuracy of the effect of L/D (section 5.2.). Moreover, the check of the application of the improved method under different soil properties resulted in an acceptable error margin when the difference between improved method and Spencer method is rather small (approximately lower 5%, see Appendix 6).

The outputs of Chapter 3 were structured and plotted in Chapter 4. Then, the final answer of the research question 1 was found out – a function representing the quantitative effect of ration L/D on landward slopes of dikes. This improved function, in turn, was incorporated into the current assessment guideline in order to form a guideline suggestion in which its applicability will satisfy the initial objectives. The context for applicability will be explained in next section.

The content of Chapter 5 involved results that were used to prove the reliability and validity of the methodology, as referred in previous paragraphs. A part of validation in this chapter was continued in Chapter 6 where a field experiment was simulated to not only check the influence of overtopping discharges on landward slopes, but also gives an examination of the assumption used in the improved method. Specifically, results of Chapter 6 include a result of a slope stability analysis and of a groundwater flow analysis. The slope stability analysis showed that the stability of downward slopes decreased with the creasing infiltration time of overtopping discharges. Besides, transferring different overtopping discharges simulating storm conditions into infiltration process was a good step in this stability analysis. This transfer actually formulated data for water boundary condition in groundwater flow calculation – the second analysis. This analysis showed an agreement between the simulated groundwater flow with the assumption used in Edelman – Joustra method. They agreed on the fact that the groundwater flow actually developed parallel to the surface of the slope, which is essential for sliding mechanism. In this sense, comparing the result of stability analysis with the improved method in terms of safety factor showed the additionally reasonable validation of the improved method.

Next following sections will focus on the significance of the improved method as well as the study of Afsluitdijk case.

7.2. The significance of the improved method

The usefulness of the improved function as well as its applicability on the assessment procedure is the serious concern in the research. This part will shed some light onto this issue and make it clear to other people in following aspects.

First thing is the relevant range of L/D ratio since it concerns how much the improvement can be made between infinite and finite calculations. From the pattern fitting with a curve, the equation showed that the difference between the two method is significant when the L/D is smaller than 25. Since the partial safety factor was ignored, the improved difference still works on the safe side, which ensured the function lying between over conservative point and exact conservative point. This means the function is conservative enough.

Second thing could be the applicability of the function. In reality, many dikes are not safe based on the first simple assessment tool like Edelman – Joustra method. Then, in order to prove these dikes are safe as they are in practice, more detailed calculations are required. Such complicated and costly tests might be not necessary if a sufficient improvement from the slope length effect can be added. For example, Table 14 presents representative dikes geometries of 53 dike rings, including their slope lengths and angles of landward slopes. These inner slope sections presented here are generally made of clay cover layer underlying by a clay core or another lower-permeable clay layer. They are diverse in crest height and slope angles.

These figures show that the diversity in dike profile in the Netherlands gives a room for using this improved function to reduce the assessment costs. For now, it is hard to determine exactly how much complicated evaluations correspond to 15% improvement of the improved method. However, hundreds of kilometers of dikes can be considered as safe without using complicated calculations. Assuming that average thickness of cover layer is 0.8m, almost representative dike rings have L/D ratio smaller than 25, which means falling into the improvement range. Take the geometry of dike ring 6 (Friesland) as an example, the material parameters include: cohesion (3.5 kPa), friction angle (22 deg); saturated unit weight of soil (17 kN/m^3), reliability class of cohesion (1.25), reliability class of friction angle (1.2), and thickness of the cover layer (0.6m). the E_J safety factor was 0.90 which was upgraded up to 1.28 with the improvement of L/D.

Table 14. Dike rings geometry

Dike ring[3]	Dike Crest (m)	Slope toe (m)	Slope angle (1:x)	Slope length (m)	L/D ratio (-)
06	3.770	2.262	2.0	3.37	4.21
09	3.62	1.433	1.5	3.92	4.90
10	5.330	3.167	3.2	7.29	9.11
11	5.390	0.700	4.0	19.36	24.20
13-2-1	3.640	0.080	2.5	9.68	12.10
20-1-1	5.060	2.440	1.6	5.00	6.25

[3] Many thanks to Deltares for allowing to extract information from projects WV21

14-2-1	7.700	2.000	3.2	18.89	23.61
38-1-1	7.040	5.344	3.5	6.18	7.73
41-1-1	11.860	9.100	2.9	8.47	10.59
41-2-1	8.800	6.500	2.6	6.41	8.01
43-1-1	7.700	1.950	4.7	27.59	34.49
43-1-3	10.300	8.233	1.9	4.44	5.55
43-1-5	14.400	12.133	4.0	9.35	11.69
45-1-1	11.990	10.167	2.5	4.91	6.14
48-1-1	18.680	13.00	4.3	25.10	31.38
16-1-1	6.400	3.840	2.9	7.85	9.81
16-1-3	4.900	0.660	1.9	8.96	11.20
17	5.300	2.800	3.0	7.91	9.89
18	5.400	0.400	3.9	20.23	25.29
21	5.330	1.800	3.6	13.22	16.53
22	4.190	0.500	3.0	11.78	14.73
24	6.280	3.800	1.6	4.68	5.85
25-2-1	5.330	1.000	2.0	9.68	12.10
34-1-1	5.280	3.468	2.5	4.88	6.10
35-1-1	5.570	3.442	3.0	6.73	8.41
36-1-1	9.720	6.567	2.9	9.67	12.09
36-1-2	---	---	---	---	---
36a	---	---	---	---	---
37-1-1	7.470	1.880	22.3	14.21	17.76
38-2-1	6.670	4.383	2.5	6.16	7.70
40	---	---	---	---	---
41-1-1	14.480	8.500	3.0	18.91	23.64
42-1-1(b)	17.600	13.167	1.7	8.74	10.93
43	7.220	5.252	2.8	5.85	7.31
44-1-1	10.600	5.400	2.8	15.46	19.33

Moreover, regarding to uncertainty of the improved method in predicting the safety factor, a randomly parametric calculation was done (see in section 5.2.4). The results of 100 random cases gave a R^2 value of 0.97, in which the safety factor of the improved method is smaller than that of Spencer method. The maximum difference is just under 10 percent. This guaranteed the safety concern for the use of the improved method, even though the accuracy is not much high.

Generally, the magnitude of the improvement is varying from 10 to 15 %, compared to the Edelman – Joustra method. This happens in case of L/D ratio varying from 10 to 25. Most of the improvement is for low dikes with short slopes, or slopes divided into two by (stability) berms. One shortcoming of the improved function is that it works properly with cohesion-dominated soil, but not sand-dominant soil. A 5-percent adjustment of the improved method was proposed if soil is strongly sand-dominant, which is distinguished from clay-dominated soil by the indicator - $c/(\gamma'.D.\tan\phi') < 1.05$ – as described in section 5.2.5.

7.3. The significance of the case study

The significance of this case study concerns the effect of average overtopping discharges on the superficial sliding mechanism. In this case, small overtopping discharges with a short time of infiltration have no significant influence on the inner slope stability until the water fills up the majority of macro pores. However, the generalization encountered the problem associated with the infiltration time concept. The time of infiltration plays an important role in this sense. The critical infiltration time for initiating the instability of the cover is dependent on both the overtopping discharge magnitude and the significant wave height. Figure 36 shows the infiltration time as the percentage of the sea state time concerning different wave height and overtopping discharges. This resulted from a probabilistic calculation following similar procedure as stated in 6.2.2, with different significant wave height H_s.

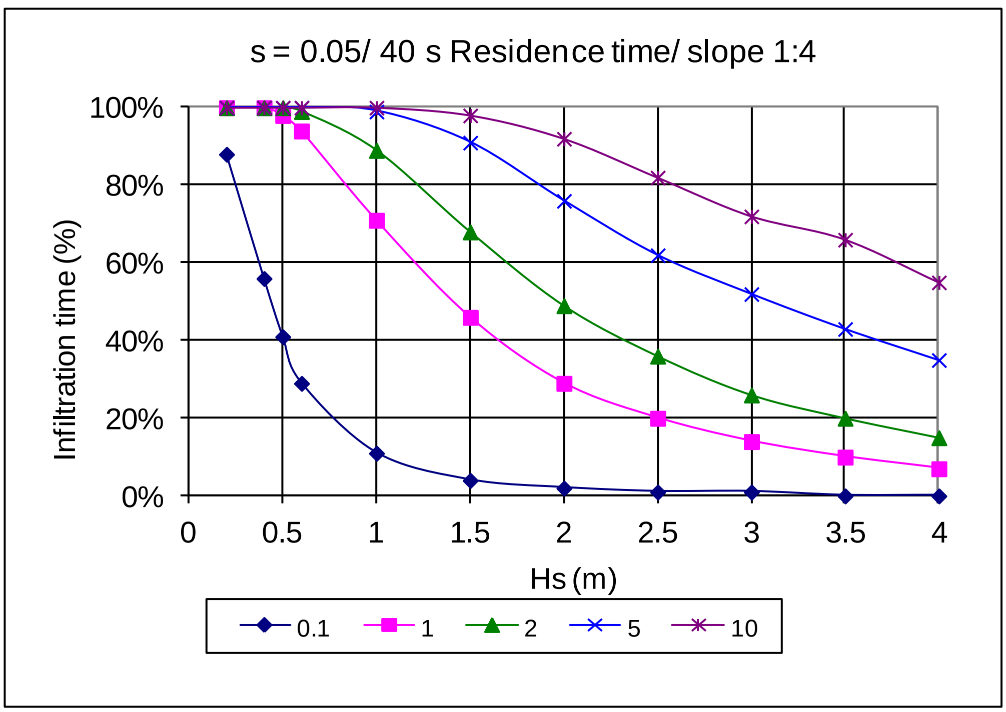

Figure 36. Infiltration time under different overtopping discharges and wave heights

The graph is formulated on the outside slope of 1:4, roughness factor of 1.0, and a wave steepness of 0.05 (-). The experiment measurements indicated that 40 seconds is the time that a superficial point is supposed to be wet due to an overtopping wave (Van Hoven, Hardeman, Van der Meer, and Steendam, 2010). Given storm duration of 6 hours, an overtopping discharge of 1 l/s per m with a wave height of 0.5m may lead to superficial sliding whereas such overtopping discharge with a 2-m wave height does not give any influence. The reason is that the former scenario has a greater infiltration time compared to the latter one (over 95% and just above 40%, respectively).

To have more insights onto the stability of the slope, the infiltration process is extended to 56 hours with the expectation of causing the failure of the inner slope. However, the superficial failure did not occur since the potential slip plane is always on the deeper layer with high safety factors (see Figure 37). From the observation, the groundwater flow decreases its discharges after 10 hours of infiltration. This means that the most dangerous moment of the cover layer is that the groundwater flow is parallel to the slope with the highest velocity or infiltration rate/ discharges. If the cover layer is still stable after this moment, attention will move to global stability. Because the affected zone developed into deeper layers, it distributed the influence of infiltration water through a wider area.

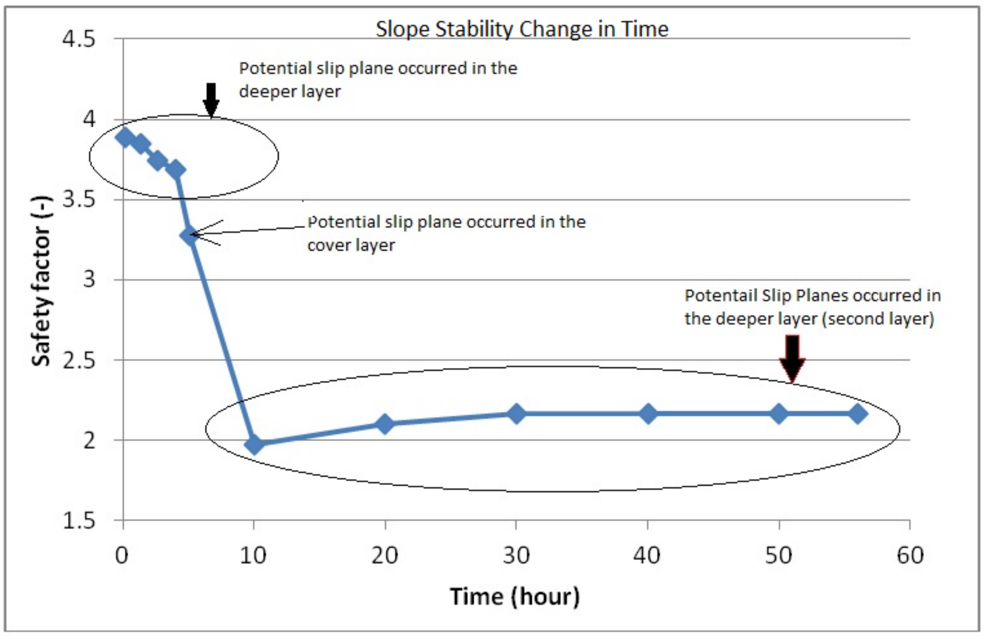

Figure 37. Safety factor versus time in Afsluitdijk case

7.4. Other issues

7.4.1. Dilation angle concern

In slope stability, dilation angle contributes to the critical slope angle. The aim of this section is to get insights onto the influence of dilation angle on stability of the simulated models. Because this understanding helps researchers determine appropriate value of dilation angle used in finite element method in order to make those simulations comparable as much as possible.

By definition, dilation angle indicates changes in volume of a soil when the soil is distorted by shearing. For example, when a soil sample is compressed or stretched, it tends to expand or contract in two other directions perpendicular to the direction of compression or expansion.

This makes the soil volume change under shearing condition. Quantitatively, it is defined as the ratio of shear displacement rate over normal displacement rate. This rate measures the soil expansion. This is quite similar to the definition of Poisson's ratio that is defined as the ratio of horizontal displacement over vertical displacement in the soil sample.

Before using of dilation angle, two concepts need to be reviewed. The first concept is of co-axial model of a soil. This concept assumes the alignment between the direction of deformation rate and the direction of applied stress. In other words, there will be no shear strain if there is no shear stress.

Another assumption is the flow rule that shows an agreement between yield function and plastic potential. In this report, the soil is considered as an associated material, which means that there is a bond connecting soil particles. This makes the soil fail as a flow. With associated materials, the plastic potential is the yield function. It is essential to clarify the definition of yield function and plastic potential. Yield function is a differential function measuring the stress state of a soil. The stress state of a soil is defined by such parameters as principle stress and shear stress. On the other end, plastic potential describes the strain rate, which is proportional to the derivative of flow function to the corresponding stress.

Therefore, when the soil accepts all of the concepts discussed above, the dilation angle can be used with different values varying from zero to friction angle, according to the soil behavior. In addition, the reason for choosing the dilation angle to be equal to the friction angle is explained as follows.

Traditionally, scientists based on simple shear stress condition to determine the stability of infinite slopes. This simple shear stress condition involves slope angles.

$$\sigma_{nt}=\gamma_n.D.\sin\alpha \tag{33}$$

$$\sigma_{tt}=\left(\gamma_n-\gamma_w\right).D.\cos\alpha \tag{34}$$

$$\frac{\sigma_{nt}}{\sigma_{tt}}=\left(\frac{\gamma_n}{\gamma_n-\gamma_w}\right).\left(\frac{\sin\alpha}{\cos\alpha}\right) \tag{35}$$

When studying the stress state on parallel failure plane, Coulomb yields a relation between the normal stress and tangential stress. This relation is defined as $\tan\phi'$.

$$\frac{\sigma_{nt}}{\sigma_{tt}}=\tan\phi' \tag{36}$$

From function 35 and 36, the critical slope angle is identified thanks to the friction angle. This is function 37.

$$\left(\frac{\gamma_n}{\gamma_n-\gamma_w}\right).\tan\alpha=\tan\phi' \tag{37}$$

On the other hand, for design purpose, the critical slope angle is necessarily determined using the condition of velocity discontinuities. This condition is used for plastic potential function. It says that for plane sliding parallel to the slope, there is no tangential strain. This means that the derivative of plastic potential with respect to tangential stress is zero. This differential equation, once it is solved, results in a function, which includes both dilation angle and friction angle.

$$\left(\frac{\gamma_n}{\gamma_n-\gamma_w}\right).\tan\alpha=\frac{\sin\phi'\cos\psi}{1-\sin\phi'\sin\psi} \qquad (38)$$

However, if the soil is considered as associated, the friction angle will be equal to dilation angle. This makes function (38) becomes (37).

Therefore, function 37, once being used in infinite stability analysis, implies that the soil is associated and the friction angle is equal to dilation angle.

7.4.2. Pore water pressure concern

In the previous paragraph, we briefly explained the difference between hydrostatic pressure and pore water pressure at the bottom of cover layer. The former is about 3.7kPa while the latter is only 1.9kPa. This value of 1.9kPa represents the pore water pressure built up at the middle of the slope. According to the prediction, the pore water pressure should be the same at any point along the interface after 5-hour infiltration due to the saturation reached. However, in the simulation at this moment, the entire cover layer is not fully saturated yet. There is still an amount of time so that the entire cover layer becomes saturated. This means that the development of pore water pressure at different locations is different to some extent.

Therefore, we checked three typical positions on the interface to see how different they are in terms of suction pressure, positive pore water pressure, and groundwater head.

In terms of suction, because of the distance between the surface and the phreatic line, the magnitude of suction at different superficial points as well as along the interface is different. The farther the distance is, the higher the suction pressure will be (Figure 38). During the infiltration process, the position close to the dike toe will experience a rapid reduction of suction, compared to other higher locations.

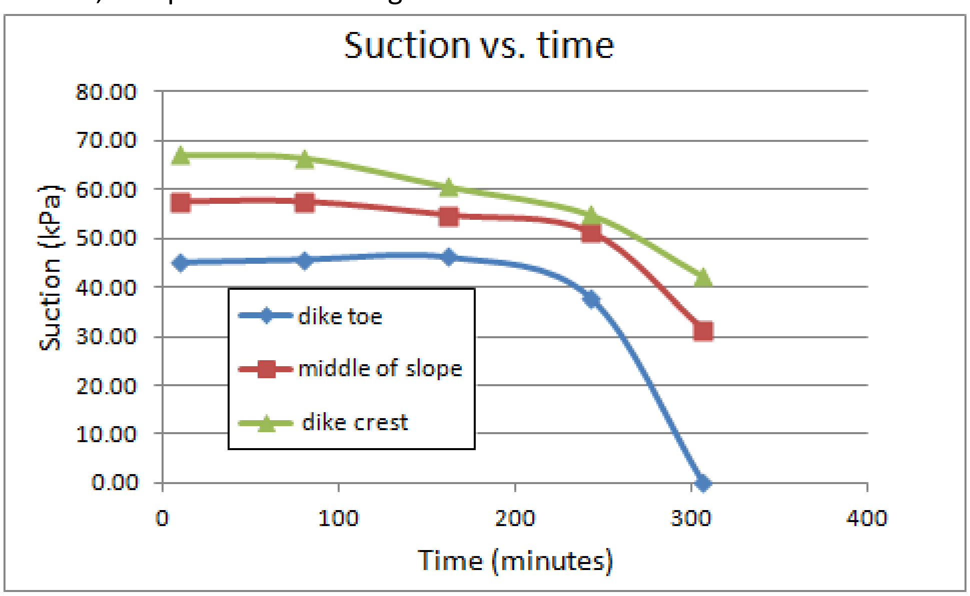

Figure 38. Reduction of suction over time

With respect to the positive pore water pressure, the toe also reaches the saturated condition first. Groundwater head is an alternative of expressing the pore water pressure, which showed that after 5 hour of infiltration; only dike toe had reached positive pore water pressure. Others are still in suction condition (Figure 39).

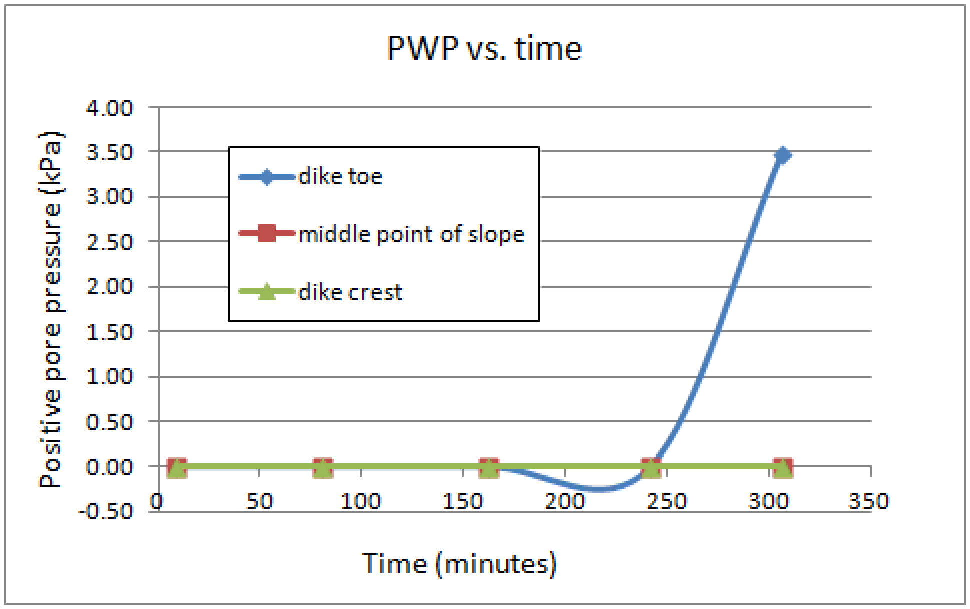

Figure 39. Pore water pressure built up

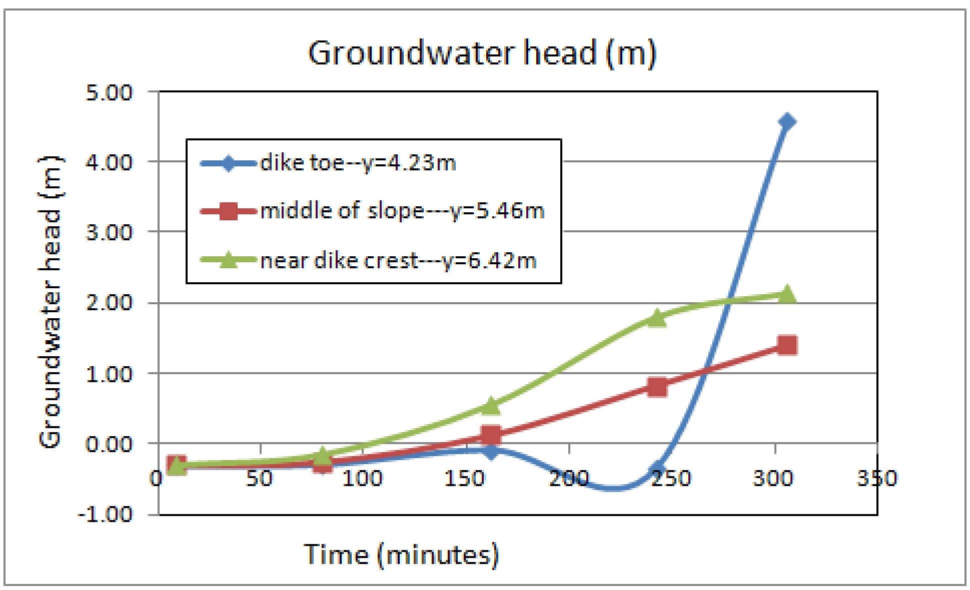

Figure 40. Groundwater head at different positions

The pore water pressure at the dike toe was checked against the measurements of the infiltration experiment on Afsluitdijk (since only two points on the slope were measured in terms of pore water pressure built up). The comparison showed a relative agreement between simulation and the experiment results.

Location	Simulation results (kPa)	Experiment results (kPa)

Dike toe	3.47	3.30

Chapter 8. Conclusions and Recommendations

8.1. Conclusions

This section will briefly summarize the whole report and gives some ideas about the contribution of the thesis. Initiating with a small aspect of problems of the project, we plan research questions and remind of finding the answers. The first main research question is about the improvement of simple assessment tool for sliding of the cover layer due to wave overtopping. This is possible as the Edelman – Joustra assessment was improved with the quantitative supplement of the effect of slope length. The definitive and important results are the improved functions, which quantified the effect of L/D ratio on superficial stability of the inner slopes.

To practical application, the thesis provides an improved method for assessing the stability against superficial sliding mechanism. The applicability of this improved method is proved in comparison discussion part (Chapter 7). Its condition is addressed in the relevant range of L/D ratio part (section 5.2.5). Furthermore, a guideline for assessing inner slope stability is suggested to incorporate into the statutory assessment tools, in which inner slope with a slope angle of 1V:3H can be accepted with corresponding conditions.

The analysis of Afsluitdijk – case study gave the answer to the second research questions, which asked for the effect of overtopping discharges on the inner slope stability. The analysis quantitatively showed the relation between overtopping discharges (characterized by q and H_s) and overtopping duration, and the slope stability. The relation was determined using readily simple methods such as wave simulation, infiltration and stability calculation. However, the analysis did not lead to a generally applicable simple method to describe this relation.

With regard to the theoretical contribution, the study gives an agreement between Edelman – Joustra assumption with FEM simulation on the ground water flow (in case study, Chapter 6). This in turn demonstrates the applicability of the adapted method. Moreover, the simulation of how the overtopping discharge is transferred to water boundary condition of infiltration process also contributes to the understanding of built-up pore water pressure.

8.2. Recommendations

From the previous discussion, it seems that there is room to improve the accuracy of the proposed method. Following recommendations target to address relevant aspects:

Firstly, both improved functions work with the ratio of L/D varying from 10 to 25. With smaller values of the ratio, the difference between improved method and Spencer method diverges considerably. This mainly happens in case of quite steep slopes, and therefore, further investigation is advisable in this aspect.

Secondly, even though a number of randomly parametric calculations were done to determine the accuracy of the improved method for predicting superficial stability of slopes, the error margin seemed to be limited in sample size. Increasing correcting the function with probabilistic analyses could be recommended.

Thirdly, the suggestion guideline stemmed from a limited number of experiments that appear not to get convincing argumentation. In addition, only one analytical method – Spencer – was used in the research approach. This can be improved by getting involved appropriate analytical methods of slope stability.

Fourthly, it would be valuable if the soil-structure of the cover layer can be investigated and a possible new soil model can be formulated to characterize the soil properties of cover layers. The shear strength of such kind of material can be determined with a new soil model if some field experiments or numerical approximation solutions successfully simulate soil behaviors.

Sixthly, we suggested that the difference in permeability between the cover layer and deeper layers should be investigated to have a clear correlation between this difference and the development of groundwater flow. By doing this, we can get insights onto the use of the assumption used in this research quantitatively, which in turn can underpin the assumption completely.

Finally, the possibility of upgrading the limitation of 0.1 l/s per m to 1.0 l/s per m in terms of average overtopping discharge is feasible. Therefore, there might be a comprehensive approach to have more evidence similar to the case study in this report so that the extension is well justified.

References

Bosman, G. (2007). “Velocity and flow depth variations during wave overtopping.” Master Thesis, Deparment of Coastal Engineering, Technology University of Delft, Netherlands.

Brinkgreve, R. B. J., Swolfs, W. M., Engin, E. (2010). *Plaxis 2D 2010.* PLAXIS bv, Delft, The Netherlands.

Budhu, M. (2007). *Soil mechanics and foundations* (pp.119-125), John Wiley & Sons, Inc, United States of America.

Cala, M., Fliksiak, J., and Tajdus, A. 2004. “Slope stability analysis with modified shear strength reduction technique.” Dept. of Geomechanics, Civil Engineering & Geotechnics, AGH University of Science & Technology, Poland.

Carpenter, J. R. (1985). “STABL5...The Spencer method of slices.” Purdue Unversity , Indiana.

Collins, B. D., and Znidarcic, D. (2004). “Stability analyses of rainfall induced Landslides.” *Journal of Geotechnical and Deoenvironmental Engineering* , Vol. 130, No. 4, pp. 362-372.

Crabb, G. I., and Atkinson, J. H. (1991). “Determinations of soil strength parameters for the analysis of highway slope failures.” *Proceedings of the international conference on slope stability*. The Institute of Civil Engineers, Isle of Wight, pp. 13-18.

Daniel Pradel, and Glen Raad. (1993). “Effect of permeability on superficial stability of homogeneous slopes.” *Journal of Geotechnical Engineering* , Vol. 119, No. 2, pp. 315-332.

Fredlund, D. (1984). “Analytical methods for slope stability analysis.” *Proceedings of the Fourth International Symposium on Landslides, State-of-the-Art*, Toronto, Canada, pp.229-250.

Griffiths, D. V., and Lane P. A. (1999). “Slope stability analysis by finite elements”. *Geotechnique 49* , No. 3, pp.387-403.

Jorissen, R., Van Loon, J. L., and Lorenzo, A. M. (2000). “Flooding risk in coastal. Risks, safety levels and probabilistic techniques in five countires along the North Sea coast.” Ministry of Transport, Public Works and Water Management.

Krishna, P. A. (2006). “Slope stability evaluations by limit equilibrium and finite element method.” PhD. Dissertation, Departmet of Civil and Transport Engineering, Norwegian University of Science and Technology, Trondheim.

Meij, R., and Sellmeijer, J. B. (2012). “A generic algorithm for solving slope stability problems: from Bishop to a free slip plane.” Deltares Institute, Delft, Netherlands.

Milledge, D. G., Griffiths, D. V., Lane, S. N., and Warburton, J. (2010). “Limits on the validity of infinite length assumptions for modelling shallow landslides.” Wiley Online Library, University of California.

Naresh C. Samtani, and Edward A. Nowatzki. (2006). *Soils and foundations,* National Highway Institute Washington, D.C.

NEN 6740 (1990). “Geotechnics - TGB 1990 – Basic Requirements and Loads.” NNI (Nederland’s Nor-malisatie-Instituut), Delft, The Netherlands.

Paul, D. L., and Jeanne, E. O. (2010). *Practical research. Planning and design. Ninth Edition.* Pearson Education Inc , New Jersey.

Reginald, H., Thamer, Y., Brent, C., and John C., (2005). “A comparison of finite element slope stability analysis with conventional limit-equilibrium investigation*.”* University of Toronto, Canada.

Steendam, G.J., Van der Meer, J.W., Hardeman, B., and Van Hoven, A. (2010). “Destructive wave overtopping tests on grass covered lanward slopes of dikes and transitions to berms.” *Proceedings of the International Conference on Coastal Engineering, No 32 (2010)*, Shanghai, China, pp. 1-14.

Sorensen, R. M. (2006). *Basic coastal engineering. Third Edition.* Springer Science, New York.

Spencer, E. (1967). “A method of analysis of the stability of embankment assuming parallel inter-slice forces.” *Journal of Geotechnique* , No. 17, pp. 11-26.

Spencer, E. (1989). “Slope stability.” Retrieved March 20, 2012, from Civil Engineering Software: http://www.finesoftware.eu/geotechnical-software/help/slope-stability/spencer/

TAW. (2001). Technical Advisory Committee for Water – Retaining Structures. Technical Report Water-retaining soil structures, Geotechnical aspects of dikes, dams and embankments.

Teunissen , J. A. M., and Spierenburg , S. E. J. (1995). “Stability of infinite slopes.” *Geotechnique* , Vol. 45, No. 2, pp. 321-323.

Trompille, V., and Eerninck, N. L. M. (2011). D-Geo Stability Version 10.1. Slope stability software for soft soil engineering. Deltares, the Netherlands.

Van Hoven, A., Hardeman, B., Van der Meer, J.W., and Steendam, G. J. (2010). “Sliding stability of landward slope clay cover layers of sea dikes subject to wave overtopping.” *Proceedings of the International Conference on Coastal Engineering, No 32 (2010)*, Shanghai, China, pp. 1-12.

Van Hoven, A., Verheij, H., and Van der Meer, J.W. (2009). “SBW Golfoverslag en Sterkte Grasbeklding.” Deltares Institute, Delft, Netherlands.

Vrouwenvelder A.C.W.M., and Siemes A.J.M. (1987). “Probabilistic calibration procedure for the derivation of partial safety factors for the Netherlands Building Codes.” Delft University of Technology.

Yu, H. S., Salgado, R., Sloan, S. W., and Kim, J. M. (1998). “Limit Analysis versus Limit Equilibrium For Slope Stability.” *Journal of Geotechnical and Geoenvironmental Engineering*, Vol. 124, No. 1, pp. 1-11.

Yu-Jie, W., and Jian-Hua, Y. (2001) “Slope stability analysis using a method with associated and non-associated flow rules.” Department of Civil & Structural Engineering, The Hong Kong Polytechnic University, Hong Kong .

Appendices

Appendix 1: Edelman – Joustra Method Calculation

SAFETY FACTORS FROM INFINITE ANALYSIS							
Parameter	Unit	Sit.1->5	Sit.6->10	Sit.11->15	Sit.16->20	Sit.21->25	Sit.26->30
Cohesion	kN/m2	4	4	4	4	4	4
Friction angle	deg	20	20	20	20	20	20
Crest height	m	2	4	6	8	10	10
Slope angle	deg	33.71	26.58	21.81	18.44	15.95	14.04
Layer thickness	m	0.6	0.6	0.6	0.6	0.6	0.6
Densityt of soil	kN/m3	20	20	20	20	20	20
Unit weight of water	kN/m3	9.81	9.81	9.81	9.81	9.81	9.81
Safety factor		**0.879**	**1.116**	**1.361**	**1.610**	**1.862**	**2.116**
Parameter	Unit	Sit.31->35	Sit.36->40	Sit.41->45	Sit.46->50	Sit.51->55	Sit.56->60
Cohesion	kN/m2	4	4	4	4	4	4
Friction angle	deg	20	20	20	20	20	20
Crest height	m	2	4	6	8	10	10
Slope angle	deg	33.71	26.58	21.81	18.44	15.95	14.04
Layer thickness	m	0.8	0.8	0.8	0.8	0.8	0.8
Densityt of soil	kN/m3	20	20	20	20	20	20
Unit weight of water	kN/m3	9.81	9.81	9.81	9.81	9.81	9.81
Safety factor		**0.729**	**0.930**	**1.136**	**1.347**	**1.559**	**1.772**
Parameter	Unit	Sit.61->65	Sit.66->70	Sit.71->75	Sit.76->80	Sit.81->85	Sit.86->90
Cohesion	kN/m2	4	4	4	4	4	4
Friction angle	deg	20	20	20	20	20	20
Crest height	m	2	4	6	8	10	10
Slope angle	deg	33.71	26.58	21.81	18.44	15.95	14.04
Layer thickness	m	1	1	1	1	1	1
Densityt of soil	kN/m3	20	20	20	20	20	20
Unit weight of water	kN/m3	9.81	9.81	9.81	9.81	9.81	9.81
Safety factor		**0.639**	**0.818**	**1.002**	**1.188**	**1.377**	**1.566**
Parameter	Unit	Sit.91->95	Sit.96->100	Sit.101->105	Sit.106->110	Sit.111->115	Sit.116->120
Cohesion	kN/m2	4	4	4	4	4	4
Friction angle	deg	20	20	20	20	20	20
Crest height	m	2	4	6	8	10	10
Slope angle	deg	33.71	26.58	21.81	18.44	15.95	14.04
Layer thickness	m	1.2	1.2	1.2	1.2	1.2	1.2
Densityt of soil	kN/m3	20	20	20	20	20	20
Unit weight of water	kN/m3	9.81	9.81	9.81	9.81	9.81	9.81
Safety factor		**0.578**	**0.743**	**0.912**	**1.083**	**1.255**	**1.429**
Parameter	Unit	Sit.121->125	Sit.126->130	Sit.131->135	Sit.136->140	Sit.141->145	Sit.1466->150
Cohesion	kN/m2	4	4	4	4	4	4
Friction angle	deg	20	20	20	20	20	20
Crest height	m	2	4	6	8	10	10
Slope angle	deg	33.71	26.58	21.81	18.44	15.95	14.04
Layer thickness	m	1.4	1.4	1.4	1.4	1.4	1.4
Densityt of soil	kN/m3	20	20	20	20	20	20
Unit weight of water	kN/m3	9.81	9.81	9.81	9.81	9.81	9.81
Safety factor		**0.536**	**0.690**	**0.848**	**1.008**	**1.169**	**1.330**

Appendix 2: Spencer's Theory Explanation

This section elaborates on the forces acting on the inter-slices, and gives a clear procedure for calculating the factor of safety (Spencer, 1967). In this method, the studied soil body above the assumed slip plane is divided into small vertical slices. Each slice has a specific height, h and a width, b (see in Figure 41). An enlarged sketch of considered forces acting on the slice is given in the Figure 42. Those forces are described as follows:

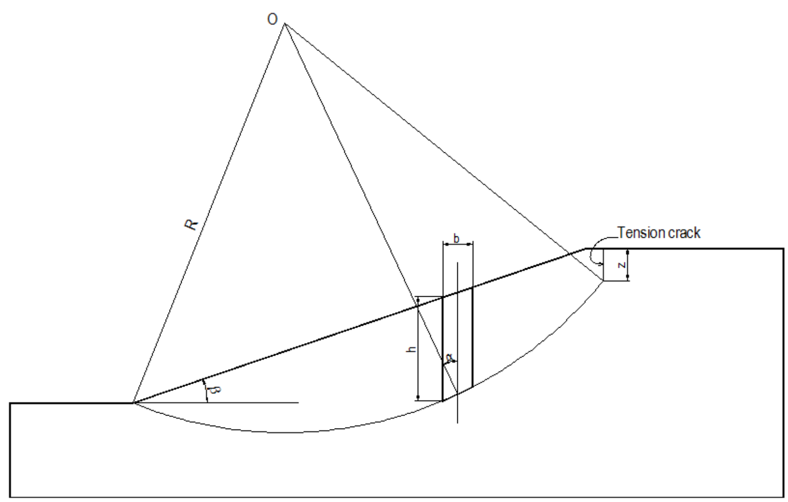

Figure 41. Slip plane

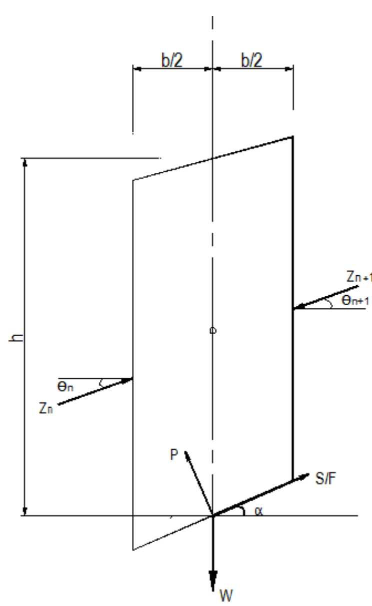

Figure 42. Considered forces

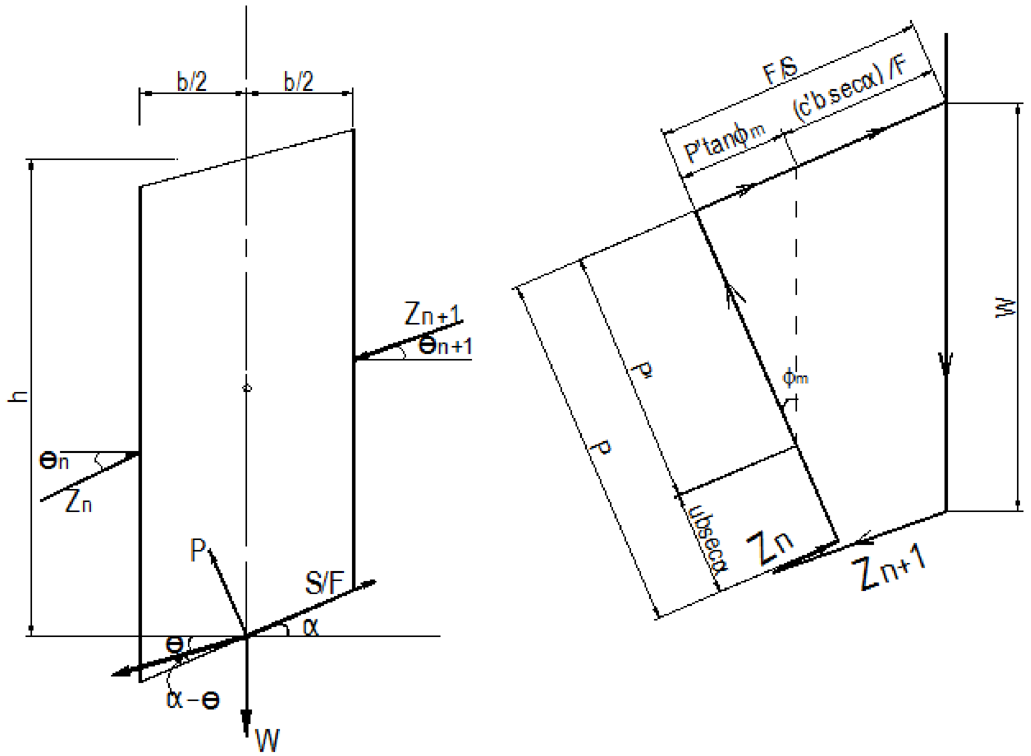

Figure 43. Force analysis

i) The weight, W

ii) The total reaction, P perpendicular to the base of the slice; this force will have two components:

a. The force P' due to the effective or inter-granular stress;

b. The force ($u.b/\cos\alpha$) due to the pore pressure;

Thus

$$P = P^{'} + u b \sec\alpha \quad [33]$$

The mobilized shear force $S_m = \frac{S}{FOS}$, [34]

where $S = c.b.\sec\alpha + P^{'}\tan\phi^{'}$ [35]

The inter-slice forces Z_n and Z_{n+1}; for equilibrium, the resultant Q of these two forces must pass through the point of intersection of the three other forces.

If the presence of the inter-slice forces is ignored, the three remaining forces are, of course, concurrent and in this case both equilibrium conditions can be satisfied by resolving moments. The following expression is obtained for the factor of safety of the embankment:

$$FOS = \frac{1}{\sum[W\sin\alpha]}\sum\left[cb\sec\alpha + \tan\phi^{'}\left(W\cos\alpha - ub\sec\alpha\right)\right] \quad [36]$$

The value FOS in this case is less than that obtained when the effect of inter-slice forces is taken into account.

Back to the consideration of the inter-slices forces, these forces in a fully rigorous solution would be separated into two components like force P. One of these components would be derived from effective stress and the other from pore pressure. In this analysis, the total force is used for the sake of simplicity.

By resolving perpendicular and parallel to the base of the slice, five forces are shown Figure 43, the following expression is obtained for the resultant Q of the two inter-slice forces:

$$Q = \frac{\frac{cb}{FOS}\sec\alpha + \frac{\tan\phi^{'}}{FOS}\left(W\cos\alpha - ub\sec\alpha\right) - W\sin\alpha}{\cos\left(\alpha-\theta\right)\left[1 + \frac{\tan\phi^{'}}{FOS}\tan\left(\alpha-\theta\right)\right]} \quad [37]$$

Now if the external forces on the embankment are in equilibrium, the vectorial sum of the inter-slice forces must be zero. In other words, the sum of the horizontal components of the inter-slice forces must be zero and the sum of their vertical components must also be zero, i.e.

$$\sum\left[Q\cos\theta\right] = 0 \quad [38]$$

And

$$\sum\left[Q\sin\theta\right] = 0 \quad [39]$$

Moreover, if the sum of the moments of the external forces about the center of rotation is zero, the sum of the moments of the inter-slice forces about the center of rotation must also be zero:

$$\sum\left[QR\cos\left(\alpha-\theta\right)\right] = 0 \quad [40]$$

And since the slip plane is assumed to be circular, the expression can be re-written as follows;

$$\sum\left[Q\cos\left(\alpha\text{-}\theta\right)\right]=0 \tag{41}$$

In a given problem, there are three equations to be solved: two with respect to forces and one in respect of moments. Value of FOS and of θ must be found so that all three equations are satisfied while the value of θ must be the same for a given slice (Carpenter, 1985).

Appendix 3: Spencer's Method Calculation

This example applies the soil model and the material parameters of the situation 1 (as stated in Chapter 3) into D Geo Stability. The calculation procedure is described in following steps.

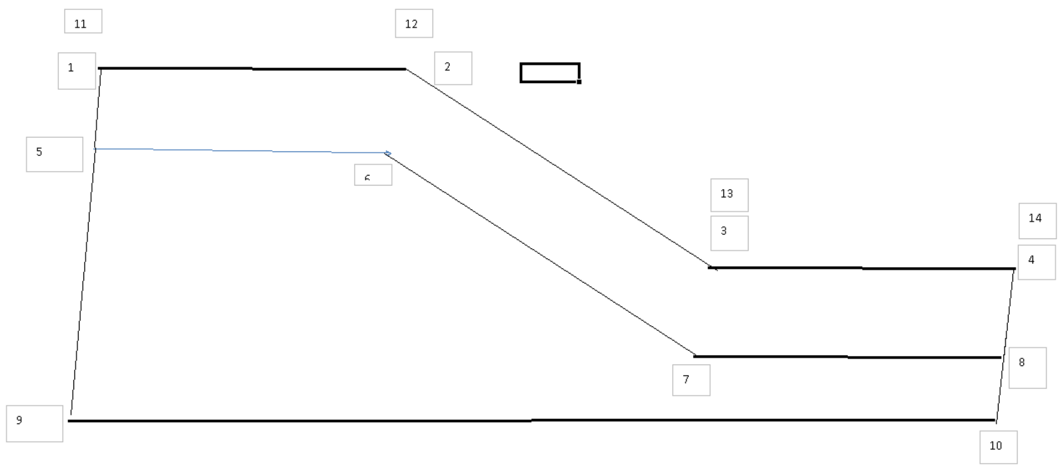

- Initial data:

  Crest height: H (m)

  Crest width: b (m)

  Thickness of cover layer: d (m)

  Slope angle: alpha (deg)

  Left and right limits: (0; x10)

  Bottom boundary: -5 (m)

- Coordinate calculation:

Table 15. Geometry coordinates of a section built up

Point	Coordinate	
	X	Y
1	X1=0	Y1=H
2	X2=b	Y2=H
3	X3= X2 + H*tan(alpha)	Y3 = Y2 - H
4	X4 = X3 + right limit	Y4 = Y3

5	X5 = X1	Y5 = H – d
6	X6 = X2 – d*tan (alpha/2)	Y6 = Y5
7	X7 = X6 + H*tan (alpha)	Y7 = Y3 – d
8	X8 = X4	Y8 = Y4 – d
9	X9 = X1	Y9 = bottom boundary
10	X10 = X9	Y10 = bottom boundary
11	X11 = X1	Y11 = Y1
12	X12 = X2	Y12 = Y2
13	X13 = X3	Y13 = Y3
14	X14 = X4	Y14 = Y4

Step 1: Impute data of geometry into Spencer model.

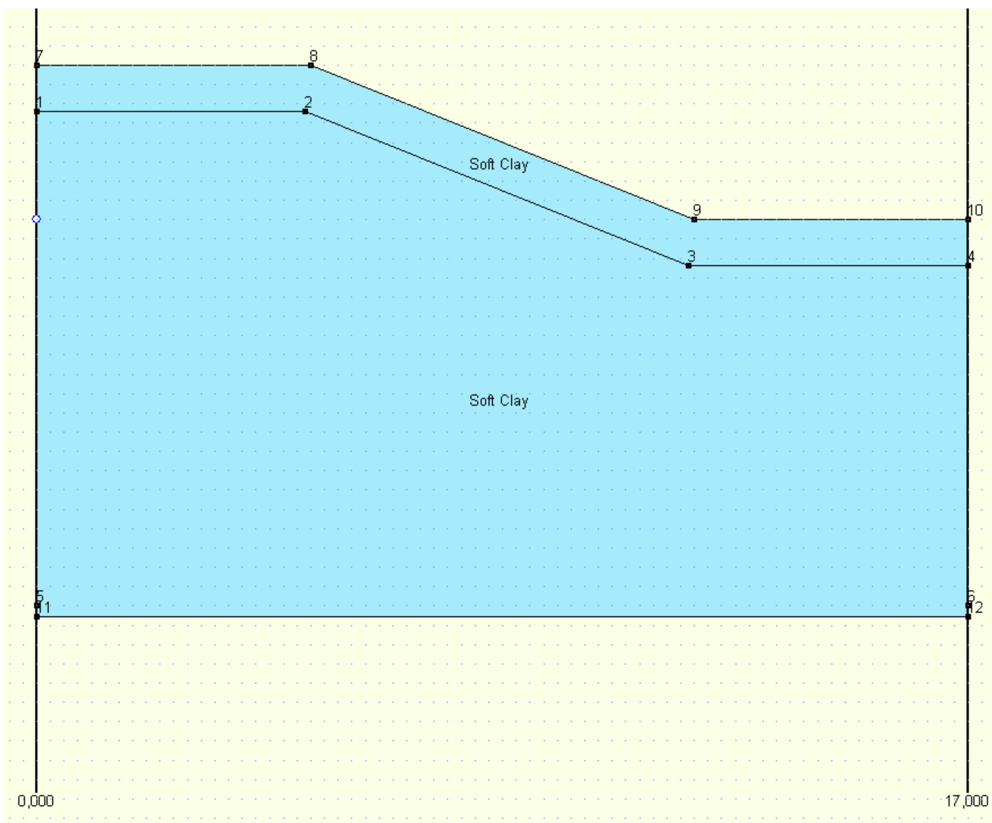

Step 2: Material properties

Define soil layers

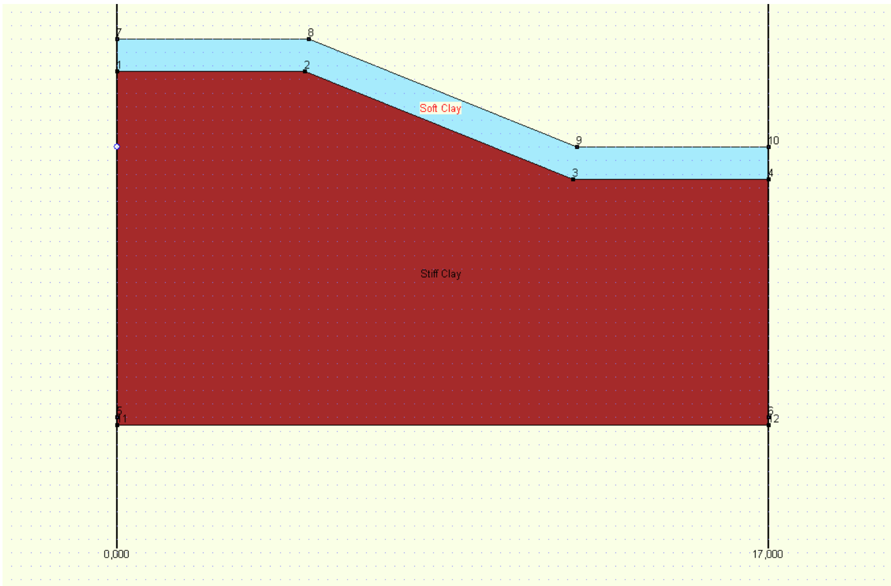

Top cover layer property:

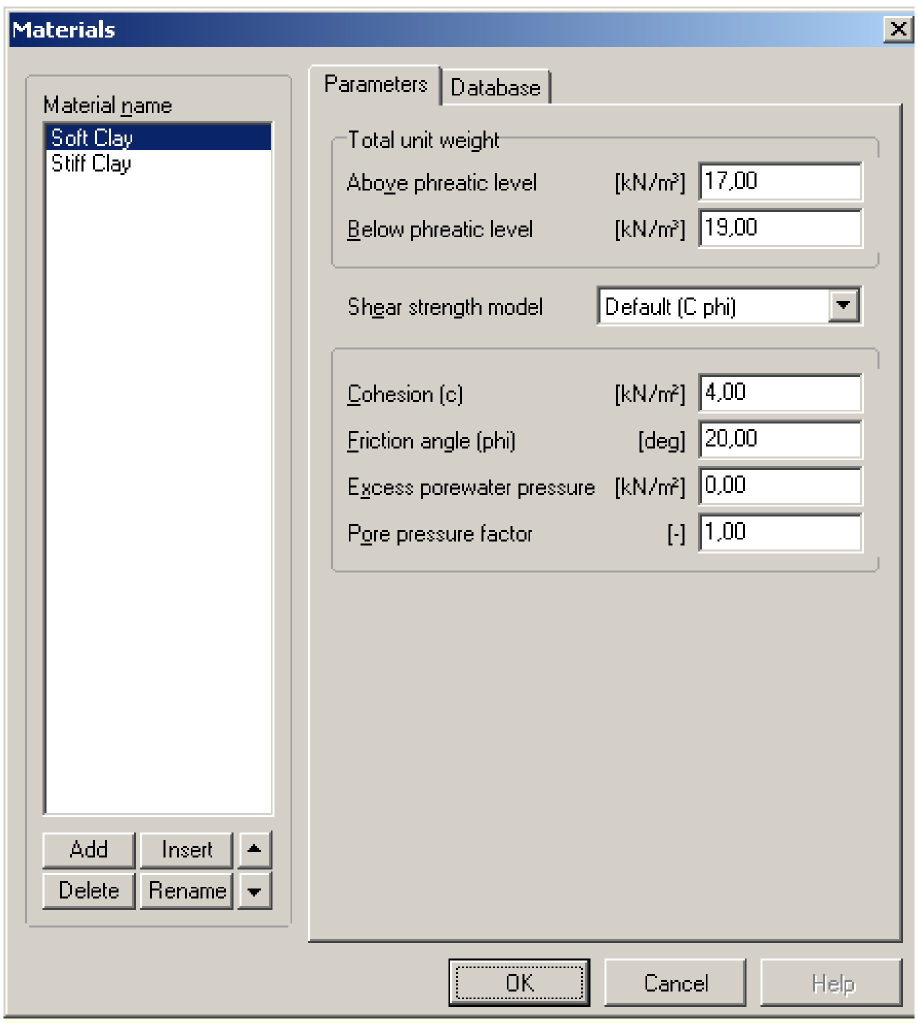

Dike core property:

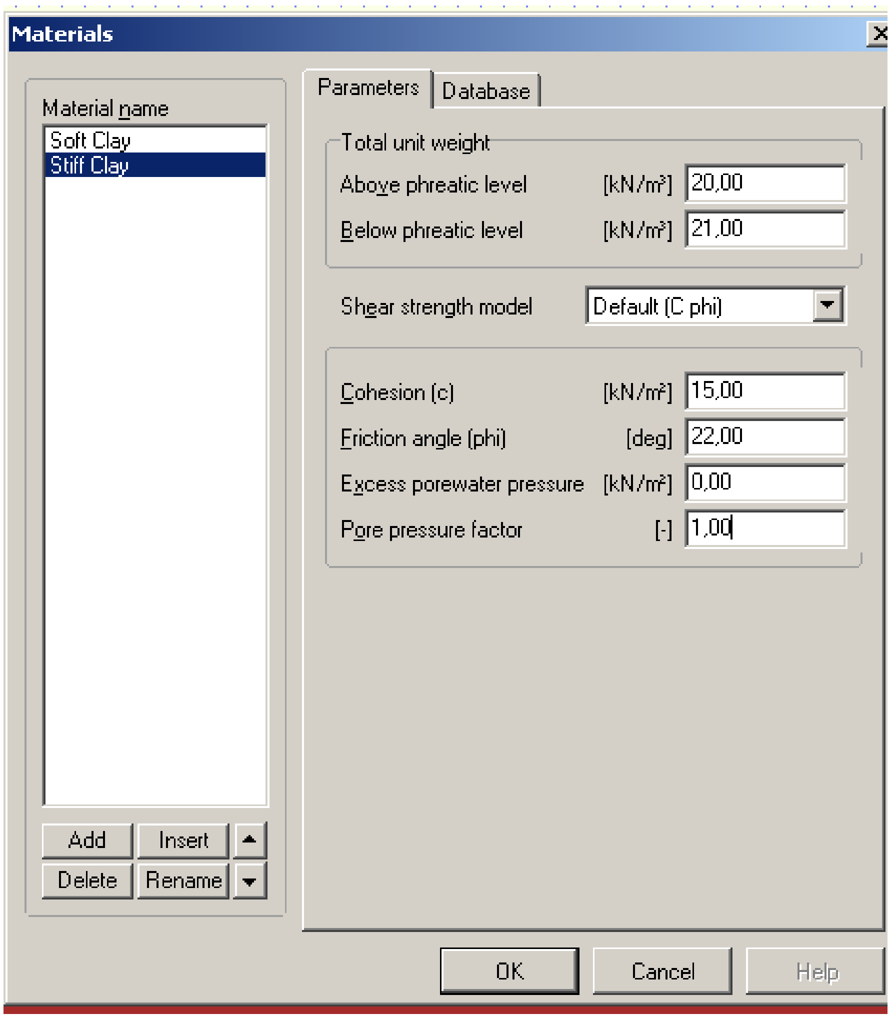

Step 3. Define slip plane

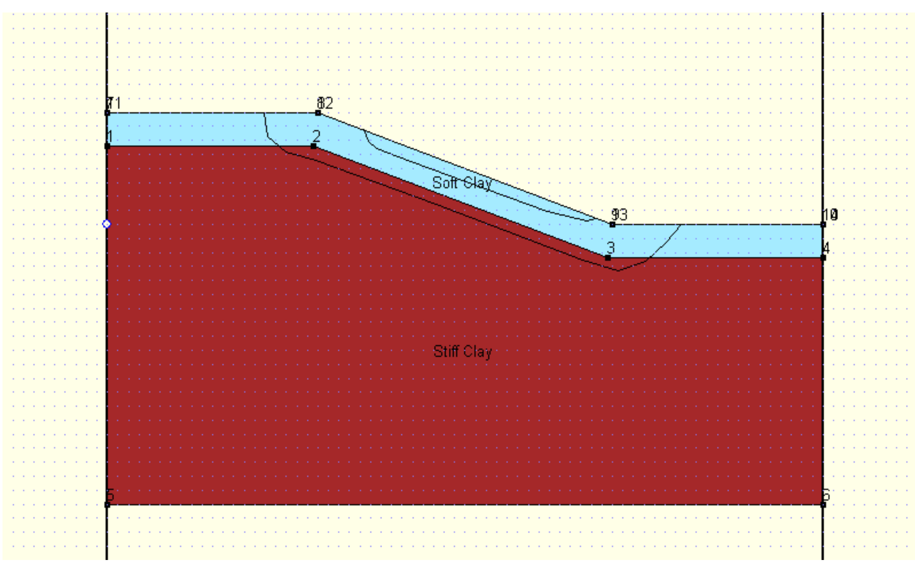

Step 4: Define phreatic line. The phreatic line is supposed to be coincided with the slope surface to ensure the assumption of saturated soil.

Step 5: Define unit weight of water: 8.162 (kN/m^3).

Step 6: Calculation and Result

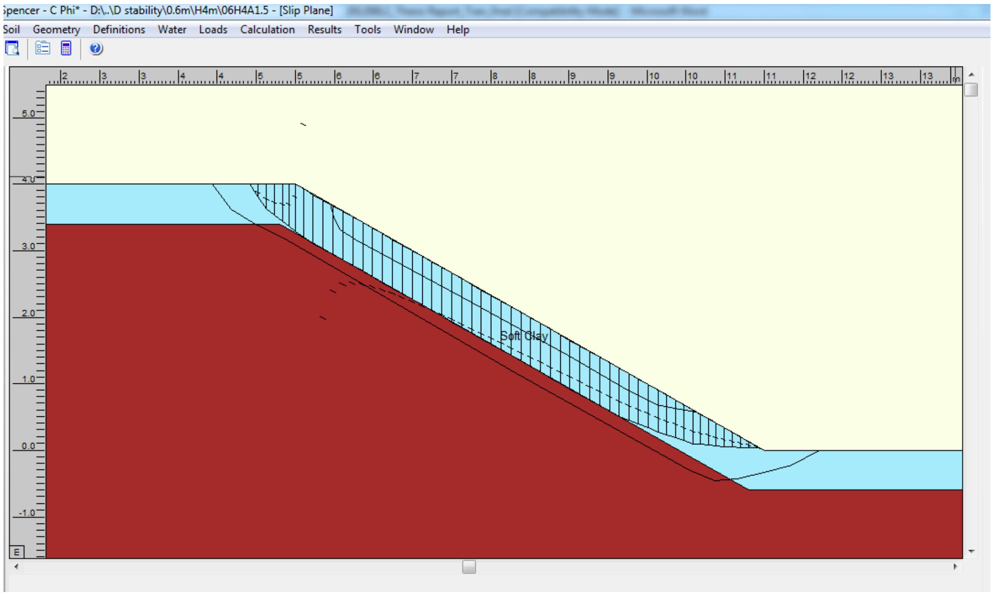

For example, the factor of safety in this situation is 1.33.

Appendix 4: Plaxis calculation

Using the same soil parameters of Spencer's model and adding some required stiffness properties, Plaxis calculation analyses the stability of inner slope of situation 1.

Step 1: import geometry from D Geo stability

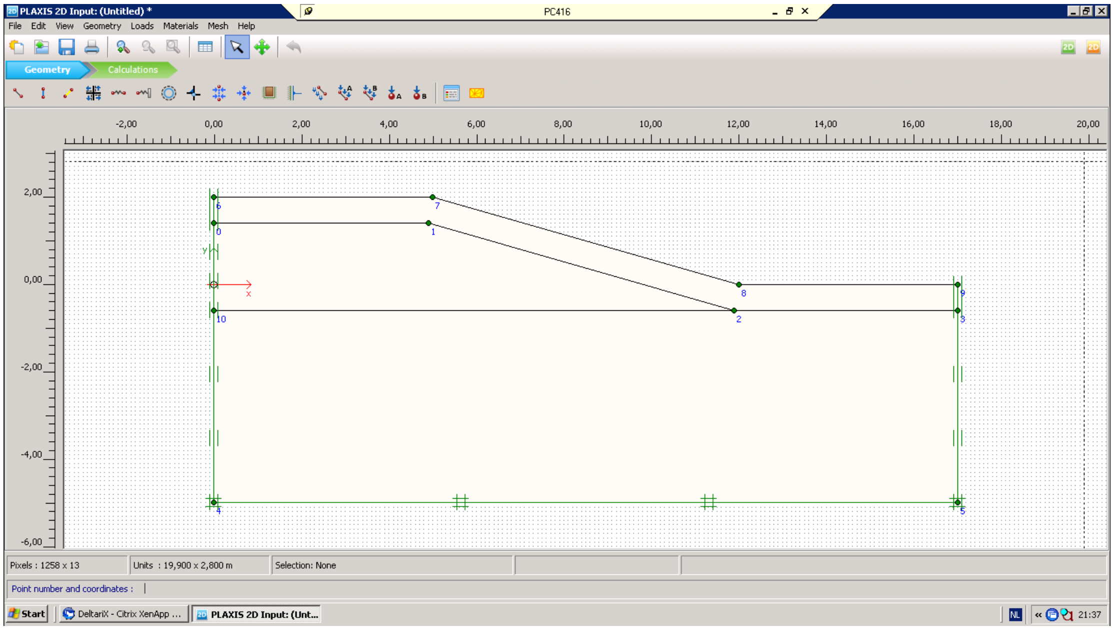

Step 2: Define material properties

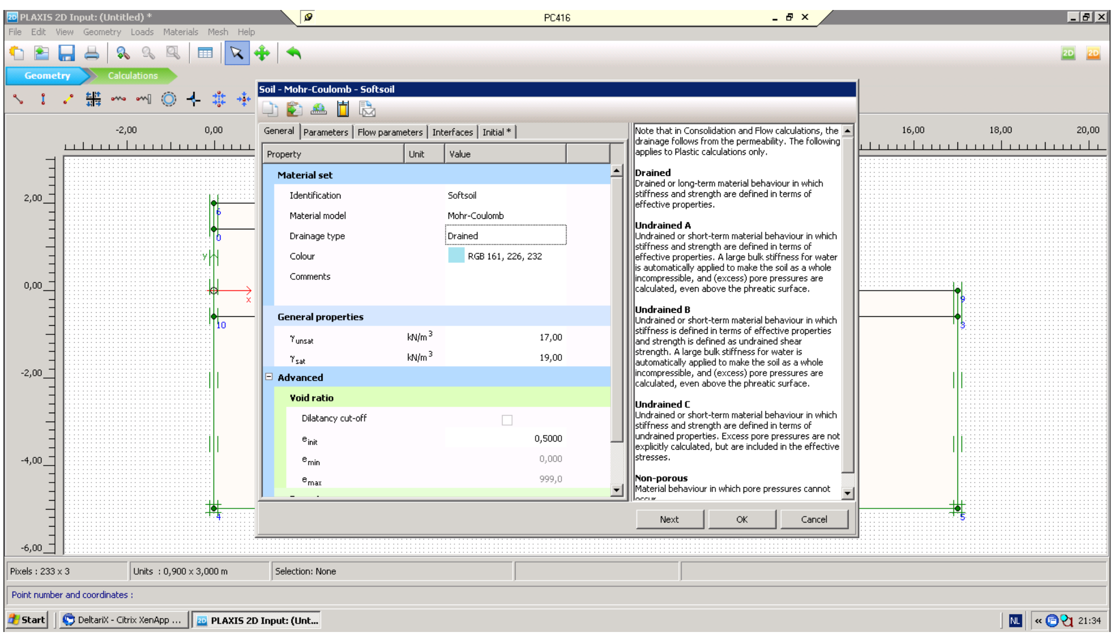

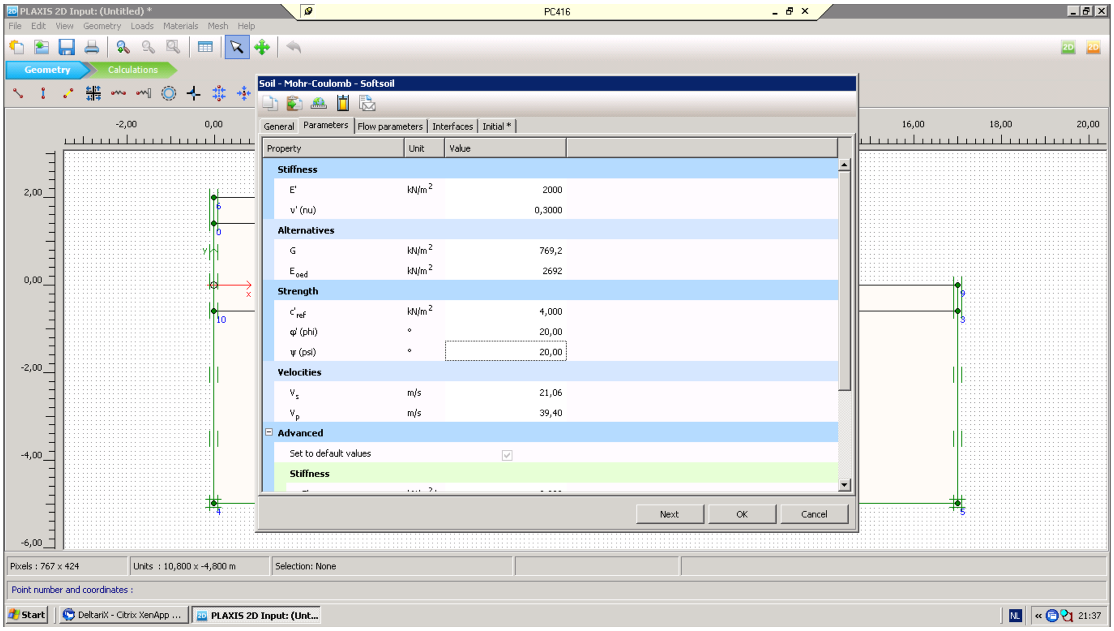

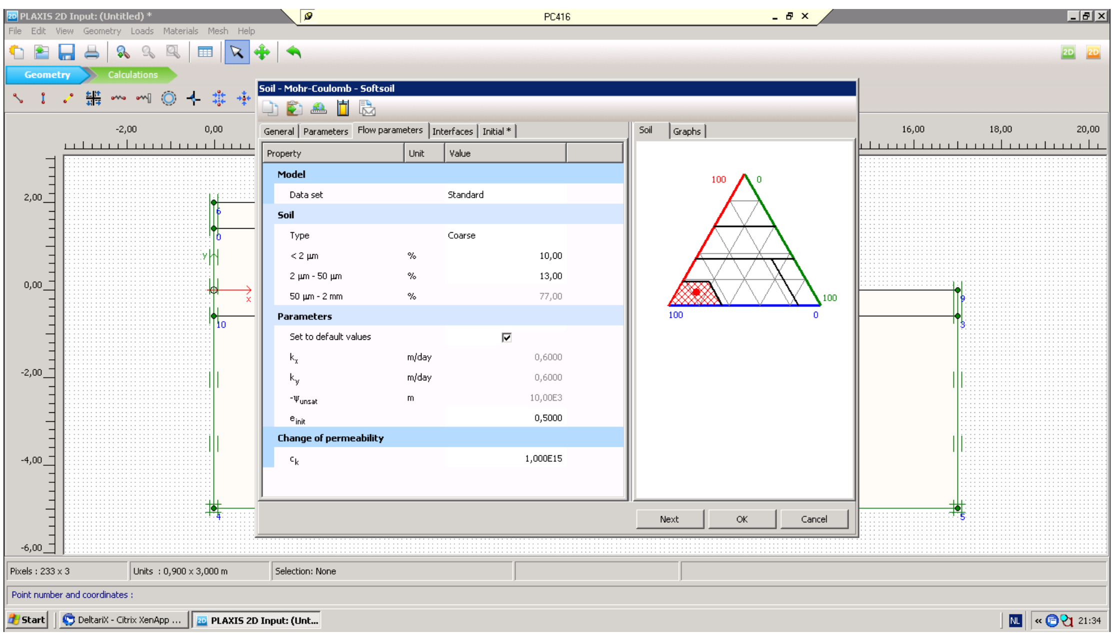

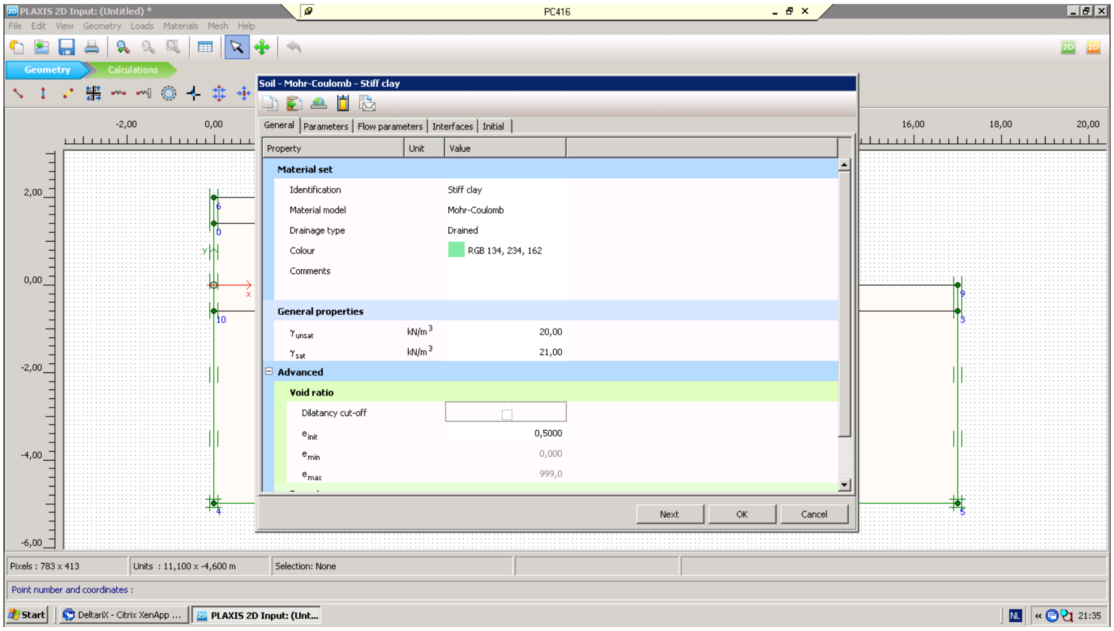
PLAXIS 2D Input: (Untitled) *
Soil - Mohr-Coulomb - Stiff clay
General
Parameters
Flow parameters
Interfaces
Initial
Property
Unit
Value
Material set
Identification
Stiff clay
Material model
Mohr-Coulomb
Drainage type
Drained
Colour
RGB 134, 234, 162
Comments
General properties
kN/m3
20,00
21,00
Advanced
Void ratio
Dilatancy cut-off
0,5000
0,000
999,0
Next
OK
Cancel

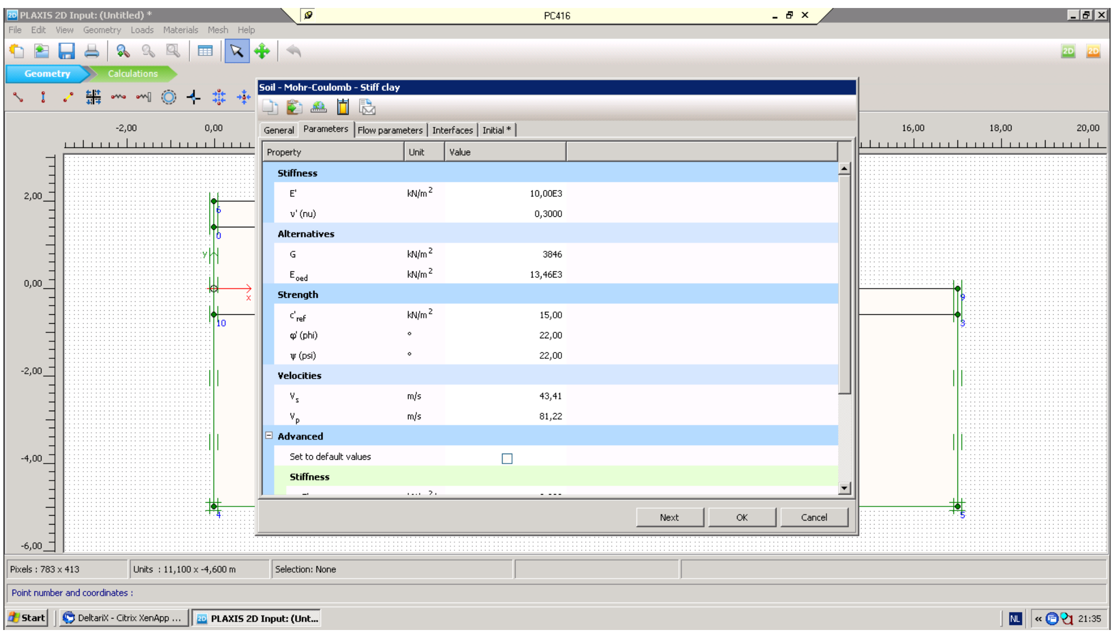
PLAXIS 2D Input: (Untitled) *
Soil - Mohr-Coulomb - Stiff clay
General
Parameters
Flow parameters
Interfaces
Initial *
Property
Unit
Value
Stiffness
E'
kN/m2
10,00E3
v' (nu)
0,3000
Alternatives
G
3846
13,46E3
Strength
15,00
φ' (phi)
22,00
ψ (psi)
22,00
Velocities
m/s
43,41
81,22
Advanced
Set to default values
Stiffness
Next
OK
Cancel

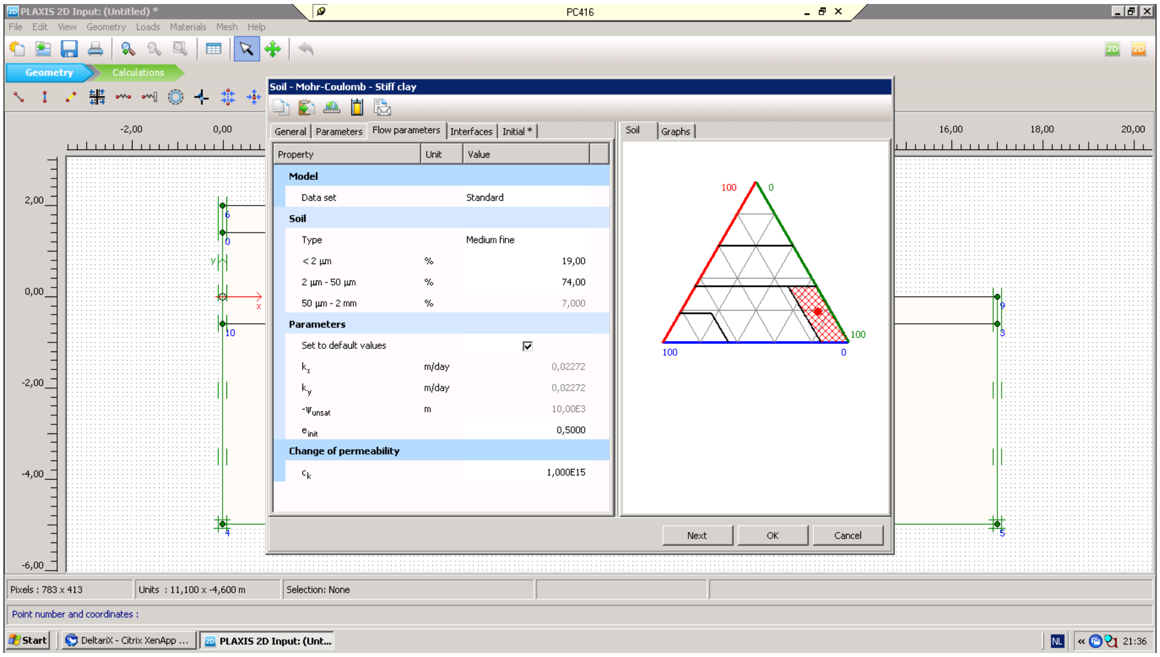

Step 3: Calculation:

This step covers some activities including generating mesh, creating profile of initial phase, construction phase and safety analysis phase. The unit weight of water is entered in each phase and corresponding to slope angle (as stated).

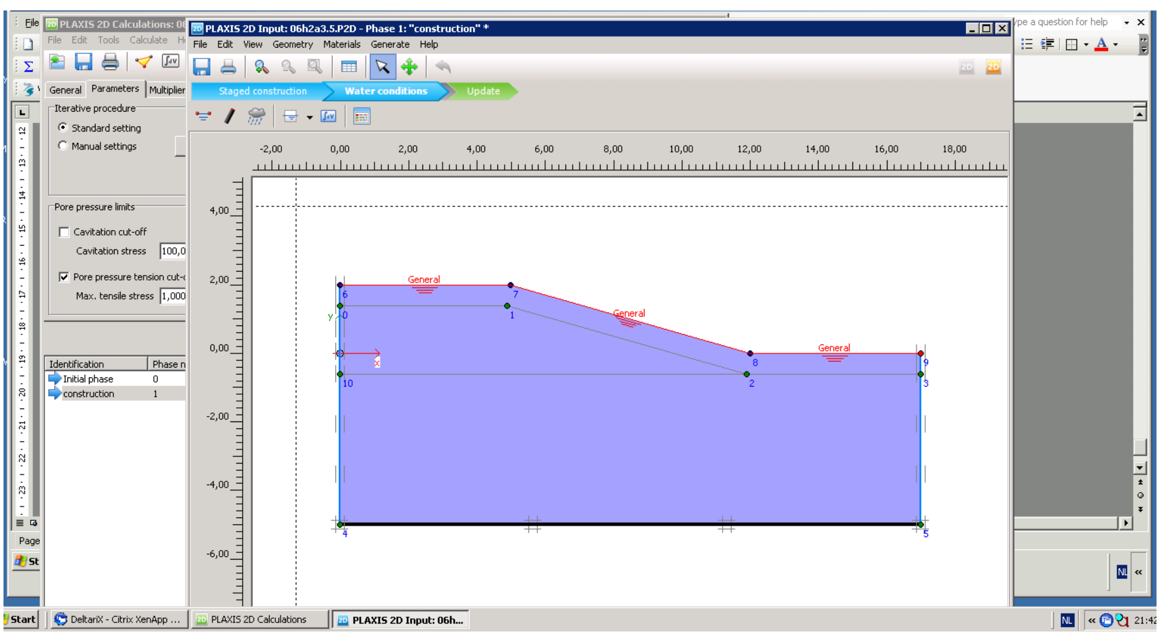

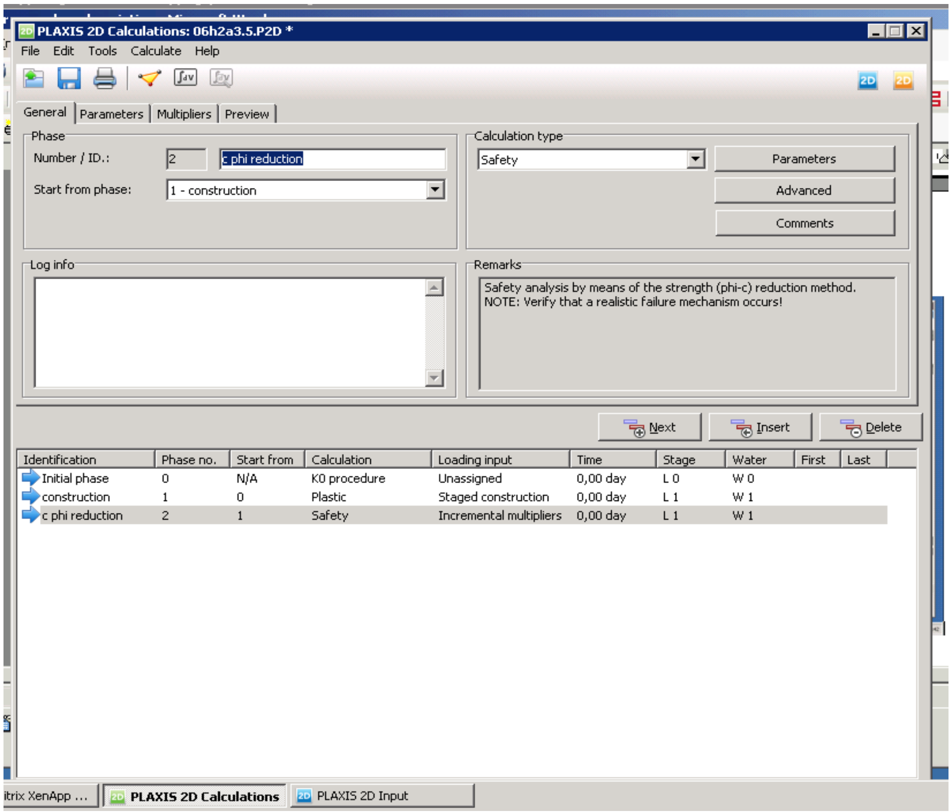

Step 4: Results

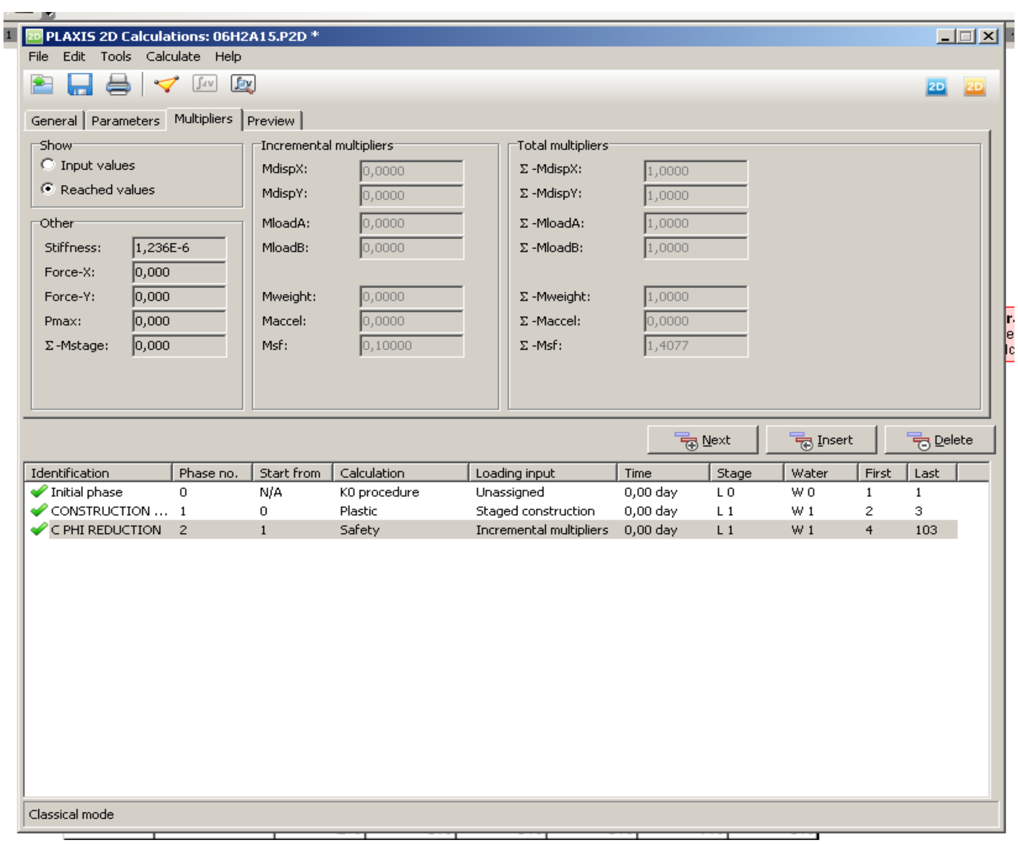

The calculated result is **1.407**, about 5% higher than the factor of safety provided by Spencer's calculation.

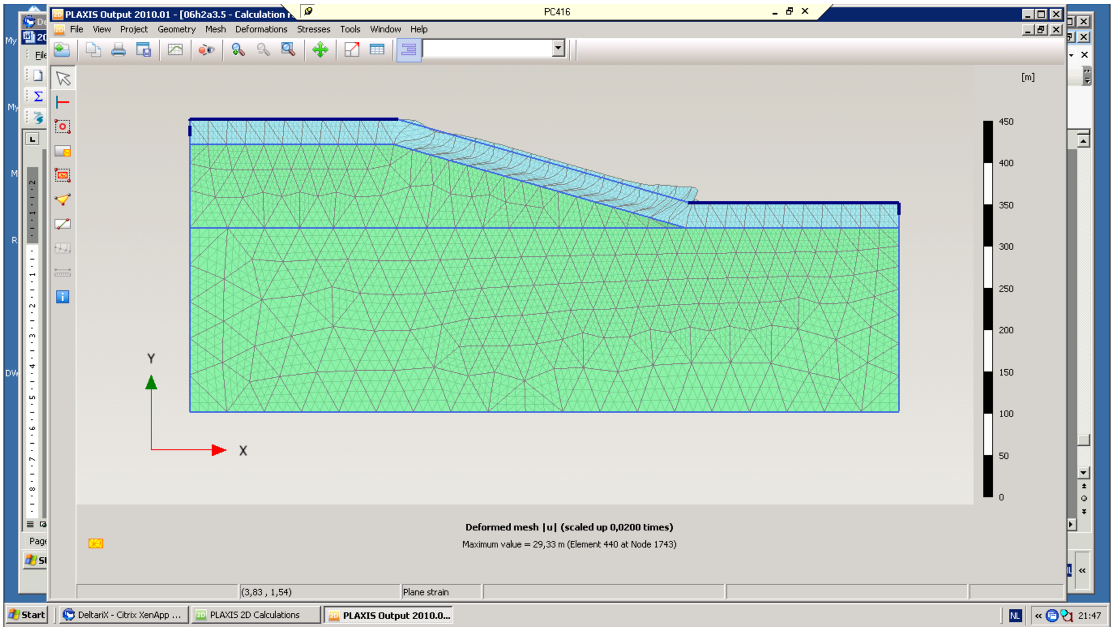

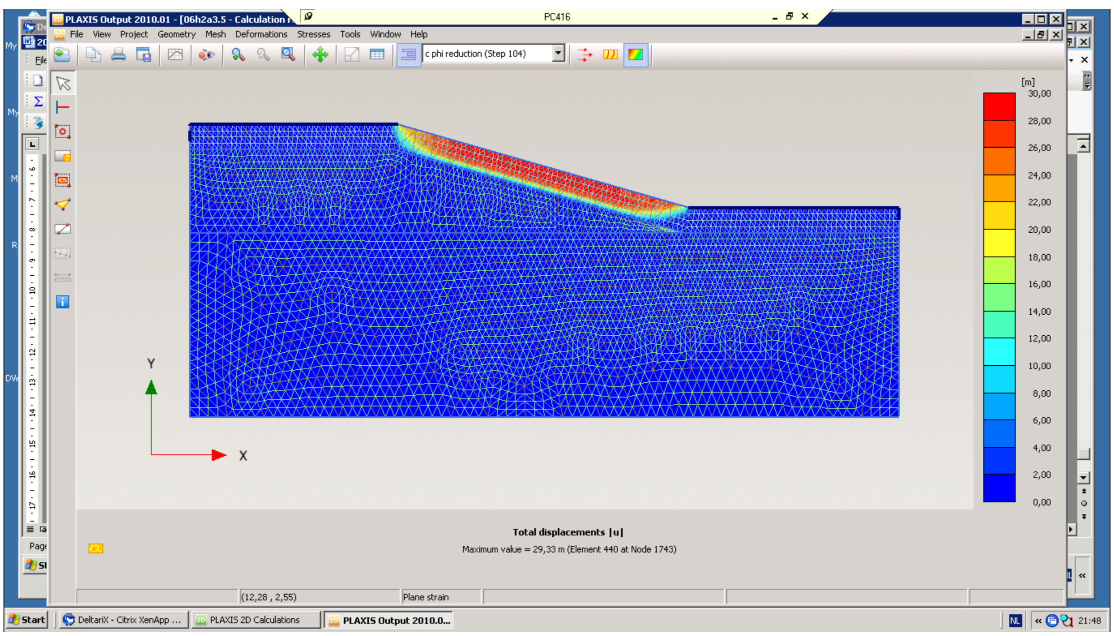

Appendix 5: Finite Element Method and Limit Equilibrium Method

H (m)	Method	Factor of safety (D=0.6m)					
		1:1.5	1:2	1:2.5	1:3	1:3.5	1:4
2	Spencer	1.33	1.6	1.81	2.05	2.31	2.57
	FEM (Plaxis)	1.407	1.613	1.88	2.113	2.39	2.58
	% difference	5%	1%	4%	3%	3%	0%
4	Spencer	1.045	1.34	1.58	1.821	2.1	2.35
	FEM (Plaxis)	1.068	1.385	1.704	1.841	2.202	2.492
	% difference	2%	3%	7%	1%	5%	6%
6	Spencer	0.98	1.27	1.51	1.75	2.01	2.26
	FEM (Plaxis)	1.056	1.369	1.545	1.766	1.925	2.468
	% difference	7%	7%	2%	1%	-4%	8%
8	Spencer	0.94	1.225	1.47	1.72	1.98	2.23
	FEM (Plaxis)	-	1.243	1.399	1.765	2.156	2.433
	% difference	-	1%	-5%	3%	8%	8%
10	Spencer	0.925	1.24	1.445	1.69	1.97	2.22
	FEM (Plaxis)	0.948	1.209	1.583	1.857	2.126	2.283
	% difference	2%	-3%	9%	9%	7%	3%

H (m)	Method	Factor of safety (D=0.8m)					
		1:1.5	1:2	1:2.5	1:3	1:3.5	1:4
2	Spencer	1.2	1.4	1.64	1.9	2.03	2.25
	FEM (Plaxis)	1.245	1.456	1.647	1.881	2.0212	2.245
	% difference	4%	4%	0%	-1%	0%	0%
4	Spencer	0.95	1.13	1.34	1.58	1.79	2
	FEM (Plaxis)		1.147	1.4263	1.6814	1.9135	2.0997
	% difference	-	1%	6%	6%	6%	5%
6	Spencer	0.85	1.05	1.25	1.51	1.7	1.92
	FEM (Plaxis)		1.0811	1.3032	1.5679	1.7949	2.065
	% difference	-	3%	4%	4%	5%	7%
8	Spencer	0.81	1.03	1.22	1.45	1.67	1.89
	FEM (Plaxis)		1.083	1.3004	1.569	1.7275	2.074
	% difference	-	5%	6%	8%	3%	9%
10	Spencer	0.797	1.01	1.23	1.43	1.65	1.87
	FEM (Plaxis)		1.068	1.3146	1.555	1.777	2.02
	% difference	-	5%	6%	8%	7%	7%

H (m)	Method	Factor of safety (D=1.0m)					
		1:1.5	1:2	1:2.5	1:3	1:3.5	1:4
2	Spencer	1.15	1.34	1.56	1.75	1.88	2.06
	FEM (Plaxis)		1.358	1.5564	1.738	1.924	2.125
	% difference	-	1%	0%	-1%	2%	3%
4	Spencer	0.852	1.04	1.221	1.42	1.61	1.797
	FEM (Plaxis)		1.058	1.29	1.4913	1.608	1.913
	% difference	-	2%	5%	5%	0%	6%
6	Spencer	0.76	0.95	1.13	1.311	1.52	1.72
	FEM (Plaxis)			1.169	1.367	1.5766	1.8034
	% difference	-	-	3%	4%	4%	5%
8	Spencer	0.718	0.931	1.088	1.275	1.49	1.673
	FEM (Plaxis)			1.1322	1.3338	1.5622	1.764
	% difference	-	-	4%	4%	5%	5%
10	Spencer	0.688	0.918	1.077	1.256	1.477	1.665
	FEM (Plaxis)			1.112	1.3127	1.543	1.753
	% difference	-	-	3%	4%	4%	5%

H (m)	Method	Factor of safety (D=1.2m)					
		1:1.5	1:2	1:2.5	1:3	1:3.5	1:4
2	Spencer	1.15	1.312	1.51	1.69	1.78	1.95
	FEM (Plaxis)		1.269	1.429	1.600	1.778	1.949
	% difference	-	-3%	-6%	-6%	0%	0%
4	Spencer	0.82	0.974	1.15	1.32	1.49	1.664
	FEM (Plaxis)			1.173	1.347	1.522	1.7212
	% difference	-	-	2%	2%	2%	3%
6	Spencer	0.715	0.873	1.053	1.215	1.387	1.576
	FEM (Plaxis)			1.078	1.263	1.448	1.6414
	% difference	-	-	2%	4%	4%	4%
8	Spencer	0.672	0.85	1.021	1.18	1.349	1.538
	FEM (Plaxis)			0.9877	1.178	1.362	1.569
	% difference	-	-	-3%	0%	1%	2%
10	Spencer	0.644	0.832	1	1.161	1.34	1.524
	FEM (Plaxis)			1.022	1.1997	1.3823	1.589
	% difference	-	-	2%	3%	3%	4%

H (m)	Method	Factor of safety (D= 1.4m)					
		1:1.5	1:2	1:2.5	1:3	1:3.5	1:4
2	Spencer	1.152	1.31	1.49	1.663	1.728	1.875
	FEM (Plaxis)		1.265	1.419	1.57	1.723	1.8824
	% difference	-	-4%	-5%	-6%	0%	0%
4	Spencer	0.79	0.95	1.09	1.252	1.418	1.577
	FEM (Plaxis)			1.079	1.254	1.4175	1.572
	% difference	-	-	-1%	0%	0%	0%
6	Spencer	0.7	0.831	0.99	1.15	1.313	1.47
	FEM (Plaxis)			1.016	1.187	1.3127	1.5272
	% difference	-	-	3%	3%	0%	4%
8	Spencer	0.628	0.81	0.95	1.11	1.278	1.44
	FEM (Plaxis)				1.1418	1.3133	1.4828
	% difference	-	-	-	3%	3%	3%
10	Spencer	0.6	0.79	0.929	1.082	1.25	1.418
	FEM (Plaxis)				1.1488	1.323	1.467
	% difference	-	-	-	6%	6%	3%

Appendix 6: Validation Calculation

Parameter	**Unit**	**Case 1**	**Case 2**	**Case 3**	**Case 4**	**Case 5**	**Case 6**	**Case 7**	**Case 8**	**Case 9**	**Case 10**	**Case 11**
Cohesion, c	kN/m2	0	1	2	3	4	5	6	7	8	9	10
Friction angle, ϕ'	deg	30	30	30	30	30	30	30	30	30	30	30
Crest height, H	m	7	7	7	7	7	7	7	7	7	7	7
Slope angle, α	deg	18.43	18.43	18.43	18.43	18.43	18.43	18.43	18.43	18.43	18.43	18.43
Layer thickness, D	m	1	1	1	1	1	1	1	1	1	1	1
Densityt of soil, γ_n	kN/m3	20	20	20	20	20	20	20	20	20	20	20
Unit weight of water, γ_w	kN/m3	9.81	9.81	9.81	9.81	9.81	9.81	9.81	9.81	9.81	9.81	9.81
Slope length, L	m	22.1359	22.136	22.1359	22.136	22.1359	22.136	22.136	22.136	22.136	22.136	22.1359
Joustra Safety factor	[-]	**0.882**	**1.041**	**1.199**	**1.357**	**1.515**	**1.673**	**1.832**	**1.990**	**2.148**	**2.306**	**2.464**
Function factor	[-]	1.083	1.083	1.083	1.083	1.083	1.083	1.083	1.083	1.083	1.083	1.083
Improved safety factor	**[-]**	**0.956**	**1.127**	**1.298**	**1.470**	**1.641**	**1.812**	**1.984**	**2.155**	**2.326**	**2.498**	**2.669**
Spencer's safety factor	**[-]**	0.85	1.07	1.25	1.431	1.613	1.8	1.982	2.16	2.346	2.527	2.71
Difference	%	11.5%	5.5%	4.2%	3.1%	2.2%	1.2%	0.6%	0.3%	-0.3%	-0.7%	-1.0%
Ratio of c/(γ'.D.tanϕ')		0.00	0.17	0.34	0.51	0.68	0.85	1.02	1.19	1.36	1.53	1.70

Parameter	**Unit**	**Case 12**	**Case 13**	**Case 14**	**Case 15**	**Case 16**	**Case 17**	**Case 18**	**Case 19**	**Case 20**	**Case 21**	**Case 22**
Cohesion, c	kN/m2	0	1	2	3	4	5	6	7	8	9	10
Friction angle, ϕ'	deg	25	25	25	25	25	25	25	25	25	25	25
Crest height, H	m	7	7	7	7	7	7	7	7	7	7	7
Slope angle, α	deg	18.43	18.43	18.43	18.43	18.43	18.43	18.43	18.43	18.43	18.43	18.43
Layer thickness, D	m	1	1	1	1	1	1	1	1	1	1	1
Densityt of soil, γ_n	kN/m3	20	20	20	20	20	20	20	20	20	20	20
Unit weight of water, γ_w	kN/m3	9.81	9.81	9.81	9.81	9.81	9.81	9.81	9.81	9.81	9.81	9.81
Slope length, L	m	22.1359	22.136	22.1359	22.136	22.1359	22.136	22.136	22.136	22.136	22.136	22.1359
Joustra Safety factor	[-]	0.713	0.871	1.029	1.187	1.345	1.504	1.662	1.820	1.978	2.136	2.295
Function factor	[-]	1.083	1.083	1.083	1.083	1.083	1.083	1.083	1.083	1.083	1.083	1.083
Improved safety factor	**[-]**	**0.772**	**0.943**	**1.115**	**1.286**	**1.457**	**1.629**	**1.800**	**1.971**	**2.143**	**2.314**	**2.485**
Spencer's safety factor	**[-]**	**0.69**	**0.9**	**1.081**	**1.26**	**1.446**	**1.626**	**1.81**	**1.99**	**2.175**	**2.36**	**2.534**
Difference	%	11.1%	5.1%	3.5%	2.5%	1.3%	0.7%	-0.1%	-0.4%	-1.0%	-1.5%	-1.5%
Ratio of c/(γ'.D.tanϕ')		0.00	0.21	0.42	0.63	0.84	1.05	1.26	1.47	1.68	1.89	2.10

Parameter	**Unit**	**Case 23**	**Case 24**	**Case 25**	**Case 26**	**Case 27**	**Case 28**	**Case 29**	**Case 30**	**Case 31**	**Case 32**	**Case 33**
Cohesion, c	kN/m2	0	1	2	3	4	5	6	7	8	9	10
Friction angle, ϕ'	deg	20	20	20	20	20	20	20	20	20	20	20
Crest height, H	m	7	7	7	7	7	7	7	7	7	7	7
Slope angle, α	deg	18.43	18.43	18.43	18.43	18.43	18.43	18.43	18.43	18.43	18.43	18.43
Layer thickness, D	m	1	1	1	1	1	1	1	1	1	1	1
Densityt of soil, γ_n	kN/m3	20	20	20	20	20	20	20	20	20	20	20
Unit weight of water, γ_w	kN/m3	9.81	9.81	9.81	9.81	9.81	9.81	9.81	9.81	9.81	9.81	9.81
Slope length, L	m	22.1359	22.136	22.1359	22.136	22.1359	22.136	22.136	22.136	22.136	22.136	22.1359
Joustra Safety factor	[-]	**0.556**	**0.715**	**0.873**	**1.031**	**1.189**	**1.347**	**1.505**	**1.664**	**1.822**	**1.980**	**2.138**
Function factor	[-]	1.083	1.083	1.083	1.083	1.083	1.083	1.083	1.083	1.083	1.083	1.083
Improved safety factor	**[-]**	**0.603**	**0.774**	**0.945**	**1.117**	**1.288**	**1.459**	**1.631**	**1.802**	**1.973**	**2.145**	**2.316**
Spencer's safety factor	**[-]**	0.54	0.74	0.922	1.105	1.284	1.47	1.659	1.837	2.02	2.19	2.38
Difference	%	10.8%	4.9%	2.9%	1.5%	0.8%	-0.2%	-1.2%	-1.4%	-1.9%	-1.6%	-2.3%
Ratio of c/(γ'.D.tanϕ')		0.00	0.27	0.54	0.81	1.08	1.35	1.62	1.89	2.16	2.43	2.70

Parameter	Unit	Case 34	Case 35	Case 36	Case 37	Case 38	Case 39	Case 40	Case 41	Case 42	Case 43
Cohesion, c	kN/m2	0	1	2	3	4	5	6	7	8	9
Friction angle, ϕ'	deg	30	30	30	30	30	30	30	30	30	30
Crest height, H	m	8	8	8	8	8	8	8	8	8	8
Slope angle, α	deg	26.57	26.57	26.57	26.57	26.57	26.57	26.57	26.57	26.57	26.57
Layer thickness, D	m	0.8	0.8	0.8	0.8	0.8	0.8	0.8	0.8	0.8	0.8
Densityt of soil, γ_n	kN/m3	20	20	20	20	20	20	20	20	20	20
Unit weight of water, γ_w	kN/m3	9.81	9.81	9.81	9.81	9.81	9.81	9.81	9.81	9.81	9.81
Slope length, L	m	17.89	17.89	17.89	17.89	17.89	17.89	17.89	17.89	17.89	17.89
Joustra Safety factor	[-]	**0.588**	**0.728**	**0.868**	**1.008**	**1.148**	**1.287**	**1.427**	**1.567**	**1.707**	**1.847**
Function factor	[-]	1.082	1.082	1.082	1.082	1.082	1.082	1.082	1.082	1.082	1.082
Improved safety factor	**[-]**	**0.637**	**0.788**	**0.939**	**1.091**	**1.242**	**1.393**	**1.545**	**1.696**	**1.847**	**1.999**
Spencer's safety factor	**[-]**	0.525	0.725	0.9	1.063	1.256	1.391	1.55	1.718	1.881	2.043
Difference	%	18%	8%	4%	3%	-1%	0%	0%	-1%	-2%	-2%
Ratio of c/(γ'.D.tanϕ')		0.00	0.21	0.42	0.64	0.85	1.06	1.27	1.49	1.70	1.91

Parameter	Unit	Case 44	Case 45	Case 46	Case 47	Case 48	Case 49	Case 50	Case 51	Case 52	Case 53
Cohesion, c	kN/m2	0	1	2	3	4	5	6	7	8	9
Friction angle, ϕ'	deg	25	25	25	25	25	25	25	25	25	25
Crest height, H	m	8	8	8	8	8	8	8	8	8	8
Slope angle, α	deg	26.57	26.57	26.57	26.57	26.57	26.57	26.57	26.57	26.57	26.57
Layer thickness, D	m	0.8	0.8	0.8	0.8	0.8	0.8	0.8	0.8	0.8	0.8
Densityt of soil, γ_n	kN/m3	20	20	20	20	20	20	20	20	20	20
Unit weight of water, γ_w	kN/m3	9.81	9.81	9.81	9.81	9.81	9.81	9.81	9.81	9.81	9.81
Slope length, L	m	17.89	17.89	17.89	17.89	17.89	17.89	17.89	17.89	17.89	17.89
Joustra Safety factor	[-]	**0.475**	**0.615**	**0.755**	**0.895**	**1.034**	**1.174**	**1.314**	**1.454**	**1.594**	**1.734**
Function factor	[-]	1.082	1.082	1.082	1.082	1.082	1.082	1.082	1.082	1.082	1.082
Improved safety factor	**[-]**	**0.514**	**0.666**	**0.817**	**0.968**	**1.120**	**1.271**	**1.422**	**1.573**	**1.725**	**1.876**
Spencer's safety factor	**[-]**	0.426	0.618	0.79	0.97	1.118	1.28	1.45	1.61	1.767	1.931
Difference	%	17.2%	7.1%	3.3%	-0.2%	0.1%	-0.7%	-2.0%	-2.3%	-2.4%	-2.9%
Ratio of c/(γ'.D.tanϕ')		0.00	0.26	0.53	0.79	1.05	1.32	1.58	1.84	2.10	2.37

Parameter	Unit	Case 54	Case 55	Case 56	Case 57	Case 58	Case 59	Case 60	Case 61	Case 62	Case 63
Cohesion, c	kN/m2	0	1	2	3	4	5	6	7	8	9
Friction angle, ϕ'	deg	20	20	20	20	20	20	20	20	20	20
Crest height, H	m	8	8	8	8	8	8	8	8	8	8
Slope angle, α	deg	26.57	26.57	26.57	26.57	26.57	26.57	26.57	26.57	26.57	26.57
Layer thickness, D	m	0.8	0.8	0.8	0.8	0.8	0.8	0.8	0.8	0.8	0.8
Densityt of soil, γ_n	kN/m3	20	20	20	20	20	20	20	20	20	20
Unit weight of water, γ_w	kN/m3	9.81	9.81	9.81	9.81	9.81	9.81	9.81	9.81	9.81	9.81
Slope length, L	m	17.89	17.89	17.89	17.89	17.89	17.89	17.89	17.89	17.89	17.89
Joustra Safety factor	[-]	**0.371**	**0.511**	**0.651**	**0.790**	**0.930**	**1.070**	**1.210**	**1.350**	**1.489**	**1.629**
Function factor	[-]	1.082	1.082	1.082	1.082	1.082	1.082	1.082	1.082	1.082	1.082
Improved safety factor	**[-]**	**0.401**	**0.553**	**0.704**	**0.855**	**1.007**	**1.158**	**1.309**	**1.461**	**1.612**	**1.763**
Spencer's safety factor	**[-]**	0.33	0.52	0.69	0.85	1.02	1.177	1.34	1.504	1.667	1.82
Difference	%	17.8%	5.9%	2.0%	0.6%	-1.3%	-1.6%	-2.3%	-3.0%	-3.4%	-3.2%
Ratio of c/(γ'.D.tanϕ')		0.00	0.34	0.67	1.01	1.35	1.69	2.02	2.36	2.70	3.03

Appendix 7. Soil Strength Parameters and Flow Parameters

Soil Strength Parameters

Data derived from the stability analysis of Afsluitdijk in Grondmechanica Delft 1987 shows that the dike was composed of a sand core covered with clayed layer and boulder clay. At that time, five Begemann boreholes were carried out to determine soil layers in the composition of Afsluitdijk. These bore holes were located in two positions (hm 14.732 and hm11.640).

Location	Clay layer thickness (m)	Boulder clay layer thickness (m)
Hm 14.734	0.15 – 0.3	1.1 – 1.8
Hm 11.640	0.35 – 0.6	1.4 – 1.7

Soil samples from 10 boreholes were sent to the laboratory for analysis. Three of them were from clay layer and the other seven samples belonged to boulder clay layer. For each sample, the cohesion c and the friction angle ϕ' (^{o}) were calculated. The results are listed in the table below.

No.	Soil type	Depth (m)	Density (t/m^3)	c' (kPa)	ϕ' (^{o})
1	Boulder clay	0.3 – 0.5	2.08	3.3	31.1
2	Boulder clay	1.3 – 1.5	2.15	4.5	29.3
3	Boulder clay	0.5 – 0.7	2.05	3.4	29.9
4	Boulder clay (including sand)	1.2 – 1.4	2.02	0	33.2
5	Boulder clay	1.3 – 1.5	2.15	4.0	35.4
6	Boulder clay	1.2 – 1.4	2.17	3.5	31.5
7	Boulder clay (strong humus, peat pieces)	0.6 – 0.6	1.80	3.8	27.8
8	Clay (included sand)	0.1 – 0.3	1.60	4.0	31.6
9	Clay, very sandy	0.4 – 0.6	1.63	1.5	26.7
10	Clay (partial sand)	0.1 – 0.25	1.48	0	36.5

The values of clay are the average of two soil samples, number 9 and 10. The result of the sample 8 is not relevant due to problems happening during the testing procedure. The values of boulder clay are also the average value of the lowest four sample tests. In this report, these values are relatively conservative in measurement.

Soil type	Density (t/m^3)	c' (kPa)	ϕ' (^{o})
Clay	1.73	0.75	31.8
Boulder clay	2.08	3.5	30.1

In DHV 2005, the strength parameters are also referred to GrondMechanica 1987. In this report, the representative values of c and ϕ' is at a high level of certainty (and even higher with the values of cohesion). Based on these data, the sliding of the cover layer did not initiated. This conclusion was also stated in Grondmechanica 1987, with a condition that the sliding occurred between clay layer and boulder clay at the depth greater than 0.6m. This is also based on limited ground investigation.

In 2009, five triaxial tests were carried on the clay cover layer. The average of maximum shear strength values is calculated, which was not much conservative. Isotropic consolidated tests worked on the samples with the controlled pressure of 5 and 10 kPa. Since the samples was compressed until they failed, the pressure rose to 20 and 30 kPa. This was about 15 and 25 kPa higher than in the field. Table 16 shows the data used to determine the shear strength parameters, of which s'= 0.5*(effective vertical stress + effective horizontal stress) and t = 0.5*(effective vertical stress – effective horizontal stress).

Table 16. Triaxial Test results

Sample	Depth (m)	s' (kPa)	t (kPa)	Weight (kN/m^3)
6-69	0.15 – 0.3	31.17	18.60	18
5-64	0.1 – 0.25	27.26	15.50	18.4
4-61	0.1 – 0.25	24.48	15.59	17.7
1-51	0.2 – 0.35	21.96	15.22	18.5
2-54	0.15 – 0.3	22.36	13.98	18.6

With the aid of linear regression of the relationship between s'- t, shear strength parameters were calculated: c= 6.2 and ϕ'= 23.4^o. However, based on these values, superficial sliding is predicted not to happen due to the high value of cohesion, even though the soil is completely saturated and the ground water flow develops parallel to the slope.

In addition, two Direct Simple Shear (DSS) tests were performed on the same clay. The advantage of this test is that soil failure can be done at a lower pressure. However, the disadvantage of Direct Simple shear test is that the horizontal pressure is more or less unknown, leading to imprecise defined points of s' and t. There are several ways to estimate the horizontal stress. An usual manner to do that is assuming the horizontal stress is equal to the vertical pressure.

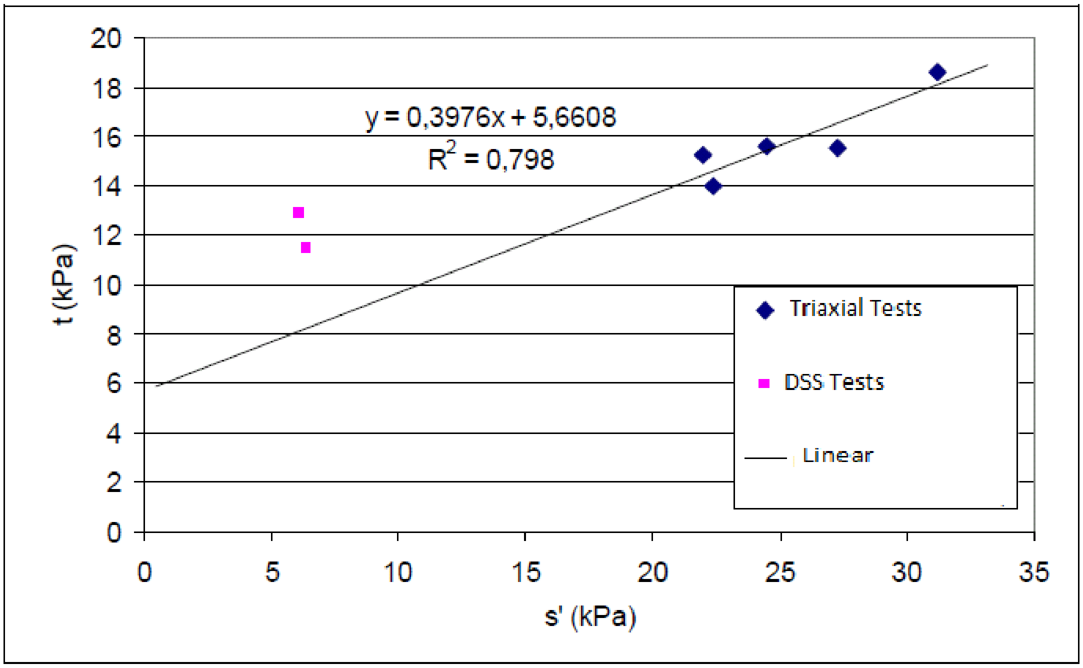

Figure 44. Triaxial and Direct Shear Tests on the clay cover layer.

As seen in the figure, DSS results is far above from the linear regression made by triaxial tests. The explanation of this are partial located in anisotropy of the sample, which causes the failure surface in triaxial tests to be different from that in DSS tests. The second possible explanation can lie on the degree of saturation. It is clear that the saturation of the samples DSS tests is less complete than that in triaxial tests due to no backpressure is placed on DSS samples.

The cohesion c and friction angle ϕ' obtained from DSS are c=11 kPa, and $\phi'=10.9^{o}$. Due to the aforementioned uncertainties, these values are not included in this report.

Flow Parameters

Table 17. Sand core permeability

Sample	Depth (m)	D10 (mm)	D50 (mm)	D60 (mm)	D70 (mm)	Packing	n (-)	k (m/s)
K56A	-1.75	0.109	1.83	0.198	0.22	Loose	0.41	1.7E-04
						Moderate	0.39	1.3E-04
						Fixed	0.37	1.1E-04
K56B	-2.2	0.118	0.201	0.221	0.245	Loose	0.4	2.0E-04
						Moderate	0.37	1.3E-04

						Fixed	0.35	1.1E-04
K63	-2.45	0.116	0.193	0.208	0.235	Loose	0.4	1.7E-04
						Moderate	0.38	1.3E-04
						Fixed	0.35	9.5E-05
K70	-1.75	0.11	0.198	0.217	0.22	Loose	0.41	1.4E-04
						Moderate	0.38	1.2E-04
						Fixed	0.35	9.0E-05

Appendix 8. Wave Overtopping Probability

This step quantifies the difference between overtopping wave discharges using probabilistic formula in described theory in Chapter 6. During a storm, a number of waves overtop the dike crests and reach the landward slope with a certain probability. Every overtopping wave has its own velocity and flow depth, which were determined by wave volume. This section gives an impression of how different overtopping discharges are quantified in terms of number of overtopping waves and wave volume per wave.

A wave condition is generally characterized by significant wave height H_s, peak wave period T_p, storm duration T_s, outer slope angle α^*, and then average overtopping discharge q (l/s per m). These basic parameters are assumed in relation with typical sea wave conditions in Dutch coastal areas. A following step-by-step procedure calculates the number of overtopping waves given certain different overtopping discharges, including number of incoming waves, probability of overtopping events, and number of overtopping waves.

a. Number of incoming waves during storm duration

Storm duration in second: T_s*3600 (s)

$$T_{m-1,0} = {T_p}/{1.1} \quad [42]$$

$$T_m = {T_{m-1,0}}/{1.15} \quad [43]$$

Number of incoming waves:

$$N_w = \frac{T_s * 3600}{T_m} \quad [44]$$

b. Probability of overtopping event of a storm

Wave steepness:

$$s_0 = \frac{H_{m,0}}{L_0} \text{ with } L_0 = \frac{g.T^2_{m-1,0}}{2\pi} \quad [45]$$

Breaker parameter:

$$\xi_0 = \frac{\tan\alpha^*}{\sqrt{s_0}} \quad [46]$$

The $R_{u,\,2\%}$ - the design crest height for 2% wave run-up is the minimum of the following formulas:

$$\frac{R_{u,2\%}}{H_{m,0}} = 1.75.\gamma_b.\gamma_\beta.\gamma_f.\xi_0 \quad [47]$$

Or

$$\frac{R_{u,2\%}}{H_{m,0}} = 1.75.\gamma_\beta.\gamma_f.\left(4.0 - \frac{1.5}{\sqrt{\xi_0}}\right) \quad [48]$$

Given an average overtopping discharge, the used crest freeboard level relative to still water level R_c is the minimum R_c between 2 following formulas:

$$\frac{q}{\sqrt{g.H_{m,0}^3}}=\frac{0.067}{\sqrt{\tan\alpha^*}}\gamma_b.\xi_0.\exp\left(-4.3\frac{R_c}{H_{m,0}}.\frac{1}{\xi_0.\gamma_b.\gamma_f.\gamma_\beta.\gamma_v}\right) \quad [49]$$

Or

$$\frac{q}{\sqrt{g.H_{m,0}^3}}=0.02\exp\left(-2.3\frac{R_c}{H_{m,0}}.\frac{1}{\gamma_f.\gamma_\beta}\right) \quad [50]$$

Minimum between these two R_c will be used to calculate probability of an overtopping event:

$$P_{ov}=\exp\left[-\left(\sqrt{-\ln(0.02)}\frac{R_c}{R_{u,2\%}}\right)^2\right] \quad [51]$$

c. Number of overtopping waves during the storm duration is:

$$N_{ov}=P_{ov}.N_w \quad [52]$$

However, within N_{ov} overtopping waves, different waves have different overtopping volumes. These volume occur with a probability calculated as follows:

- Probability of occurrence of N_i number of overtopping waves.

$$P_v=\frac{N_i}{(N_{ov}+1)} \quad [53]$$

- The maximum volumes of overtopping wave corresponding to P_v.

Figure 25 illustrates the difference between overtopping discharges in terms of number of overtopping waves and the overtopping volumes, of which the different overtopping volumes during a storm can be described by a Weibull distribution:

$$P_v=1-\exp\left[-\left(\frac{V}{a}\right)^{0.75}\right]$$ (Eurotop 2007) [54]

Where $a=0.84.T_m\frac{q}{P_{ov}}=0.84.q\frac{T_s}{N_{ov}}$ (Van der Meer, 2006a) [55]

List of Tables

List of Figures

List of Symbols and Abbreviations

Greek symbols

α : inclination of slip surface at the middle of the slice (deg)

$\alpha*$: seaward slope angle (deg)

τ_c : shear strength at the base of the slice (kN/m^2)

τ_o : mobilized shear stress at the base of the slice (kN/m^2)

ϕ' : effective friction angle (deg)

σ : total stress at the base of slice (kN/m^2)

σ' : effective stress at the base of slice (kN/m^2)

γ_n : unit weight of saturated soil (kN/m^3)

γ_w : unit weight of water (kN/m^3)

γ_S , γ_R : partial safety factor of driving forces and resistance forces (-)

γ_b : reduction factor for a berm effect, called dike coefficient (-)

γ_f : reduction factor for the roughness of the outer slope, or friction coefficient (-)

γ_β : reduction factor for the angle of wave attack (-)

ξ_0 : breaker parameter (-)

γ_v : influence factor for a vertical wall on slope (-)

θ : constant inter-slices force inclination (deg)

υ : Poisson's ratio (-)

Roman symbols

c : effective cohesion (kN/m^2)

d_{fil} : depth of infiltration (m)

D : depth perpendicular distance to the surface of slope from the base of slice (m)

E : Young's modulus of elasticity (kPa)

e : Void ratio (-)

E_1, E_2 : horizontal/normal inter-slice forces.

F_m : safety factor that meets the moment equilibrium condition (-)

F_f : safety factor that meets forces equilibrium condition (-)

g : acceleration due to gravity ($9.81\ m/s^2$)

H_s : significant height wave (m)

H_{m0} : significant wave height or spectral wave height (m)

I_{fil} : Infiltration time (%)

k_{ave} : average permeability (m/s)

L_0 : deep water wave length (m)

n : porosity (-)

$N^{'}$: effective force at the base of the slice (N)

q : average wave overtopping discharge per meter (m^3/s per meter)

Q* : dimensionless overtopping discharge (-)

R_c : crest freeboard relative to still water level (m)

Ru,2% : run-up level exceeded by 2% of the incoming waves (m)

s_0 : wave steepness (-)

T : shear force at the base of the slice (kN/m^2)

s' : principle effective stress in Triaxial test (kPa)

S^*, R* : design value of driving forces, design value of resistance forces

S_k , R_k : mean measured value of driving forces, mean measured value of resistance forces

t : shear stress or deviatoric stress in triaxial test (kPa)

t_s : infiltration time (second)

T_s : Storm duration (hour)

$T_{m-1,0}$: spectral wave period at toe of dike (second)

T_1, T_2 : vertical/shear inter-slice forces

u : pore pressure (kN/m^2)

V_{fil} : infiltration volume (l per m^2)

V_{thr} : saturated threshold (l per m^2)

W : weight of the soil of the slice (kN/m^2)

W_1 : slope-parallel stress generated by soil weight (kN/m^2)

W_2 : slope-perpendicular force/stress generated by soil weight (kN/m^2)

Abbreviations

DSS : Direct Shear Stress

L/D : ratio of slope length over the thickness of cover layers

FOS : Factor of safety

FEM : Finite element method

LEM : limit equilibrium method

PWP : pore water pressure

SWL : Still water level